APPLICATIONS OF UAS IMAGERY IN WHEAT BREEDING

By

ANDREW WALTER HERR

A dissertation submitted in partial fulfillment of
the requirements for the degree of

DOCTOR OF PHILOSOPHY

WASHINGTON STATE UNIVERSITY
Program of Molecular Plant Science

MAY 2024

To the Faculty of Washington State University:

The members of the Committee appointed to examine the dissertation of ANDREW WALTER HERR find it satisfactory and recommend that it be accepted.

Arron H. Carter, Ph.D., Chair

Kimberly Garland Campbell, Ph.D.

Lav R. Khot, Ph.D.

Robert Brueggeman, Ph.D.

ACKNOWLEDGMENT

I want to thank Dr. Arron Carter, who agreed to take on a (still) young and naive Ph.D. student, giving me the tools and the freedom to let my curiosity drive my research. Dr. Carter has shown me what it looks like to be a successful scientist without sacrificing family or faith. He has shown me the balance of asking intriguing questions without losing sight of an applied objective. The decision to join the winter wheat program has changed my life for the better in more ways than one and is a chapter of my life that I will never forget.

I want to thank my Ph.D. committee members, Dr. Kimberly Garland Campbell, Dr. Lav Khot, and Dr. Robert Brueggeman, for guiding me in my research, highlighting the importance of perspective, and showing interest in my work. I also want to thank those who I have had a chance to work with, learn from, and bounce ideas off of: Dr. Lance Merrick, Dr. Dennis Lozada, Dr. Sindhuja Sankaran, Dr. Osval Montesinos-López, Dr. Samuel Revolinski, Dr. Xianran Li, and Peter Schmuker.

None of my research would have been possible without the work done by the winter wheat breeding team members, especially Gary Shelton, Kyall Hagemeyer, and Brandon Libey, for maintaining all of the yield trials I utilized and vandalized with my research equipment, most certainly making their lives harder.

APPLICATIONS OF UAS IMAGERY IN WHEAT BREEDING

Abstract

by Andrew Walter Herr, Ph.D.
Washington State University
May 2024

Chair: Arron H. Carter

Plant breeding is a field of study with goals that have not changed significantly over time: develop cultivars with high yield, disease resistance, and drought tolerance, to name a few. While the goals of a breeding program may not change frequently, the form and technology used with which those goals are achieved are constantly evolving. High throughput phenotyping (HTP) with unoccupied aerial systems (UAS) shows significant promise in improving how crops are bred. Data collected from UAS can provide a breeder with new insights into how cultivars respond to stress and a particular environment, creating potential use cases for improving other areas of breeding, such as genomic selection and how field experiments are designed and analyzed. These new technologies, however, should not be adopted without consideration. The first study, outlined here, utilized three different HTP platforms and collection methodologies, two ground systems and one UAS-based, to determine if there is a difference in the quality of data collected. Across four years, data collected from ground systems only moderately correlated to UAS. It was also shown that data collected with UAS produced more heritable data than that collected with either ground-based system. While manufacturing specifications of the data collected from remote sensors may be similar, it is essential to be aware of the methodology used in the collection. Reflectance data standardization, sensor platform, and environmental conditions can significantly impact the quality of the data obtained and limit utility across platforms and methodologies. In the second study, spectral reflectance indices (SRI) were evaluated for their ability to improve genomic selection (GS). SRIs collected on 11,593 plots across four years were used with genomic data in univariate models as covariates and in multivariate models as secondary response variables for the assessment of prediction accuracy of grain yield. Including SRI data as covariates in univariate genomic prediction models improved prediction accuracy over the control GS model but was unreliable across years. In multivariate models, SRIs improved prediction performance across years, but due to the dataset size, high-performance computational resources were required, which could limit feasibility in an applied setting. The final study highlights the potential for SRI to improve how a breeder deals with field variability in yield trial experiments. Across three years, 47 breeding trials were evaluated under three spatial analysis strategies: linear models incorporating block-effect, row-column effect, and 2D splines. Model fit was improved across all spatial analysis methods when SRIs were incorporated as covariates. Model fitness was most greatly improved in unreplicated early-generation trials. This study highlighted the potential of SRIs to enhance how breeding trials are analyzed despite extreme environmental variables and climate conditions. This collective research highlights the challenges and benefits of utilizing UAS imagery in an applied breeding pipeline. When used strategically, the insights gained from UAS will, like genomic selection, make it an invaluable tool in the plant breeder's toolbelt.

TABLE OF CONTENTS

Page

CHAPTERS

LIST OF TABLES

Page

CHAPTER 2

CHAPTER 3

CHAPTER 4

LIST OF FIGURES

Page

CHAPTER 1

CHAPTER 2

CHAPTER 3

CHAPTER 4

CHAPTER 5

Dedication

To those whom I love deeply and who have supported me along this journey.

CHAPTER ONE: INTRODUCTION TO UAS IN PLANT BREEDING

Andrew W. Herr[1], Alper Adak[2], Matthew E. Carroll[3], Dinakaran Elango[3], Soumyashree Kar[3], Changying Li[4], Sarah E. Jones[3], Arron H. Carter[1], Seth C. Murray[2], Andrew Paterson[4], Sindhuja Sankaran[5], Arti Singh[3], Asheesh K. Singh[3]

[1]Department of Crop and Soil Sciences, Washington State University, Pullman, WA 99164-1222

[2]Dept. Soil and Crop Science; Texas A&M University; College Station, TX 77843-2474

[3]Department of Agronomy, Iowa State University, Ames, IA 50011-1051

[4]Plant Genome Mapping Laboratory, University of Georgia, Athens GA 30602-1539

[5]Department of Biological Systems Engineering, Washington State University, Pullman, WA 99164

(Portions of the chapter are taken from contributions published in an invited review in Crop Science)

Citation

Herr, A.W.; Adak, A.; Carroll, M.E.; Elango, D.; Kar, S; Li, C; Jones, S.E.; Carter, A.H.; Murray, S.C.; Paterson, A.; Sankaran, S.; Singh, A.; Singh, A.K. (2023) UAS imagery for phenotyping in cotton, maize, soybean, and wheat breeding. Crop Science, 63 (4).

Attributions

The author contributions for CHAPTER ONE: INTRODUCTION TO UAS IN PLANT BREEDING for the first author Andrew W. Herr include the conceptualization, original draft preparation, review, and editing. The contributions of co-author Arron H. Carter include conceptualization, review, editing, and funding acquisition. All other authors include review and editing of presented sections. All authors contributed to the article and approved the published version.

Trends in UAS and Crop Science

Plant breeding is a field of research that will utilize any tools it can to improve the efficiency of the cultivar development process. In an age of growing demand, unreliable growing conditions, and limited resources, breeders must use any tools they can to release cultivars that are reliable, efficient, and meet producer needs. Remote sensing tools are the latest technology showing promise in aiding a breeder in their efforts.

Over the last two decades, the primary applications of small plot research remote sensing have been unoccupied/uncrewed aerial systems (UAS, also called drones or sometimes UAVs representing the vehicles themselves and ignoring the sensors on board), which have benefited the agricultural community in phenotyping and precision agriculture applications. For example, Costa et al. (2019) reported on compiled data from the Scopus database and other sources (Nardi et al., 2016; Pallottino et al., 2018) noting that published work on phenotyping in context of omics, forestry, and precision agricultural applications has increased since 2009, where the current frequency of publications in phenotyping is up about 20% (2009-2017). These trends can be seen in Figure 1.

Similarly, in a recent meta-analysis of UAS for agricultural and environmental applications (n = 163, last 20 years) utilizing machine learning and statistical models (Eskandari et al., 2020), found that visible (RGB) imagery was most common. Among these, 62% of studies mostly used linear regression. Applications of deep learning approaches to analyze UAS data are also increasing, given high overall accuracies in varied applications (Eskandari et al., 2020; Osco et al., 2021). With continuing technological development in sensor/sensing systems and data analytics comes a greater number of images/sensor data, a greater possibility of multicollinearity of variables, and interest in increasing the speed of decision making.

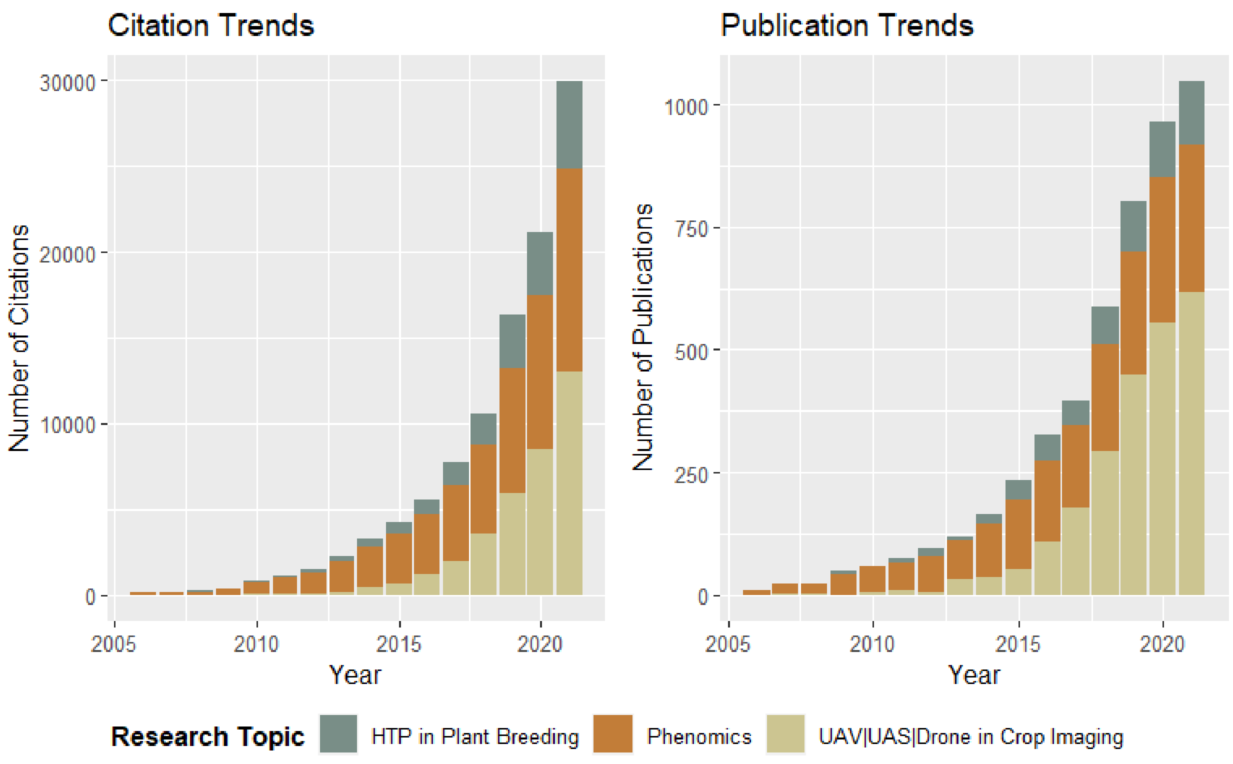

Figure 1. Recent trends of key terms in UAS crop phenotyping in publications since 2006. Adapted from data provided by Web of Science™

Advancements in sensors and sensing platforms have continued to improve over time, positively impacting tools for diverse fields of research such as medicine, material science, and microbiology, in addition to agriculture (Andukar et al., 2016; Hirano et al., 2015; Jaeger et al., 2016; Khanal et al., 2017; Zhao et al., 2017). With several companies developing sensors with real-time analytic outputs, it can be anticipated that sensors' (RGB, multispectral camera, hyperspectral camera, light detection and ranging (LiDAR) systems, etc.) spectral resolution, spatial resolution, pixel dimension, compactness, and affordability will further improve, similar to DNA sequencing (Hayden, 2014). In terms of sensing platforms and systems, UAS are becoming more affordable and sophisticated in their operation (automation, communication, stability, payload, battery life, etc.). Multiple companies continue to focus on adapting UAS technology for agricultural applications.

UAS are a crucial component of high throughput phenotyping (HTP), defined as the use of sensors in conjunction with aerial, ground, or controlled environment systems to rapidly phenotype large numbers of plants with some level of automation (D. P. Singh et al., 2021). The benefits of adopting phenomics or HTP technologies in crop breeding programs are strongly tied to factors such as genetic gain, costs and returns, rate of technology development, and breeders' comfort with technological adoption (Awada et al., 2018). Removal of human bias of objectively estimated traits will also improve accuracy. For example, Sankaran et al. (2015) correlated UAS-based sensing to ground truth data on visual rating of emergence and spring stand at 0.86, and although high, the discrepancy was more likely due to errors in ground truth measurements, and not the sensor image. It is important to recognize that discussing ground "truth" data can be misleading, as human measures are also subject to errors, in some cases more so, than automated systems (Cobb et al., 2013). For novel traits, unlike existing traits, the confirmation of utility cannot be determined by simple correlations with existing measurements, as they can from manually measured plant height, plant lodging or stand counts. Instead, estimates of repeatability or heritability must be made to show that these measurements reliably discriminate between different varieties and genotypes. Phenomics has potential to improve both selection accuracy and accelerate generation cycles to improve genetic gain through prediction (Adak et al., 2022; Adak et al., 2021c; Rincent et al., 2019), although beneficial breeding outcomes are yet to be demonstrated in practice. Wide-spread adoption of UAS phenotyping approaches into plant breeding is reliant on some combination of three factors: significant evidence of human bias in manually collected trait data, increased overall genetic gain established with UAS technologies, or overall decreased cost of UAS data collection and analysis (Araus et al., 2018).

Phenotyping of Routine Traits in Wheat

As shown in cotton, soybean, and maize above, high throughput phenotyping with UAS spectral data can have positive breeding applications in small grain crops. Small grains like wheat [*Triticum aestivum* L.] are no exception and novel approaches compared with other crops have been developed even as biology and breeding process among each differs. As with any novel high throughput strategy, one of the first approaches in utilizing UAS systems is to reduce labor and resource costs in sampling routine traits like grain yield and plant height.

Plant Height and Biomass

Plant height is an essential trait of interest in small grain crops. In wheat, a moderate plant height is a critical factor in reduced lodging (Berry et al., 2003) and increased yield potential (Carver, 2009). Plant height is also important for biomass prediction, plant stress evaluation, and cultivar distinction (Aasen et al., 2015). Traditional strategies for plant height phenotyping are simple yet labor intensive when sampling many plots. UAS-based RGB and multispectral cameras can be used to generate a Digital Surface Model (DSM), a combined model of underlying topography and crop features allowing for distinction in crop height relative to ground level (Granshaw, 2016). Using the DSM method, Holman et al. (2016) found that wheat plant height by UAS is highly predictable ($R^2 = 0.99$) and as effective as terrestrial LiDAR. Similar results were found by Madec et al. (2017) and Hassan et al. (2019a). Volpato et al. (2021b) validated these efficient and scalable findings under extensive wheat breeding trials across several growth stages and determined that genotypic selection using UAS data as covariates was equivalent to that of manual ground measurements.

Traditionally, evaluating above ground biomass is destructive, labor intensive, and infeasible on a large scale. As mentioned above with plant height, biomass is important for increasing harvest index, a limiting factor for improving grain yield (M. P. Reynolds et al., 2017). With accurate plant height estimates from DSMs, it is possible to evaluate plant biomass more efficiently and without crop destruction (Bendig et al., 2015). Several studies have shown that biomass can accurately be estimated using UAS strategies (Jin et al., 2015; Sangjan et al., 2022).

Biotic Stress

Disease resistance is a critical feature in wheat cultivar development and can be responsible for up to 100% yield loss under severe conditions. Growers demand disease resistance to maximize yield potential and reduce other input costs for controlling the disease. Because of this, regularly screening breeding populations against disease susceptibility is compulsory, but resource intensive using current methods. UAS-based RGB and multispectral imaging is an appealing option in crop disease infection and severity detection and has shown to be effective with various wheat diseases, including leaf rust (*Puccinia triticina*), stripe rust (*P. striiformis* f. sp. *tritici*, also known as yellow rust), and fusarium head blight (*Fusarium graminearum*) (Bauriegel et al., 2011; Dammer et al., 2011; Dehkordi et al., 2020; W. Guo et al., 2021).

Canopy Cover

Canopy coverage is a secondary trait that can provide helpful insight into key agronomic traits for wheat. In large plot applications, UAS collected vegetative indices can separate plant canopy from the soil within the plot area based on a predetermined threshold. This methodology is outlined well by Sankaran et al. (2015) in the determination of fall seedling emergence and can also allow for the evaluation of other essential traits such as planting density and spring stand in winter wheat (Jin et al., 2017; Kipp et al., 2014; Prey et al., 2018). Assessing canopy coverage temporally also allows observation of canopy closure speed, a critical factor in drought tolerance (Mullan et al., 2010).

Phenotyping of Previously Infeasible Traits in Wheat

Grain Yield-Related Traits

For breeders working with almost all crops, grain yield is a critical trait of interest and an ideal gauge of overall biological and economic performance. Thus, grain yield is an appealing trait for a wheat breeder to focus on when implementing high throughput phenotyping approaches (M. Reynolds et al., 2020). It is well established that vegetation indices like NDVI and NDRE, through UAS-based multispectral imaging, collected at heading or grain fill correlate highly with small grain crop grain yields (Gracia-Romero et al., 2017; Lozada et al., 2020b). These indices work by contrasting the maximum absorption of red or red edge in the leaf through chlorophyll and the maximum reflectance of near infrared due to leaf cellular structure (Gitelson & Merzlyak, 1996; Rouse, 1974). In wheat breeding programs, chlorophyll targeted vegetation indices are the established index of choice for versatility in trait sampling and grain yield predictions (Magney et al., 2016). Hassan et al. (2019b) conducted a study validating NDVI's performance for in-season selection and grain yield temporally throughout the growth cycle and across a diverse population of genotypes, indicative of a practical breeding strategy. The study validated that NDVI correlations to grain yield are inconsistent before anthesis, yet consistently high during anthesis and grain fill. High heritability between vegetation indices and grain yield has been well established and allows for indirect selection in a breeding program (Duan et al., 2017; Lozada et al., 2020a). As technology improves and hyperspectral sensors become available in UAS applications, new strategies can be used in yield evaluation. Montesinos-López et al. (2017) showed that utilizing a full range of available narrow spectral bands (250) from a hyperspectral camera improved yield prediction modeling over vegetation indices based on a few, often wide bands, as used in NDVI.

Canopy Temperature and Stomatal Conductance

Early use of handheld thermal imaging systems showed remote sensing technologies' potential to evaluate previously impractical traits like stomatal conductance. Amani et al. (1996) evaluated thermal image data from 24 spring wheat cultivars under water stress conditions across two years. Thermal data was used to calculate the plant canopy temperature relative to the ambient air temperature and it was found that this temperature depression was highly correlated to yield (r = 0.84), indifferent to growth stage or sample timing relative to irrigation. This study also found that canopy temperature depression was significantly correlated to the mean stomatal conductance (r = 0.76), a key factor in developing heat and drought tolerant cultivars. In later work, Pinto et al. (2010) found 15 QTL in wheat associated with heat and drought tolerance in a biparental mapping population by evaluating canopy temperature. These QTL were also associated with improved root architecture (Pinto & Reynolds, 2015). High throughput thermal imaging created the opportunity for this discovery and improved the breeder's ability to screen and select drought tolerant cultivars.

Thermal imaging for canopy temperature currently has challenges for routine and practical applications. Thermal data needs to be standardized relative to the ambient air temperature and humidity. Standardized relative canopy temperature has been more useful in evaluating genotypes than unstandardized temperatures, as outlined in Jones et al. (2009), Pinto et al. (2010), and Pinto & Reynolds (2015). Another factor when maximizing utility of thermal data in evaluating canopy temperature of small grains is to remove the background temperature of the soil and dead leaves. Segmentation of thermal images allows for the isolation of green canopy, minimizing unwanted noise and bias (Rischbeck et al., 2017). Given the promise thermal imaging already shows for use in wheat, improvements in thermal methodology and technology could make adoption and use routine.

Small grains require a relatively small amount of water when compared to other staple crops. This makes crops like wheat and barley ideal for semi-arid regions like those found in the United States, Mexico, and Australia. As climate change makes farming difficult in these regions, breeders need to identify drought tolerant varieties. UAV based thermal imaging for canopy temperature and stomatal conductance can be a valuable tool in this pursuit.

Chlorophyll and Senescence

Chlorophyll is essential for photosynthesis by converting light energy to usable chemical energy, so plant health, growth, and yield are directly influenced by chlorophyll content, making it a trait of high interest in breeding. Spectral imaging has opened new avenues to estimate chlorophyll content nondestructively during the growing season on a large scale. Munden et al. (1994) looked at chlorophyll contents' relationship to specific spectral bands in winter wheat and found that red edge and NIR wavelengths most accurately related to chlorophyll content. Red, red-edge, and NIR absorption in the plant canopy indicates chlorophyll *a-b* content, an indicator for overall plant health (Xie & Yang, 2020). Standard spectral indices that effectively evaluate chlorophyll content and overall plant health in wheat are NDVI and NDRE. These indices work by contrasting the maximum absorption of red or red edge in the leaf through chlorophyll and the maximum reflectance of near-infrared due to leaf cellular structure (Rouse, 1974; Gitelson & Merzlyak, 1996).

The evaluation of chlorophyll content and plant health is approachable compared to other traits evaluated using UAV spectral data. Because of chlorophylls activity in the red wavelengths, it has also been shown that canopy chlorophyll content can be estimated using an inexpensive RGB digital camera in both wheat and rice from a handheld and UAV platform (Baresel et al., 2017; Saberioon et al., 2014).

Yield potential is a major influence on the success of a wheat cultivar. One method to achieve this potential is to maximize photosynthetic potential throughout the growth cycle by selecting extended leaf area duration or "staygreen" (Parry et al., 2011). Radiation use efficiency traits like staygreen are also crucial in stress conditions like drought by maximizing photosynthetic activity through grain fill (Spano et al., 2003). The main feature of the staygreen trait is delayed senescence, resulting in maintained chlorophyll content in the canopy for longer when compared to a genotype without staygreen. In wheat, when spectral imaging data is collected temporally during grain fill, delayed senescence can be observed with standard vegetation indices like NDVI (Lopes & Reynolds, 2012). This strategy for identifying cultivars with staygreen in wheat has produced precise estimations and has been repeatably validated in breeding applications (Hassan et al., 2018; Zahra, 2017).

Targeting chlorophyll content using spectral data also allows for the potential to estimate plant nitrogen content. The close relationship between nitrogen status and chlorophyll content in wheat is well established (Baresel et al., 2017; Bojović & Marković, 2009; Fitzgerald et al., 2010). This relationship allows a farmer to utilize precision nitrogen applications based on spectral field data (Xie et al., 2018). For breeders, observing chlorophyll content allows for the potential of nitrogen status variability to be observed in large field trials. This variability can be accounted for, and spatial corrections can be made, providing more accurate trial data.

Nitrogen Use Efficiency

UAV spectral imaging for the observation and management of nitrogen is a promising area of study, providing breeders with the tools to improve nitrogen use efficiency (NUE) in wheat cultivars, reducing the risk of nitrogen runoff and fertilizer input costs. Li et al. (2009) demonstrated the high throughput potential in evaluating the NUE of winter wheat by collecting NDVI measurements on five cultivars across ten field locations in Northern China. Estimations of plant nitrogen concentration and uptake from NDVI were low (R2 = 0.25 and R2 = 0.43, respectively) when considering all locations. However, in a few locations, NDVI had a significant relationship to both nitrogen concentration and uptake (R2 = 0.89 and R2 = 0.87, respectively). This study shows both the potential and challenges associated with assessing NUE with remote sensing strategies. Another study, conducted in the state of New York, found similar results using the Maccioni vegetation index in evaluating nitrogen utilization and uptake efficiency (Frels et al., 2018).

In another study by Pavuluri et al. (2015), multiple regression and Pearson's correlation models of spectral data were used and able to explain most of the variability in both yield and nitrogen uptake (84 and 83%, respectively) under diverse genetic and environmental variability. The study also found that predictability was better when the wheat was subjected to a low nitrogen regimen. Adequate nitrogen applications minimize variability in plant chlorophyll content and limit the ability of spectral data to make accurate predictions of NUE.

NUE can be an impactful trait for breeders to target. The introduction of nitrogen efficient wheat cultivars can minimize environmental impact while lessening farmers' fertilizer costs. Historically NUE was impractical to evaluate on a large scale in a breeding program. UAV spectral imaging now allows breeders to consider nitrogen traits across an extensive breeding program.

UAS in Wheat Breeding

The underlying success of UAS-based high throughput phenotyping in a breeding program is the ability to improve genetic gain. Providing breeders with additional phenotypic and phenomic trait data allows for more accurate selections leading to increased genetic gain in cultivar development. In wheat, UAS data has been used in three strategies to improve the prediction in essential traits of interest. Phenotypic data has been used independently, used in conjunction with genomic prediction strategies, or to account for spatial variability on a trial level.

Indirect Selection

Indirect selection is an effective method for estimating grain yield in winter wheat (Lozada et al., 2020; Prasad et al., 2007). In this strategy, Indirect selection evaluates a secondary trait that correlates to the primary trait of interest. The success of Indirect selection relies upon the secondary trait's heritability and the genetic correlation of the secondary and primary trait of interest (Falconer, 1989).

In breeding, even high throughput resources are limited. When dealing with several breeding trial locations, collecting multiple data points across growth stages is not always realistic. In winter wheat, research has been done identifying heading, flowering, and grain fill as key growth stages to collect spectral data to maximize secondary trait heritability and grain yield prediction (Babar et al., 2007; Lozada et al., 2020). Hassan, Yang, Rasheed, et al. (2019) evaluated UAV-NDVI data collected on 32 cultivars in high and low water stress environments and found that heritability for NDVI was highest at flowering (h^2=0.95). Despite this high heritability, correlations of NDVI to grain yield were low in both the irrigated and unirrigated locations (R^2=0.40 and 0.08, respectively), indicating a limited genetic correlation of traits.

When used alone, Indirect selection poses a few challenges when being implemented to evaluate complex agronomic traits. Indirect selection using spectral indices lacks the robustness needed to work under all breeding trial scenarios. Diverse sample populations and unreplicated trials create the potential for low heritability values for indices, decreasing predictive power (Bowman et al., 2015). While reflectance indices have limited effectiveness when used in Indirect selection, great potential has been shown when used in combination with genomic selection (Lozada et al., 2020).

Phenotypic & Genomic Selection

Beyond UAS, it has been shown that secondary traits associated with the primary trait of interest can improve prediction accuracy when used as fixed effects. For example, large effect QTL linked with winter wheat baking quality improved predictions when used as fixed effects in ridge regression models (Michel et al., 2019). Likewise, Bernardo (2014) found that when major genes are responsible for ≥10% of genetic variation are present, and are used as fixed effects in genomic selection, prediction accuracy improves. Secondary phenotypic traits have also been shown to improve genomic selection when used as fixed effects. Compared with only DNA marker genomic data, the prediction accuracy of genomic selection models like rrBLUP can be improved when secondary phenotypic traits like UAS reflectance indices when incorporated as fixed effects in a prediction model (Krause et al., 2019, 2020; Lozada et al., 2020a). This strategy utilizes correlated traits from indirect selection but accounts for genotypic variability, creating a more robust prediction methodology. Lozada et al. (2020a) recently found that multiple HTP reflectance indices, when used individually and in conjunction with one another in a genomic prediction model, significantly increased the prediction accuracy for grain yield.

Despite the growing interest and utilization of genomic selection in breeding strategies, success has been limited when looking at highly quantitative traits across breeding cycles. It is known that genomic selection models need to be updated over cycles (Merrick et al., 2022). However when utilized in conjunction with HTP data across breeding cycles, as outlined in Figure 2, it is possible to account for more error in models, improving overall genomic selection performance; yet it remains unknown if that allows longer cycles between updating models. Using the findings mentioned above, J. Sun et al. (2019) evaluated the potential of genomic selection with and without secondary traits, UAS derived canopy temperature and green normalized difference vegetation index, to improve grain yield prediction ability across cycles. Three advanced wheat yield trials, consisting of 1092 unique genotypes, were evaluated across three years. Their results showed that prediction accuracy of grain yield across breeding cycles increased by an average of 146% when secondary traits were included. This showed that UAS derived phenotypic data can capture variation genomics cannot and reduces prediction error.

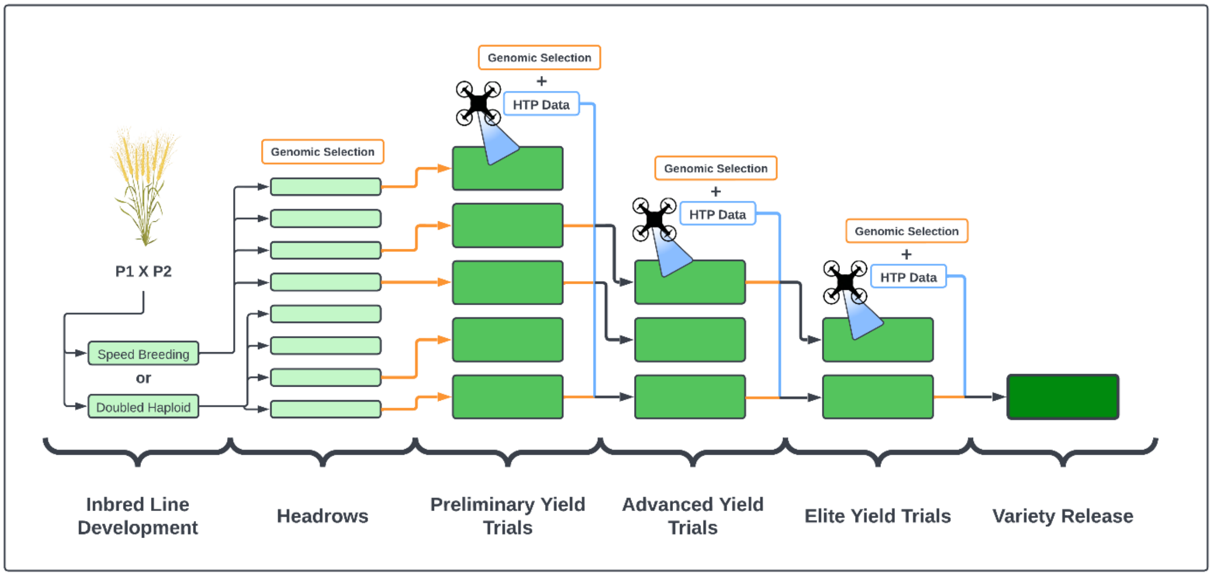

Figure 2. Sample wheat breeding pipeline with potential points of implementation of HTP in combination with genomic selection.

Confounding Factors and Limitations in Field Phenotyping

As with any breeding program, resources are limited, and decisions must be made when collecting phenotypic data across an extensive breeding program. UAV-based phenotyping platforms allow large amounts of spectral data to be collected; however, to minimize error, it is imperative to plan flights within a defined timeframe of solar noon on days with consistent irradiance. These factors limit the number of possible flights across the growing season. Breeding scenarios with many yield trial locations across diverse environments may only collect data at each location at a single growth stage. For example, in wheat, research has shown that a breeder with a focus on drought tolerance and grain yield potential can reduce data collection across growth stages and focus on collecting spectral data at heading and grain fill, allowing for more locations to be evaluated (Babar et al., 2007; Hassan, Yang, Rasheed, et al., 2019; Lozada et al., 2020; Sun et al., 2019).

References

Aasen, H., Burkart, A., Bolten, A., & Bareth, G. (2015). Generating 3D hyperspectral information with lightweight UAV snapshot cameras for vegetation monitoring: From camera calibration to quality assurance. *ISPRS Journal of Photogrammetry and Remote Sensing*, *108*, 245–259. https://doi.org/10.1016/j.isprsjprs.2015.08.002

Adak, A., Murray, S. C., Božinović, S., Lindsey, R., Nakasagga, S., Chatterjee, S., Anderson, S. L., & Wilde, S. (2021). Temporal vegetation indices and plant height from remotely sensed imagery can predict grain yield and flowering time breeding value in maize via machine learning regression. *Remote Sensing*, *13*(11), 2141.

Amani, I., Fischer, R. A., & Reynolds, M. P. (1996). Canopy Temperature Depression Association with Yield of Irrigated Spring Wheat Cultivars in a Hot Climate. *Journal of Agronomy and Crop Science*, *176*(2), 119–129. https://doi.org/10.1111/j.1439-037X.1996.tb00454.x

Andukar, A., Deshmukh, R., & Bansod, B. (2016). A review on imaging techniques in food safety and its advancements. *Int. J. Adv. Res. Electr. Electron. Instrum. Eng*, *5*, 980–983.

Araus, J. L., Kefauver, S. C., Zaman-Allah, M., Olsen, M. S., & Cairns, J. E. (2018). Translating High-Throughput Phenotyping into Genetic Gain. *Trends in Plant Science*, *23*(5), 451–466. https://doi.org/10.1016/j.tplants.2018.02.001

Awada, L., Phillips, P. W., & Smyth, S. J. (2018). The adoption of automated phenotyping by plant breeders. *Euphytica*, *214*(8), 1–15.

Babar, M. A., Ginkel, M. van, Reynolds, M. P., Prasad, B., & Klatt, A. R. (2007). Heritability, correlated response, and indirect selection involving spectral reflectance indices and grain yield in wheat. *Australian Journal of Agricultural Research*, *58*(5), 432–442. https://doi.org/10.1071/AR06270

Baresel, J. P., Rischbeck, P., Hu, Y., Kipp, S., Hu, Y., Barmeier, G., Mistele, B., & Schmidhalter, U. (2017). Use of a digital camera as alternative method for non-destructive detection of the leaf chlorophyll content and the nitrogen nutrition status in wheat. *Computers and Electronics in Agriculture*, *140*, 25–33. https://doi.org/10.1016/j.compag.2017.05.032

Bauriegel, E., Giebel, A., Geyer, M., Schmidt, U., & Herppich, W. (2011). Early detection of Fusarium infection in wheat using hyper-spectral imaging. *Computers and Electronics in Agriculture*, *75*(2), 304–312.

Bendig, J., Yu, K., Aasen, H., Bolten, A., Bennertz, S., Broscheit, J., Gnyp, M. L., & Bareth, G. (2015). Combining UAV-based plant height from crop surface models, visible, and near infrared vegetation indices for biomass monitoring in barley. *International Journal of Applied Earth Observation and Geoinformation*, *39*, 79–87. https://doi.org/10.1016/j.jag.2015.02.012

Bernardo, R. (2014). Genomewide Selection when Major Genes Are Known. *Crop Science*, *54*(1), 68–75. https://doi.org/10.2135/cropsci2013.05.0315

Berry, P. M., Sterling, M., Baker, C. J., Spink, J., & Sparkes, D. L. (2003). A calibrated model of wheat lodging compared with field measurements. *Agricultural and Forest Meteorology*, *119*(3), 167–180. https://doi.org/10.1016/S0168-1923(03)00139-4

Bojović, B., & Marković, A. (2009). Correlation between nitrogen and chlorophyll content in wheat (Triticum aestivum L.). *Kragujevac Journal of Science*, *31*(5827), 69–74.

Bowman, B. C., Chen, J., Zhang, J., Wheeler, J., Wang, Y., Zhao, W., Nayak, S., Heslot, N., Bockelman, H., & Bonman, J. M. (2015). Evaluating Grain Yield in Spring Wheat with Canopy Spectral Reflectance. *Crop Science*, *55*(5), 1881–1890. https://doi.org/10.2135/cropsci2014.08.0533

Carver, B. F. (2009). *Wheat: Science and Trade*. John Wiley & Sons.

Cobb, J. N., DeClerck, G., Greenberg, A., Clark, R., & McCouch, S. (2013). Next-generation phenotyping: Requirements and strategies for enhancing our understanding of genotype–phenotype relationships and its relevance to crop improvement. *Theoretical and Applied Genetics*, *126*(4), 867–887.

Costa, C., Schurr, U., Loreto, F., Menesatti, P., & Carpentier, S. (2019). Plant phenotyping research trends, a science mapping approach. *Frontiers in Plant Science*, *9*, 1933.

Dammer, K.-H., Möller, B., Rodemann, B., & Heppner, D. (2011). Detection of head blight (Fusarium ssp.) in winter wheat by color and multispectral image analyses. *Crop Protection*, *30*(4), 420–428.

Dehkordi, R. H., El Jarroudi, M., Kouadio, L., Meersmans, J., & Beyer, M. (2020). Monitoring Wheat Leaf Rust and Stripe Rust in Winter Wheat Using High-Resolution UAV-Based Red-Green-Blue Imagery. *Remote Sensing*, *12*(22), Article 22. https://doi.org/10.3390/rs12223696

DeSalvio, A. J., Adak, A., Murray, S. C., Wilde, S. C., & Isakeit, T. (2022). Phenomic data-facilitated rust and senescence prediction in maize using machine learning algorithms. *Scientific Reports*, *12*(1), 7571.

Duan, T., Chapman, S. C., Guo, Y., & Zheng, B. (2017). Dynamic monitoring of NDVI in wheat agronomy and breeding trials using an unmanned aerial vehicle. *Field Crops Research*, *210*, 71–80. https://doi.org/10.1016/j.fcr.2017.05.025

Eskandari, R., Mahdianpari, M., Mohammadimanesh, F., Salehi, B., Brisco, B., & Homayouni, S. (2020). Meta-analysis of unmanned aerial vehicle (UAV) imagery for agro-environmental monitoring using machine learning and statistical models. *Remote Sensing*, *12*(21), 3511.

Falconer, D. S. (1989). *Introduction to quantitative genetics*. Longman Scientific and Technical, New York.

Fitzgerald, G., Rodriguez, D., & O'Leary, G. (2010). Measuring and predicting canopy nitrogen nutrition in wheat using a spectral index—The canopy chlorophyll content index (CCCI). *Field Crops Research*, *116*(3), 318–324.

Frels, K., Guttieri, M., Joyce, B., Leavitt, B., & Baenziger, P. S. (2018). Evaluating canopy spectral reflectance vegetation indices to estimate nitrogen use traits in hard winter wheat. *Field Crops Research*, *217*, 82–92. https://doi.org/10.1016/j.fcr.2017.12.004

Gitelson, A. A., & Merzlyak, M. N. (1996). Signature Analysis of Leaf Reflectance Spectra: Algorithm Development for Remote Sensing of Chlorophyll. *Journal of Plant Physiology*, *148*(3), 494–500. https://doi.org/10.1016/S0176-1617(96)80284-7

Gracia-Romero, A., Kefauver, S. C., Vergara-Díaz, O., Zaman-Allah, M. A., Prasanna, B. M., Cairns, J. E., & Araus, J. L. (2017). Comparative Performance of Ground vs. Aerially Assessed RGB and Multispectral Indices for Early-Growth Evaluation of Maize Performance under Phosphorus Fertilization. *Frontiers in Plant Science*, *8*. https://www.frontiersin.org/journals/plant-science/articles/10.3389/fpls.2017.02004

Granshaw, S. I. (2016). Photogrammetric Terminology: Third Edition. *The Photogrammetric Record*, *31*(154), 210–252. https://doi.org/10.1111/phor.12146

Guo, A., Huang, W., Dong, Y., Ye, H., Ma, H., Liu, B., Wu, W., Ren, Y., Ruan, C., & Geng, Y. (2021). Wheat yellow rust detection using UAV-based hyperspectral technology. *Remote Sensing*, *13*(1), 123.

Hassan, M. A., Yang, M., Fu, L., Rasheed, A., Zheng, B., Xia, X., Xiao, Y., & He, Z. (2019). Accuracy assessment of plant height using an unmanned aerial vehicle for quantitative genomic analysis in bread wheat. *Plant Methods*, *15*(1), 1–12.

Hassan, M. A., Yang, M., Rasheed, A., Jin, X., Xia, X., Xiao, Y., & He, Z. (2018). Time-Series Multispectral Indices from Unmanned Aerial Vehicle Imagery Reveal Senescence Rate in Bread Wheat. *Remote Sensing*, *10*(6), Article 6. https://doi.org/10.3390/rs10060809

Hassan, M. A., Yang, M., Rasheed, A., Yang, G., Reynolds, M., Xia, X., Xiao, Y., & He, Z. (2019). A rapid monitoring of NDVI across the wheat growth cycle for grain yield prediction using a multi-spectral UAV platform. *Plant Science*, *282*, 95–103. https://doi.org/10.1016/j.plantsci.2018.10.022

Hayden, E. C. (2014). Technology: The $1,000 genome. *Nature*, *507*(7492), 294–296.

Hirano, Y., Matsuda, A., & Hiraoka, Y. (2015). Recent advancements in structured-illumination microscopy toward live-cell imaging. *Microscopy*, *64*(4), 237–249.

Holman, F. H., Riche, A. B., Michalski, A., Castle, M., Wooster, M. J., & Hawkesford, M. J. (2016). High Throughput Field Phenotyping of Wheat Plant Height and Growth Rate in Field Plot Trials Using UAV Based Remote Sensing. *Remote Sensing*, *8*(12), Article 12. https://doi.org/10.3390/rs8121031

Jaeger, B. M., Hong, A. S., Letter, H., & Odell, M. C. (2016). Advancements in imaging technology for detection and diagnosis of palpable breast masses. *Clinical Obstetrics and Gynecology*, *59*(2), 336–350.

Jin, X., Liu, S., Baret, F., Hemerlé, M., & Comar, A. (2017). Estimates of plant density of wheat crops at emergence from very low altitude UAV imagery. *Remote Sensing of Environment*, *198*, 105–114. https://doi.org/10.1016/j.rse.2017.06.007

Jin, X., Yang, G., Xu, X., Yang, H., Feng, H., Li, Z., Shen, J., Lan, Y., & Zhao, C. (2015). Combined Multi-Temporal Optical and Radar Parameters for Estimating LAI and Biomass in Winter Wheat Using HJ and RADARSAR-2 Data. *Remote Sensing*, *7*(10), Article 10. https://doi.org/10.3390/rs71013251

Jones, H. G., Serraj, R., Loveys, B. R., Xiong, L., Wheaton, A., & Price, A. H. (2009). Thermal infrared imaging of crop canopies for the remote diagnosis and quantification of plant responses to water stress in the field. *Functional Plant Biology*, *36*(11), 978–989.

Khanal, S., Fulton, J., & Shearer, S. (2017). An overview of current and potential applications of thermal remote sensing in precision agriculture. *Computers and Electronics in Agriculture*, *139*, 22–32.

Kipp, S., Mistele, B., Baresel, P., & Schmidhalter, U. (2014). High-throughput phenotyping early plant vigour of winter wheat. *European Journal of Agronomy*, *52*, 271–278. https://doi.org/10.1016/j.eja.2013.08.009

Krause, M. R., González-Pérez, L., Crossa, J., Pérez-Rodríguez, P., Montesinos-López, O., Singh, R. P., Dreisigacker, S., Poland, J., Rutkoski, J., Sorrells, M., Gore, M. A., & Mondal, S. (2019). Hyperspectral Reflectance-Derived Relationship Matrices for Genomic Prediction of Grain Yield in Wheat. *G3 Genes|Genomes|Genetics*, *9*(4), 1231–1247. https://doi.org/10.1534/g3.118.200856

Krause, M. R., Mondal, S., Crossa, J., Singh, R. P., Pinto, F., Haghighattalab, A., Shrestha, S., Rutkoski, J., Gore, M. A., Sorrells, M. E., & Poland, J. (2020). *Aerial High-Throughput Phenotyping Enabling Indirect Selection for Grain Yield at the Early-generation Seed-limited Stages in Breeding Programs* (p. 2020.04.21.054163). https://doi.org/10.1101/2020.04.21.054163

Li, X., Quigg, R. J., Zhou, J., Xu, S., Masinde, G., Mohan, S., & Baylink, D. J. (2006). A critical evaluation of the effect of population size and phenotypic measurement on QTL detection and localization using a large F2 murine mapping population. *Genetics and Molecular Biology*, *29*(1), 166–173. https://doi.org/10.1590/S1415-47572006000100030

Lopes, M. S., & Reynolds, M. P. (2012). Stay-green in spring wheat can be determined by spectral reflectance measurements (normalized difference vegetation index) independently from phenology. *Journal of Experimental Botany*, *63*(10), 3789–3798. https://doi.org/10.1093/jxb/ers071

Lozada, D. N., Godoy, J. V., Ward, B. P., & Carter, A. H. (2020). Genomic Prediction and Indirect Selection for Grain Yield in US Pacific Northwest Winter Wheat Using Spectral Reflectance Indices from High-Throughput Phenotyping. *International Journal of Molecular Sciences*, *21*(1), Article 1. https://doi.org/10.3390/ijms21010165

Madec, S., Baret, F., de Solan, B., Thomas, S., Dutartre, D., Jezequel, S., Hemmerlé, M., Colombeau, G., & Comar, A. (2017). High-Throughput Phenotyping of Plant Height: Comparing Unmanned Aerial Vehicles and Ground LiDAR Estimates. *Frontiers in Plant Science*, *8*, 2002. https://doi.org/10.3389/fpls.2017.02002

Magney, T. S., Eitel, J. U. H., Huggins, D. R., & Vierling, L. A. (2016). Proximal NDVI derived phenology improves in-season predictions of wheat quantity and quality. *Agricultural and Forest Meteorology*, *217*, 46–60. https://doi.org/10.1016/j.agrformet.2015.11.009

Merrick, L. F., Herr, A. W., Sandhu, K. S., Lozada, D. N., & Carter, A. H. (2022). Optimizing Plant Breeding Programs for Genomic Selection. *Agronomy*, *12*(3). https://doi.org/10.3390/agronomy12030714

Michel, S., Loeschenberger, F., Hellinger, J., Strasser, V., Ametz, C., Pachler, B., Sparry, E., & Buerstmayr, H. (2019). Improving and maintaining winter hardiness and frost tolerance in bread wheat by genomic selection. *Frontiers in Plant Science*, *10*. https://doi.org/10.3389/fpls.2019.01195

Montesinos-López, O. A., Montesinos-López, A., Crossa, J., de los Campos, G., Alvarado, G., Suchismita, M., Rutkoski, J., González-Pérez, L., & Burgueño, J. (2017). Predicting grain yield using canopy hyperspectral reflectance in wheat breeding data. *Plant Methods*, *13*(1), 4. https://doi.org/10.1186/s13007-016-0154-2

Mullan, D. J., Reynolds, M. P., Mullan, D. J., & Reynolds, M. P. (2010). Quantifying genetic effects of ground cover on soil water evaporation using digital imaging. *Functional Plant Biology*, *37*(8), 703–712. https://doi.org/10.1071/FP09277

Munden, R., Curran, P., & Catt, J. (1994). The relationship between red edge and chlorophyll concentration in the Broadbalk winter wheat experiment at Rothamsted. R*emote Sensing*, *15*(3), 705–709.

Nardi, P., Di Matteo, G., Palahi, M., & Scarascia Mugnozza, G. (2016). Structure and evolution of Mediterranean forest research: A science mapping approach. *PloS One*, *11*(5), e0155016.

Osco, L. P., Junior, J. M., Ramos, A. P. M., de Castro Jorge, L. A., Fatholahi, S. N., de Andrade Silva, J., Matsubara, E. T., Pistori, H., Gonçalves, W. N., & Li, J. (2021). A review on deep learning in UAV remote sensing. *International Journal of Applied Earth Observation and Geoinformation*, *102*, 102456.

Pallottino, F., Biocca, M., Nardi, P., Figorilli, S., Menesatti, P., & Costa, C. (2018). Science mapping approach to analyze the research evolution on precision agriculture: World, EU and Italian situation. *Precision Agriculture*, *19*(6), 1011–1026.

Parry, M. A., Reynolds, M., Salvucci, M. E., Raines, C., Andralojc, P. J., Zhu, X.-G., Price, G. D., Condon, A. G., & Furbank, R. T. (2011). Raising yield potential of wheat. II. Increasing photosynthetic capacity and efficiency. *Journal of Experimental Botany*, *62*(2), 453–467.

Pavuluri, K., Chim, B. K., Griffey, C. A., Reiter, M. S., Balota, M., & Thomason, W. E. (2015). Canopy spectral reflectance can predict grain nitrogen use efficiency in soft red winter wheat. *Precision Agriculture*, *16*(4), 405–424. https://doi.org/10.1007/s11119-014-9385-2

Pinto, R. S., & Reynolds, M. P. (2015). Common genetic basis for canopy temperature depression under heat and drought stress associated with optimized root distribution in bread wheat. *Theoretical and Applied Genetics*, *128*(4), 575–585. https://doi.org/10.1007/s00122-015-2453-9

Pinto, R. S., Reynolds, M. P., Mathews, K. L., McIntyre, C. L., Olivares-Villegas, J.-J., & Chapman, S. C. (2010). Heat and drought adaptive QTL in a wheat population designed to minimize confounding agronomic effects. *Theoretical and Applied Genetics*, *121*(6), 1001–1021.

Prasad, B., Carver, B. F., Stone, M. L., Babar, M. A., Raun, W. R., & Klatt, A. R. (2007). Potential Use of Spectral Reflectance Indices as a Selection Tool for Grain Yield in Winter Wheat under Great Plains Conditions. *Crop Science*, *47*(4), 1426–1440. https://doi.org/10.2135/cropsci2006.07.0492

Prey, L., Von Bloh, M., & Schmidhalter, U. (2018). Evaluating RGB Imaging and Multispectral Active and Hyperspectral Passive Sensing for Assessing Early Plant Vigor in Winter Wheat. *Sensors*, *18*(9), Article 9. https://doi.org/10.3390/s18092931

Reynolds, M., Chapman, S., Crespo-Herrera, L., Molero, G., Mondal, S., Pequeno, D. N. L., Pinto, F., Pinera-Chavez, F. J., Poland, J., Rivera-Amado, C., Saint Pierre, C., & Sukumaran, S. (2020). Breeder friendly phenotyping. *Plant Science*, *295*, 110396. https://doi.org/10.1016/j.plantsci.2019.110396

Reynolds, M. P., Pask, A. J. D., Hoppitt, W. J. E., Sonder, K., Sukumaran, S., Molero, G., Pierre, C. S., Payne, T., Singh, R. P., Braun, H. J., Gonzalez, F. G., Terrile, I. I., Barma, N. C. D., Hakim, A., He, Z., Fan, Z., Novoselovic, D., Maghraby, M., Gad, K. I. M., … Joshi, A. K. (2017). Strategic crossing of biomass and harvest index—Source and sink—Achieves genetic gains in wheat. *Euphytica*, *213*(11), 257. https://doi.org/10.1007/s10681-017-2040-z

Rincent, R., Malosetti, M., Ababaei, B., Touzy, G., Mini, A., Bogard, M., Martre, P., Le Gouis, J., & van Eeuwijk, F. (2019). Using crop growth model stress covariates and AMMI decomposition to better predict genotype-by-environment interactions. *Theoretical and Applied Genetics*, *132*(12), 3399–3411. https://doi.org/10.1007/s00122-019-03432-y

Rischbeck, P., Cardellach, P., Mistele, B., & Schmidhalter, U. (2017). Thermal phenotyping of stomatal sensitivity in spring barley. *Journal of Agronomy and Crop Science*, *203*(6), 483–493.

Rouse, J. W., Hass, R. H., Schell, J. A., Deering, D. W., & Harlan, J. C. (1974). *Monitoring the vernal advancement and retrogradation (green wave effect) of natural vegetation* (NASA/GSFC Final Report, pp. 1–137). NASA.

Saberioon, M. M., Amin, M. S. M., Anuar, A. R., Gholizadeh, A., Wayayok, A., & Khairunniza-Bejo, S. (2014). Assessment of rice leaf chlorophyll content using visible bands at different growth stages at both the leaf and canopy scale. *International Journal of Applied Earth Observation and Geoinformation*, *32*, 35–45. https://doi.org/10.1016/j.jag.2014.03.018

Sangjan, W., McGee, R. J., & Sankaran, S. (2022). Optimization of UAV-Based Imaging and Image Processing Orthomosaic and Point Cloud Approaches for Estimating Biomass in a Forage Crop. *Remote Sensing*, *14*(10), 2396.

Sankaran, S., Khot, L. R., & Carter, A. H. (2015). Field-based crop phenotyping: Multispectral aerial imaging for evaluation of winter wheat emergence and spring stand. *Computers and Electronics in Agriculture*, *118*, 372–379. https://doi.org/10.1016/j.compag.2015.09.001

Singh, D. P., Singh, A. K., & Singh, A. (2021). *Plant Breeding and Cultivar Development*. Academic Press.

Spano, G., Di Fonzo, N., Perrotta, C., Platani, C., Ronga, G., Lawlor, D., Napier, J., & Shewry, P. (2003). Physiological characterization of 'stay green'mutants in durum wheat. *Journal of Experimental Botany*, *54*(386), 1415–1420.

Sun, J., Poland, J. A., Mondal, S., Crossa, J., Juliana, P., Singh, R. P., Rutkoski, J. E., Jannink, J.-L., Crespo-Herrera, L., Velu, G., Huerta-Espino, J., & Sorrells, M. E. (2019). High-throughput phenotyping platforms enhance genomic selection for wheat grain yield across populations and cycles in early stage. *Theoretical and Applied Genetics*, *132*(6), 1705–1720. https://doi.org/10.1007/s00122-019-03309-0

Volpato, L., Pinto, F., González-Pérez, L., Thompson, I. G., Borém, A., Reynolds, M., Gérard, B., Molero, G., & Rodrigues, F. A. (2021). High Throughput Field Phenotyping for Plant Height Using UAV-Based RGB Imagery in Wheat Breeding Lines: Feasibility and Validation. *Frontiers in Plant Science*, *12*, 185. https://doi.org/10.3389/fpls.2021.591587

Xie, C., & Yang, C. (2020). A review on plant high-throughput phenotyping traits using UAV-based sensors. *Computers and Electronics in Agriculture*, *178*, 105731. https://doi.org/10.1016/j.compag.2020.105731

Xie, C., Yang, C., Hummel Jr, A., Johnson, G. A., & Izuno, F. T. (2018). Spectral reflectance response to nitrogen fertilization in field grown corn. *International Journal of Agricultural and Biological Engineering*, *11*(4), 118–126.

Zahra, S. (2017). *Characterization of a Wheat Mapping Population for Growth Pattern and Studying Staygreen Wheat Canopy Using Multispectral UAV Images* [Thesis]. https://oaktrust.library.tamu.edu/handle/1969.1/165863

Zhao, X., He, S., & Tan, M. C. (2017). Advancements in infrared imaging platforms: Complementary imaging systems and contrast agents. *Journal of Materials Chemistry B*, *5*(23), 4266–4275.

CHAPTER TWO: REMOTE SENSING CONTINUITY: A COMPARISON OF HTP PLATFORMS AND POTENTIAL CHALLENGES WITH FIELD APPLICATIONS

Andrew W. Herr[1] and Arron H. Carter [1]

[1]Department of Crop and Soil Sciences, Washington State University, Pullman, Washington, USA

(Published in Frontiers in Plant Science)

Citation

Herr, A.W. & Carter, A.H. (2023) Remote Sensing Continuity: A Comparison of HTP platforms and Potential Challenges with Field Applications. Frontiers in Plant Science, 14, 1233892.

Attributions

The author contributions for CHAPTER TWO: REMOTE SENSING CONTINUITY: A COMPARISON OF HTP PLATFORMS AND POTENTIAL CHALLENGES WITH FIELD APPLICATIONS for the first author Andrew W. Herr include the conceptualization, data collection, analysis, original draft preparation, review, and editing. The contributions of co-author Arron H. Carter include conceptualization, review, editing, and funding acquisition. All authors contributed to the article and approved the published version.

Abstract

In an era of climate change and increased environmental variability, breeders are looking for tools to maintain and increase genetic gain and overall efficiency. In recent years the field of high throughput phenotyping (HTP) has received increased attention as an option to meet this need. There are many platform options in HTP, but ground-based handheld and remote aerial systems are two popular options. While many HTP setups have similar specifications, it is not always clear if data from different systems can be treated interchangeably. In this research, we evaluated two handheld radiometer platforms, Cropscan MSR16R and Spectra Vista Corp (SVC) HR-1024i, as well as a UAS-based system with a Sentera Quad Multispectral Sensor. Each handheld radiometer was used for two years simultaneously with the unoccupied aircraft systems (UAS) in collecting winter wheat breeding trials between 2018-2021. Spectral reflectance indices (SRI) were calculated for each system. SRI heritability and correlation were analyzed in evaluating the platform and SRI usability for breeding applications. Correlations of SRIs were low against UAS SRI and grain yield while using the Cropscan system in 2018 and 2019. Dissimilarly, the SVC system in 2020 and 2021 produced moderate correlations across UAS SRI and grain yield. UAS SRI were consistently more heritable, with broad-sense heritability ranging from 0.58 to 0.80. Data standardization and collection windows are important to consider in ensuring reliable data. Furthermore, practical aspects and best practices for these HTP platforms, relative to applied breeding applications, are highlighted and discussed. The findings of this study can be a framework to build upon when considering the implementation of HTP technology in an applied breeding program.

Introduction

Severe weather and climate change are creating new challenges in maintaining and improving global food production. Plant breeding is an important tool in adapting to these difficulties (Brown et al., 2015). However, the plant breeding process is not immune to extreme or unpredictable environmental conditions, impacting selection efficiency and genetic gain (Xiong et al., 2022). Despite steady increases in genetic gain, global cereal crop demand is projected to surpass production by 2050 (Ray et al., 2013). A practical method for increasing crop production is through the release of new cultivars by increasing genetic gain. On average, it takes 7-12 years to release a new winter wheat cultivar (Carver, 2009). Thus, it is imperative to look at new methods that increase genetic gain, decrease cycle time, and improve grain yield in an era of climate change and extreme environmental variables (Xiong et al., 2022). Recent advancements in genomic technologies have provided breeders with large amounts of data to utilize genomic and marker-assisted selections. However, genomic data has limited use without the backing of phenotypic data, creating a new bottleneck in the industry, and limiting cultivar development efficiency (Mir et al., 2019). One proposed solution to this limitation is implementing high throughput phenotyping (HTP) methods associated with established breeding strategies (Reynolds et al., 2020).

The development of HTP results from advancements in imaging sensors, image processing technology, and an understanding of secondary phenotypic traits (Pauli et al., 2016; Mir et al., 2019). Despite these advancements, unoccupied aircraft systems (UAS) technology can be fastidious and resource intensive for simple plant breeding applications. Most HTP strategies require the purchase of expensive specialized equipment and tedious data standardization and processing pipelines. There is a continued need to identify and adapt HTP technology to better aid the breeder while maintaining cost-effectiveness (Reynolds et al., 2020).

There are three primary options in field-based HTP. Satellites allow for the high throughput collection of field-scale images yet are limited by image frequencies and resolution, critical factors in plot-level research applications. Alternatively, ground-based and handheld systems provide high resolution imaging across a wide range of frequencies but can be challenging to handle and capture larger-scale, multi-plot images quickly. UAS provide a “goldilocks” ratio of utility, temporal frequency, and spatial resolution (Araus and Cairns, 2014; Song et al., 2021). Rotocopters are a versatile platform that allows for high throughput, high resolution image capture. Due to power usage and battery capacity, the limitations of the platform arise in payload capacity and flight time (Sankaran et al., 2015b; Xie and Yang, 2020).

The spectral reflectance data collected from handheld radiometers and UAS cameras has minimal uses in its raw form. Spectral reflectance indices (SRI) are used to evaluate target features and remove image noise creating a practical, standardized trait value (Myneni et al., 1995; Xue and Su, 2017). Vegetation indices are developed by evaluating the reflectance value of the plant canopy at specific light bands associated with photosynthetic mechanisms. Normalized Difference Vegetation Index (NDVI) is a prevalent index used to evaluate plant health by evaluating contrast in the maximum absorption of red in the leaf through chlorophyll pigmentation and the maximum reflectance of near-infrared due to leaf cellular structure (Rouse Jr, 1974). Normalized Difference Red-edge Index (NDRE), another popular standard vegetation index, works similarly to NDVI but replaces red with red-edge absorption relative to NIR (Gitelson and Merzlyak, 1996). The vegetation index used depends on the crop, growth stage, and target trait. These factors influence reflectance values and relative index effectiveness (Wientjes et al., 2017; Lozada et al., 2020; Herr et al., 2023). Vegetation indices have many applications in capturing routine trait estimates like plot quality, biotic, and abiotic stress (Sankaran et al., 2015a; Guo et al., 2021; Sarkar et al., 2022; Sapkota et al., 2023), as well as previously infeasible traits like chlorophyll content and nitrogen content (Xie and Yang, 2020; Yin et al., 2022). Unlike vegetation indices, water indices such as Normalized Water Index (NWI) use infrared range reflectance to evaluate stomatal conductance and overall photosynthetic efficiency (Babar et al., 2006). Water indices can evaluate and predict relative water content, leaf osmotic potential, stomatal conductance, and canopy temperature(Gutierrez et al., 2010; Bal et al., 2021; Visitacion et al., 2022).

For most breeders working with cereal crops, grain yield is the critical trait of interest and an ideal gauge of overall biological and economic performance. Grain yield in wheat is highly quantitative and can make selection efficiency difficult (Reynolds et al., 2012). It is well established that NDVI and other vegetation indices like NDRE and NWI, through high throughput multispectral imaging, correlate with cereal crop grain yields (Geipel et al., 2014; Gracia-Romero et al., 2017; Lozada et al., 2020). It has also been shown that SRI data can be utilized to improve tools like genomic selection for grain yield. Thus, grain yield is an appealing trait for a breeder to focus on when implementing HTP approaches (Reynolds et al., 2020; Montesinos López et al., 2022; Herr et al., 2023).

SRI heritability and correlation to grain yield are leading indicators of SRI and platform utility. A strong repeatable relationship to grain yield can determine data quality and efficiency of selection in large-scale field-based breeding applications. While the sensors evaluated in this study collected the same SRIs, each has a different manufacturer, sensor type, and processing pipeline. Sensor differences create the potential for variances in data value and quality. These variances are compared and discussed. Finally, the practical aspects of the platforms are compared for their potential cost relative to the benefit they could provide (i.e., the improved resolution of ground collected data is not worth the extra logistics required in data collection).

With the growing interest in utilizing high throughput phenotyping technology in plant breeding, this study aimed to compare the SRI data collected from breeding trials between ground systems and UAS and determine if the use of ground-based handheld systems provides an increased resolution and data quality that justify the negative aspects of the platform, like collection time, data noise, and secondary applications.

Materials and Methods

Study Population

The Washington State University (WSU) winter wheat breeding program has collected multispectral data with three different phenotyping systems as indicated in Figure 1: A handheld multispectral radiometer, the Cropscan MSR16R (CROPSCAN Inc., Rochester, MN, USA), a handheld full-range hyperspectral spectro-radiometer, the Spectra Vista Corporation (SVC) HR-1024i (Spectra Vista Corporation, Poughkeepsie, NY, USA), and a UAS-based system, a Sentera Quad Multispectral Sensor (Sentera Inc., Minneapolis, MN, USA) mounted on a DJI Inspire 1 rotor copter platform.

Data for all platforms was collected at anthesis due to its established relationship with grain yield (Duan et al., 2017; Lozada et al., 2020). Each population evaluated was sampled on the same day by both the UAS and compared handheld system. Handheld data was collected within a six-hour window of solar noon, which was the typical time required to collect data given the number of plots in the trials. UAS data was collected within a four-hour window of solar noon. In these trials, UAS data was often collected at or near solar noon to try and be in the middle of the handheld data collection timeframe, and flights often took 20 minutes. The UAS mounted with the Sentera camera flew a programmed route at an altitude of 45 m, with an 85% longitudinal and lateral overlap of georeferenced images. All data was collected on days with clear skies to limit variability in solar radiation. All trials were grown in Pullman, WA, as shown in Figure 1, and include:

- A genetically diverse Quality Association Mapping (QAM) panel;
- Unreplicated single plot yield trials of soft white and hard red winter wheat;

- Replicated alpha-lattice preliminary yield trials of soft white and hard red winter wheat;
- Replicated alpha-lattice advanced yield trials of soft white and hard red winter wheat.

Table 1 outlines the study populations' characteristics, including year, trial design, total number of unique entries, number of total plot observations, and HTP data type collected. Plots were planted using a double-disc 8-row small plot planter at a seed density of 250 seed per square meter. Total plot size was 1.5 meter wide by 3.5 meter long. Ground was prepared by grower cooperators using minimum-tillage techniques and practices customary of the region. Grain yield data were collected at all locations with a Zurn 150 harvester (Zurn Harvesting GmbH & Co. KG, Waldenburg, Germany). Weather data for each year can be found at weather.wsu.edu for the Pullman, WA location. Single environment adjusted means were calculated for all observations of grain yield. Grain yield was the focus of observation given its importance as the final end-value selection parameter in many plant breeding programs.

UAS Phenotypic Data

The Sentera Quad Multispectral Sensor covered target bands of interest for winter wheat evaluation. The camera has four sensors that cover eight broad spectral bands between 450 nm and 970 nm. Collected UAS images are stitched and prepared for data extraction in Pix4Dmapper (Pix4D Inc., Denver, CO, USA), creating a single orthomosaic image for each sensor per location. Orthomosaic images were transferred to Quantum Geographic Information System (QGIS) for plot identification and then further processed with a custom R code for calibration, index calculation, and single plot mean data extraction. In 2018 and 2019, a single reflectance panel (85% reflectance) was used for radiometric calibration on RBG and red edge bands. Quantum efficiency coefficients were used to calculate NIR using:

$$NIR = (2.921 \times Blue) - (0.754 \times Red).$$

The NIR band was then normalized with a coefficient of 3.07 during the calculation of SRIs (Ortiz et al., 2021). In 2020 and 2021, a set of calibration panels (five panels ranging from 2% – 85% reflectance, MosaicMill Oy, Vantaa, Finland) was implemented. Iqbal et al. (2018) developed a simple radiometric calibration methodology using a set of calibration panels with a known variation of reflectance at each broadband wavelength of interest. The band layers are adjusted based on the relationship:

$$SR = DN \times m \pm b,$$

where digital numbers (DN) are the raw observed pixel values for collected orthomosaic images and Surface Reflectance (SR) is the true reflectance value. Slope (m) and intercept (b) are variables explaining the relationship between observed and true values of the reflectance panels. Once slope and intercept are calculated based on the reflectance panels' regression, the corresponding bands can be adjusted.

Ground Phenotypic Data

Like the Sentera sensor, the CROPSCAN MSR16R covers target bands of interest. The CROPSCAN radiometer has 16 broad spectral bands that range from 430 nm to 970 nm. Before data collection the sensor is calibrated using manufacture provided calibration panel. The sensor was attached to a pole and placed 1m directly above the wheat canopy in the middle of the plot. One plot is collected at a time, and a mean value for each spectral band is logged for that plot. An irradiance light sensor accounts for light variation and reduces noise in reflectance values. The CROPSCAN MSR system software is used to retrieve collected band values. Plot reflectance values were normalized across all observations by dividing each plot reflectance value by the standard deviation of reflectance values within a trial.

The SVC HR-1024i is a hyperspectral sensor collecting thousands of narrow band values between 338 nm and 2515 nm for each plot. Before sampling, the sensor was calibrated using the manufacture provided calibration panel. The SVC was held by hand at a height of 0.75 m above the plot at an approximate 20-degree angle. Collected SVC data reflectance curves were observed for each plot. Observations with abnormal reflectance curves below 1000 nm were removed from the evaluation. Band reflectance values were normalized as done with CROPSCAN data. Broadband values that reciprocate the collected UAS bands were then calculated by averaging all SVC narrowband values within the 50 nm desired broadband window.

Spectral Reflectance Indices Calculation and Data Analysis

Comparing these systems is based on three overlying factors: grain yield correlation with water indices, grain yield correlation with vegetation indices, and overall utility for a large-scale breeding program. The processed spectral reflectance data collected from each plot for both the handheld and UAS platforms were used to calculate the vegetation indices NDVI, NDRE, Transformed Chlorophyll Absorption Reflectance Index (TCARI), Modified Triangular Vegetation Index (MTVI), and the water index, NWI. NDVI and NWI are the most commonly used in each of their corresponding categories and are ideal measures of plant stress and canopy water stress, respectively, in winter wheat (Prasad et al., 2007; Lozada et al., 2020). NDRE, TCARI and MTVI were chosen because of their past success in our breeding program in correlating to yield and accounting for environmental variability. The spectral reflectance bands used and formulas for these indices are shown in Table 2.

Broad-sense heritability (H2) was calculated for SRIs across all sampled locations for grain yield. Genotype, replication, block, environment, and genotype by environment variation were used as random effects in the calculation of H2 with the formula:

$$H^2 = \frac{\sigma_G^2}{\sigma_G^2 + \frac{\sigma_{GE}^2}{x} + \frac{\sigma_\varepsilon^2}{xr}}$$

where σ_G^2 is genetic variance, σ_{GE}^2 is variation due to genotype by environmental effect, σ_ε^2 represents variation due to error, x signifies the number of environments, and r represents the number of replications (Bernardo, 2002). Variance components used in heritability calculations were estimated using the "lme4" package in R. Heritability, in conjunction with correlation to grain yield, will indicate an index's success in indirect selection.

Phenotypic correlations among traits were calculated within the two datasets as Pearson correlations using "cor' function in R. Scatterplots and regressions for each unique year and platform combination was generated using "ggplot2" in R.

Principal component analysis (PCA) was conducted for the 2018-2019 and 2020-2021 populations using NDVI, NDRE, TCARI, MTVI and NWI for each platform as well as grain yield. PCA was conducted using the "FactoMineR" package in R.

Results

SRI Correlation Across Platforms and with Grain Yield

Within each population, the correlation of indices was evaluated between collection methods as well as between indices and grain yield. In 2018-2019 correlations with grain yield were close to zero or slightly negative with handheld NWI, ranging from -0.23 to 0.22. Handheld NDVI was negatively associated with UAS NDVI with a correlation of -0.48, whereas handheld NWI and NDRE had a small positive association with UAS with a correlation of 0.24 and 0.2, respectively. In the 2020-2021 population, NDVI and NDRE had a moderate to high positive correlation between collection strategies and grain yield, as seen in Figure 2 and reinforced by PCA in Figure 3. NWI had a low correlation between UAS and handheld, with a coefficient of 0.07. When correlated to grain yield, UAS and handheld NWI had a negative association of -0.34 and -0.67, respectively. The negative correlation between water-based indices and grain yield was supported in PCA. This negative correlation is expected in NWI with both vegetation indices and grain yield. A lower NWI value indicates higher water content in crop canopy.

Linear Relationship of SRIs to Grain Yield

A clearer relationship can be seen when linear regressions are conducted with SRIs and grain yield, as seen in Figure 3. Across all years and environmental conditions, UAS NDVI has an expected linear distribution relative to grain yield. Both handheld systems used in this study produced high NDVI values across observations while producing more non-normal distributions relative to grain yield. UAS NDVI generally has a stronger linear relationship to grain yield over the handheld counterpart. Only NDVI is shown because of its relevance to wheat. All other SRIs evaluated have similar trends.

PCA of SRIs Across Platforms and Grain Yield

The first principal component (Dim1) captured between 35.6% and 55.8% of the phenotypic variation. The second principal component (Dim2) was only able to explain between 30.9% and 22.4% of trait variation. PCA biplots of individuals in both populations group years along Dim1, indicating strong between-year environmental variability. QAM diversity panels group closely within their given year, while breeding trials (single plot, preliminary, and advanced) tend to spread across Dim2. As seen in Figure 4, the 2020 observations are tightly grouped due to ideal growing conditions reducing genetic expression in trait variability. In 2018-2019 handheld generated indices contributed most in Dim1 while UAS generated indices contributed more in Dim2. This differs from 2020-2021 where most indices were contributing to Dim1 whereas only handheld MTVI and UAS NWI were major contributors to Dim2.

Heritability of Grain Yield and SRIs in Evaluated Trials

Broad-sense heritability for spectral indices of all years evaluated was moderate to high, with a range of 0.50 to 0.80. Grain yield heritability was also calculated at 0.65 in 2018-2019 and 0.76 in 2020-2021, as seen in Table 3. Across both populations, UAS collected indices had a higher heritability than handheld collected indices. This difference was greater with NDVI and NDRE than with NWI.

Discussion

In this study, we have outlined the differences in the correlation and heritability performance of SRIs collected from handheld and UAS systems relative to grain yield. This study evaluated HTP data of a breeding population from a single location, over four highly differing years. This is typical of most breeding programs where lines are evaluated initially and selected based on performance at one location. Despite these factors, there are clear differences in the capability of the tested HTP systems for application in a breeding pipeline to improve grain yield selection potential as secondary traits. Both phenotypic correlation and heritability of SRIs were assessed to evaluate the utility in improving selection for grain yield. This section, along with the discussion of analytical results, will break down the less tangible aspects of the HTP systems used in this study and their relative potential utility in breeding applications.

SRI Correlation and Precision Across Platforms

The correlations of SRIs in the 2018-2019 dataset were generally lower than that of the 2020-2021 dataset. It is important to note that NWI is a water index that negatively associates with canopy water content. A higher NWI value indicates lower canopy water content, meaning that a strong negative correlation to grain yield is ideal (Bandyopadhyay et al., 2014). This relatively low correlation in 2018-2019 is potentially due to inadequate data quality caused by more primitive data standardization and poor sensor quality, where only one calibration panel was used. The poor data quality in 2018-2019 is also exemplified in the low correlations of corresponding SRIs between handheld and UAS. Similar findings were shown by Deng et al. (2018) and Díaz-Delgado et al. (2019), both highlighting inconsistencies in sensor performance and correlation, especially when sensor quality or calibration methods are inadequate. Finally, despite moderate heritability, the 2018-2019 SRI data correlates poorly with grain yield. This suggests that the collected data was not capturing the chlorophyll or water content targeted by SRIs, possibly because of the reduced calibration panel set. Ensuring that data collected is of the highest quality is always essential. As additional research was published suggesting the move from a single calibration panel to multiple panels, subsequent data was improved and yielded higher correlations with grain yield (Duan et al., 2017; Guo et al., 2019).

Unlike the 2018-2019 dataset, in 2020 and 2021, correlations are improved to moderate or high across SRI and platform. UAS data correlations are most likely improved over the 2018-2019 population due to an improved image calibration strategy using a set of five calibration panels. The 2020-2021 data also displays expected patterns across the correlation table between grain yield, handheld and UAS data indicating a more successful capture of target physiological characteristics relative to the 2018-2019 dataset. There are generally stronger correlations among grain yield UAS data in 2020-2021 relative to 2018-2019. These differences between datasets collected by the two ground based systems could possibly be because of variation in climatic conditions of the years. More likely, the improved correlations in 2020 and 2021 were because of improved data quality with the enhanced calibration strategies that were implemented.

The variation shown between sensors in this study is most likely not due to the sensor itself but in the methods by which those sensors were used. Theoretically each sensor should be able to capture the same reflectance values. Error in end SRI values is not being introduced by the sensor itself but in how the sensor is calibrated, the platform used, and the manufacture methodologies.

The handheld radiometer systems do not have as quick of a collection speed as UAS, allowing for the introduction of error, similar results were found by Tattaris et al. (2016). This issue will be discussed in later sections. This study also validated Tattaris et al. (2016) in higher correlations of UAS derived vegetation indices to yield relative to ground based proximal sensors. In 2020 and 2021, handheld platforms did outperform UAS with NWI correlations. The outlier in correlation is most likely due to NWI's susceptibility to environmental variability and general sensor quality. These results are corroborated in Gutierrez et al. (2010) and Bandyopadhyay et al. (2014), highlighting difficulties in working with NWI. The SVC sensor used in 2020 and 2021 is a hyperspectral sensor capable of greater precision in reflectance evaluations. Reflectance bands used in calculating NWI are within the median reflectance range of the SVC sensor, whereas the UAS camera works with secondary modified sensors.

SRI Heritability and Reliability in Selection

Across all evaluated SRIs in both populations, UAS data produced a higher broad-sense heritability than handheld systems. This difference in heritability between systems is most likely due to the increased variability of SRI data introduced during a lengthened data collection window. Handheld systems have the disadvantage of collection efficiency, taking approximately 10 seconds per plot, whereas a UAS system can average under 2 seconds per plot. While the UAS, Cropscan and SVC all have methods for sensor calibration, slight changes in solar position and intensity likely impacted reflectance readings. It has been well established that minimization of error during the spectral reflectance data collection process is critical to the final data quality (Guo et al., 2016; Ortiz et al., 2021). Because the UAS system captures several plots at a time and the same plot multiple times, all within a 20-30 min window, it is likely that UAS reflectance data has a reduced potential for error relative to the handheld radiometers used. This difference in data quality is also observed in NDVI's relationships to grain yield across years, shown in Figure 3.

The moderate SRI heritability observed in this study is expected due to a portion of the study population being unreplicated trials. We also expect heritability in the 2018-2019 population to be lower than the 2020-2021 population due to the increased variability of the population from the inclusion of the QAM diversity panel (Bowman et al., 2015). SRI heritability was generally lower than grain yield, limiting the potential application for indirect selection. However, the moderate correlation and heritability of SRIs suggest the potential for improved genetic gain when utilized as secondary traits in selection. The utilization of SRI data for utilization in breeding for grain yield is most promising when incorporated in genomic selection strategies as a covariate or in multivariate models as shown my Lozada et al. (2020) and Montesinos López et al. (2022) respectively.

Platform Utility in a Breeding Program

For most plant breeding programs grain yield is the primary trait of interest. The highly quantitative nature of the trait can make selection and prediction efficiency difficult (Reynolds et al., 2012). There is evidence that SRI data can complement and improve tools like genomic selection and machine learning prediction for use in the breeding strategy of grain yield (Montesinos López et al., 2022; Herr et al., 2023). It is important to validate that the methods used in secondary trait data collection are high quality, heritable, and correlate well to the primary trait of interest.

The overarching goal of this study was to determine if the use of ground-based handheld systems provides an increased resolution and data quality that justify the negative aspects of the platform, like collection time, data noise, and secondary applications. As mentioned above, handheld systems have the disadvantage of collection speed; this difference is amplified when capturing large breeding trails. A UAS can collect all data of a 1000 plot breeding trial in approximately 30 min, whereas the handheld system will take roughly 3 hours. In smaller research programs and applications, this difference would have minimal impact on the ability to collect desired datasets. However, in large breeding programs with multiple trial locations, collecting reflectance data across all locations at more than one or two critical time points can be difficult. Solar and weather limitations create narrow windows for image capture, and UAS imaging allows for flexibility in data collection timing. Under ideal environmental conditions, UAS allows for quick data capture across several locations in a single day. The variability seen in heritability and correlation between handheld and UAS is partly due to the differential in capture time. The increased time it takes a handheld radiometer system to collect data on an entire breeding trial, 2-3 hours, creates the potential for changes in solar radiation caused by solar angle or cloud cover. This will produce within field errors in collected reflectance data, creating challenges in distinguishing genetic, phenotypic, and environmental variability (Tattaris et al., 2016).

The HTP systems used in this study highlight the reality of working with technology in long term breeding research applications. When first evaluating the potential of HTP, UAS sensors were not common, thus the Cropscan system was utilized as a platform that was easy to implement in a field-based breeding program. In 2018, as more UAS and sensors became available, they were used in tandem with the hand-held Cropscan. When the Cropscan broke in 2020, alternative solutions were pursued for a ground based radiometer, leading to the use of the SVC system. Similarly, with the UAS calibration, when starting in 2018 the manufacturer recommendations of a single white panel were used. As new research came out it became evident for the need to implement higher quality, multi-panel radiometric calibration in 2020 and 2021. With technology constantly changing and improving, it is important to recognize the potential improvements these can make. It also important to note that new methodology or equipment can impact the quality and reliability of SRI data as shown in this study. As other breeding programs begin using HTP, it is valuable to evaluate different UAS calibration strategies and handheld platforms within the same population and year, and across a diverse set of environments, to clearly identify each technology's reliability.

Each of the three phenotyping systems used in this study has a different method of calibration, collection, and processing that influence the quality of data collected. The SVC and Cropscan radiometer systems initially use a white reference panel to calibrate the sensor. These radiometers do not collect actual images but a range of mean reflectance bands within the sensor field of view. The Cropscan system requires custom software for post-processing to populate reflectance values, and the SVC requires normalization and conversion of narrow hyperspectral band values to multispectral broadbands. A major disadvantage of these radiometers is their inability to screen for reflectance noise within the sensor field of view. The UAS used in this study collects images which are later stitched into an orthomosaic containing the desired reflectance values. These orthomosaics can be used to create soil masks, removing soil and other non-plant reflectance in calculating mean plot reflectance for later use in SRI calculation.

Calibration is another strategy for minimizing reflectance noise and standardizing collected data. All platforms in 2018-2019 and the handheld system in 2020-2021 used a simple single-panel radiometric calibration technique that utilizes the know reflectance of a white panel to adjust sensor readings based on the observed panel reflectance. This method is effective but is more limited in accurately adjusting each reflectance band (Iqbal et al., 2018). Radiometric calibration with a range of calibration panels, a method used for 2020-2021 UAS data collection, improves the former strategy by utilizing three to five reflectance panels with a known range of solar absorption. The range of panels can be used to produce a regression of expected reflectance against observed for each reflectance band of interest. This technique allows for more precise adjustment in individual band readings, producing more reliable reflectance values (Wang and Myint, 2015; Iqbal et al., 2018). The removal of soil noise, robust radiometric calibration, and short flight times minimize the error in the data collected, ensuring reflectance data quality across time and locations.

It is important to maximize limited resources in large-scale applied plant breeding research. Any implementation of HTP can be costly and time consuming. Because of this, when looking at implementing HTP into a breeding program, it is important to consider the versatility and range of the platform selected. The handheld radiometers used in this study can collect high resolution reflectance data across a broad spectral range with the potential for producing SRIs with moderate heritability and correlation to yield, yet are limited in their ability to account for soil noise or inconsistent solar radiation. The data capture speed limits the quality of data collection across locations and time. The lack of orthomosaic image capture in these systems also limits access to secondary traits of interest like plant height and canopy coverage estimates.

With the continual improvement in technology and software, the barrier to entry for UAS phenotyping continues to drop. The speed and efficiency of UAS minimizes labor and cost while providing quality data for further use in breeding strategies. However, it is important to consider best practices that will minimize unwanted environmental variability in collected UAS data. One way that this can be done is by utilizing multiple radiometric calibration panels as outlined in 2020 and 2021 UAS data collection (Iqbal et al., 2018). Another practice that can minimize unwanted variability is in timing of UAS flights. Most sensors utilized on a UAS are passive sensors, therefore, it is important to adjust for shadowing and variability of solar radiation. For best results it is recommended to fly within a 4-5 hour window of solar noon on days without clouds (Ortiz et al., 2021). In plant breeding programs looking to incorporate high throughput phenotyping, the UAS is an efficient and versatile option that when used properly can produce high quality data.

Overall, it is important to know that not all HTP systems for data collection are created equal. Knowing what HTP traits are most important to the program, frequency and scale of data collection, and resources allocation will help determine which platform will be most beneficial in HTP data collection. When implemented properly, UAS are the more promising system for SRI collection in large-scale breeding programs.

Tables and Figures

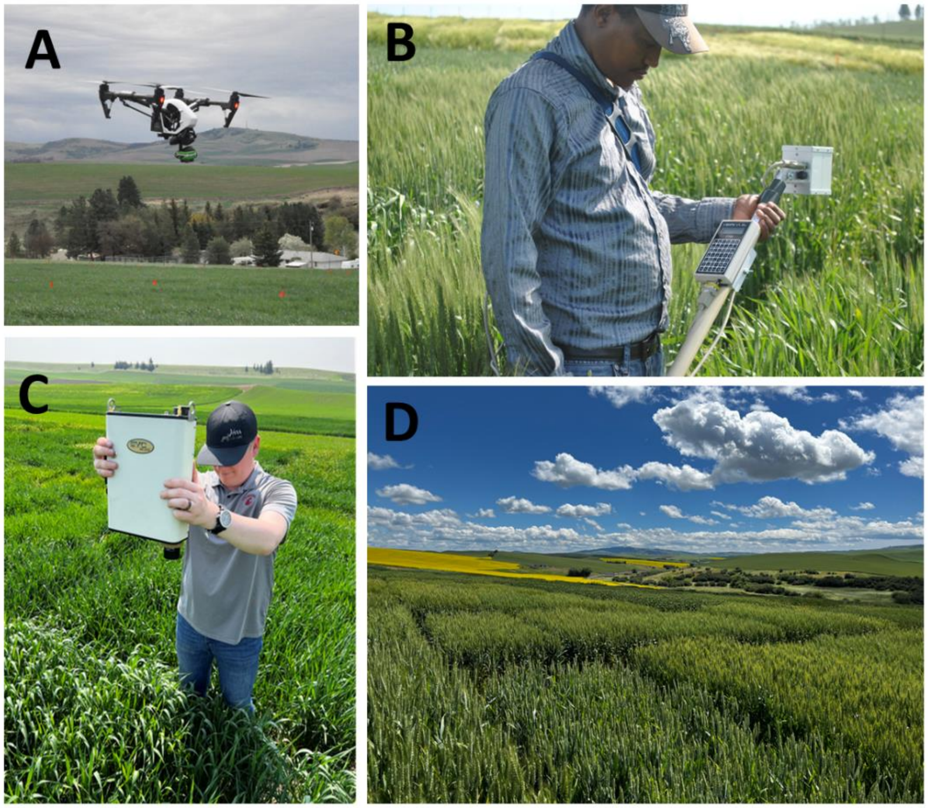

Figure 1. The imaging systems used in this study were (A) a DJI Inspire 1 UAS with a Sentera Quad Multispectral Sensor, (B) Cropscan MSR16R, and (C) SVC HR-1024i. (D) highlights the study location.

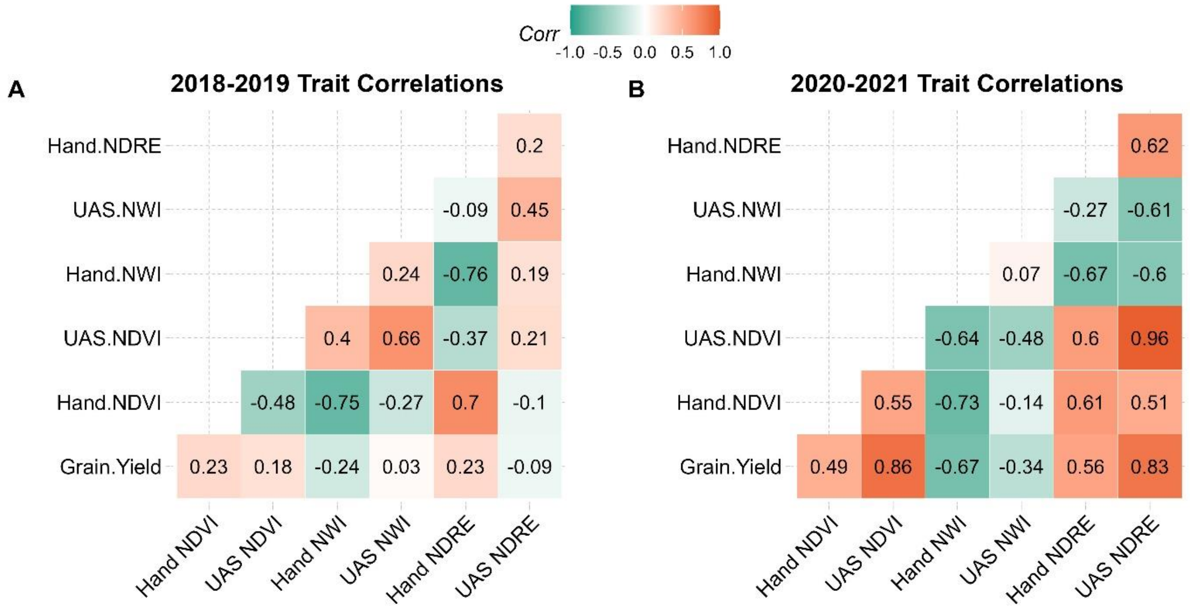

Figure 2. Correlation table of grain yield, handheld collected SRIs, and UAS collected SRIs in (A) 2018-2019 population and (B) 2020-2021 population. NDVI – Normalized Difference Vegetation Index; NDRE – Normalized Difference Red Edge; NWI – Normalized Water Index.

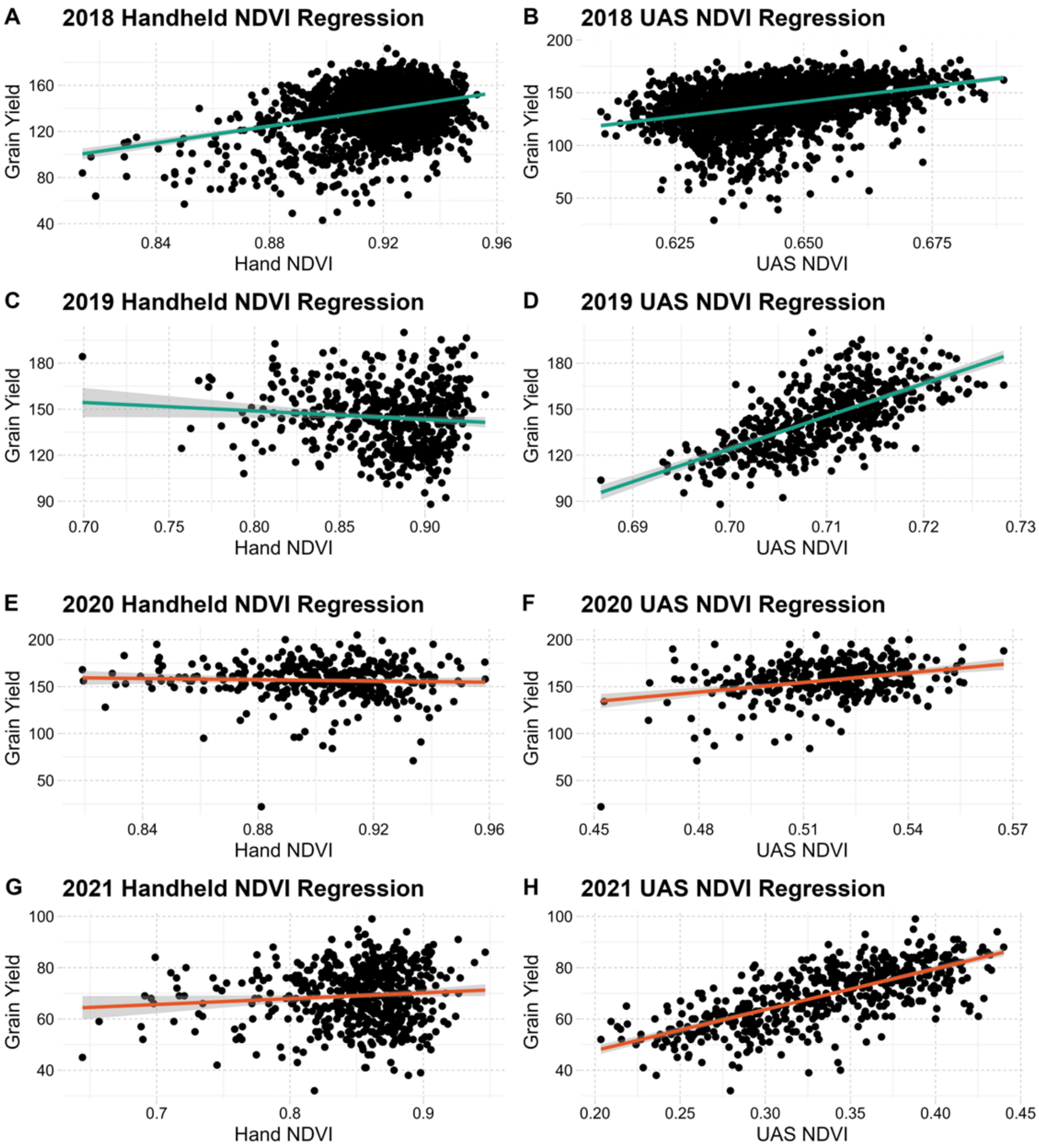

Figure 3. Linear regression of grain yield and handheld NDVI (A, C, E, G) or UAS NDVI (B, D, F, H) in each year evaluated. NDVI – Normalized Difference Vegetation Index.

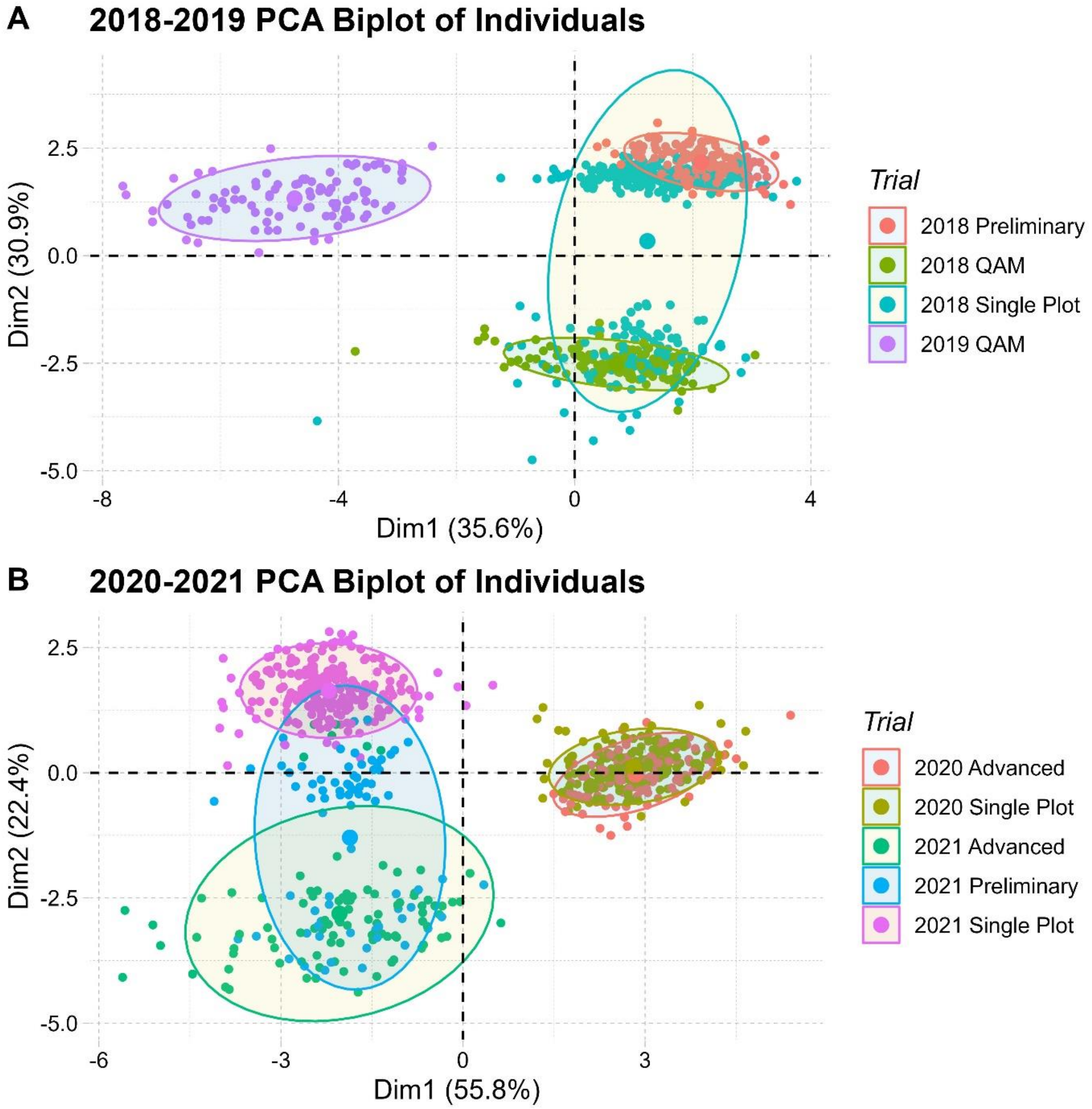

A 2018-2019 PCA Biplot of Individuals

B 2020-2021 PCA Biplot of Individuals

Figure 4. Principal component biplot of individuals and vector of variables in (A) 2018-2019 population and (B) 2020-2021 population showing the genetic relationships of QAM diversity panel, early generation single plot, preliminary, and advanced trials.

Table 1. Study populations for HTP platform comparison.

Trial	Year	Design	Replication	Number of Entries	Total Observations	UAS	Cropscan	SVC
Single Plot	2018	Augmented Design with repeating checks	1	1438	1503	X	X	
Preliminary	2018	Alpha-Lattice	3	168	504	X	X	
QAM	2018	Augmented Design with repeating checks	1	480	528	X	X	
QAM	2019	Augmented Design with repeating checks	1	480	528	X	X	
Single Plot	2020	Augmented Design with repeating checks	1	178	195	X		X
Advanced	2020	Alpha-Lattice	3	48	144	X		X
Single Plot	2021	Augmented Design with repeating checks	1	213	227	X		X
Preliminary	2021	Alpha-Lattice	3	54	162	X		X
Advanced	2021	Alpha-Lattice	3	46	138	X		X

QAM: Quality Association Mapping Panel; X: Indicates HTP Data Type Collected

1

Table 2. Spectral reflectance index equations.

Spectral Reflectance Index	Abbreviation	Equation	Reference
Normalized Difference Vegetation Index	NDVI	$(R800 - R680)/(R800 + R680)$	(Rouse Jr, 1974)
Normalized Difference Red Edge	NDRE	$(R800 - R700)/(R800 + R700)$	(Gitelson and Merzlyak, 1996)
Transformed Chlorophyll Absorption Reflectance Index	TCARI	$3 \times [(R700 - 680) - 0.2 \times (R700 - R550)(R700/R680)]$	(Haboudane et al., 2002)
Normalized Water Index	NWI	$(R970 - R800)/(R970 + R800)$	(Gao, 1996)
Modified Triangular Vegetation Index	MTVI	$((R700 - R550))/\surd((2 * R800 + 1)^{2} - (6 * R800 - 5 * \surd R680) - 0.5))$	(Haboudane et al., 2004)

Table 3. Broad-sense heritability (H^2) of grain yield, UAS indices, and handheld indices.

Population	Grain Yield	Handheld NDVI	UAS NDVI	Handheld NWI	UAS NWI	Handheld NDRE	UAS NDRE
2018-2019	0.65	0.52	0.80	0.50	0.58	0.50	0.60
2020-2021	0.76	0.55	0.68	0.62	0.70	0.58	0.67

Conflict of Interest

The authors declare that the research was conducted in the absence of any commercial or financial relationships that could be construed as a potential conflict of interest.

Author Contributions

The project conceptualization and development of methodology was done by AWH & AHC.The formal investigation, analysis, visualization, original draft preparation, and data curation was conducted by AWH. The resources, review and editing, funding acquisition, and supervision was done by AHC. All authors have read and agreed to the published version of the manuscript.

Funding

Research was partially supported by the Agriculture and Food Research Initiative Competitive Grant awards 2022-67013-36426 and 2022-68013-36439 (WheatCAP) from the National Institute of Food and Agriculture, Hatch project 1014919, and the O.A. Vogel Research Endowment at Washington State University.

Acknowledgments

The authors would like to thank Dr. Sinduja Sankaran for use of the SVC equipment, and for many years of collaboration in helping establish an HTP system within the breeding program.

Data Availability Statement

The datasets generated for this study can be found in the Washington State University Research Exchange https://doi.org/10.7273/000004802.

References

Araus, J. L., and Cairns, J. E. (2014). Field high-throughput phenotyping: the new crop breeding frontier. *Trends in Plant Science* 19, 52–61. doi: 10.1016/j.tplants.2013.09.008.

Araus, J. L., Kefauver, S. C., Zaman-Allah, M., Olsen, M. S., and Cairns, J. E. (2018). Translating High-Throughput Phenotyping into Genetic Gain. *Trends in Plant Science* 23, 451–466. doi: 10.1016/j.tplants.2018.02.001.

Babar, M., Reynolds, M., Van Ginkel, M., Klatt, A., Raun, W., and Stone, M. (2006). Spectral reflectance to estimate genetic variation for in-season biomass, leaf chlorophyll, and canopy temperature in wheat. *Crop science* 46, 1046–1057.

Bal, S. K., Wakchaure, G., Potekar, S., Choudhury, B. U., Choudhary, R. L., and Sahoo, R. N. (2021). Spectral signature-based water stress characterization and prediction of wheat yield under varied irrigation and plant bio-regulator management practices. *Journal of the Indian Society of Remote Sensing* 49, 1427–1438.

Bandyopadhyay, K., Pradhan, S., Sahoo, R., Singh, R., Gupta, V., Joshi, D., et al. (2014). Characterization of water stress and prediction of yield of wheat using spectral indices under varied water and nitrogen management practices. *Agricultural Water Management* 146, 115–123.

Bernardo, R. (2002). *Breeding for quantitative traits in plants*. Stemma press Woodbury, MN.

Bowman, B. C., Chen, J., Zhang, J., Wheeler, J., Wang, Y., Zhao, W., et al. (2015). Evaluating Grain Yield in Spring Wheat with Canopy Spectral Reflectance. *Crop Science* 55, 1881–1890. doi: https://doi.org/10.2135/cropsci2014.08.0533.

Brown, M., Antle, J., Backlund, P., Carr, E., Easterling, B., Walsh, M., et al. (2015). Climate change, global food security and the US food system.

Carver, B. F. (2009). *Wheat: Science and Trade*. John Wiley & Sons.

Deng, L., Mao, Z., Li, X., Hu, Z., Duan, F., and Yan, Y. (2018). UAV-based multispectral remote sensing for precision agriculture: A comparison between different cameras. *ISPRS journal of photogrammetry and remote sensing* 146, 124–136.

Díaz-Delgado, R., Ónodi, G., Kröel-Dulay, G., and Kertész, M. (2019). Enhancement of ecological field experimental research by means of UAV multispectral sensing. *Drones* 3, 7.

Duan, T., Chapman, S. C., Guo, Y., and Zheng, B. (2017). Dynamic monitoring of NDVI in wheat agronomy and breeding trials using an unmanned aerial vehicle. *Field Crops Research* 210, 71–80. doi: 10.1016/j.fcr.2017.05.025.

Gao, B.-C. (1996). NDWI—A normalized difference water index for remote sensing of vegetation liquid water from space. *Remote sensing of environment* 58, 257–266.

Geipel, J., Link, J., and Claupein, W. (2014). Combined Spectral and Spatial Modeling of Corn Yield Based on Aerial Images and Crop Surface Models Acquired with an Unmanned Aircraft System. *Remote Sensing* 6, 10335–10355. doi: 10.3390/rs61110335.

Gitelson, A. A., and Merzlyak, M. N. (1996). Signature Analysis of Leaf Reflectance Spectra: Algorithm Development for Remote Sensing of Chlorophyll. *Journal of Plant Physiology* 148, 494–500. doi: 10.1016/S0176-1617(96)80284-7.

Gracia-Romero, A., Kefauver, S. C., Vergara-Díaz, O., Zaman-Allah, M. A., Prasanna, B. M., Cairns, J. E., et al. (2017). Comparative Performance of Ground vs. Aerially Assessed RGB and Multispectral Indices for Early-Growth Evaluation of Maize Performance under Phosphorus Fertilization. *Front. Plant Sci.* 8. doi: 10.3389/fpls.2017.02004.

Guo, A., Huang, W., Dong, Y., Ye, H., Ma, H., Liu, B., et al. (2021). Wheat yellow rust detection using UAV-based hyperspectral technology. *Remote Sensing* 13, 123.

Guo, J., Wang, Q., Tong, Y., Fei, D., and Liu, J. (2016). Effect of solar radiation intensity and observation angle on canopy reflectance hyperspectra for winter wheat. *Transactions of the Chinese Society of Agricultural Engineering* 32, 157–163.

Gutierrez, M., Reynolds, M. P., and Klatt, A. R. (2010). Association of water spectral indices with plant and soil water relations in contrasting wheat genotypes. *J Exp Bot* 61, 3291–3303. doi: 10.1093/jxb/erq156.

Haboudane, D., Miller, J. R., Pattey, E., Zarco-Tejada, P. J., and Strachan, I. B. (2004). Hyperspectral vegetation indices and novel algorithms for predicting green LAI of crop canopies: Modeling and validation in the context of precision agriculture. *Remote Sensing of Environment* 90, 337–352. doi: 10.1016/j.rse.2003.12.013.

Haboudane, D., Miller, J. R., Tremblay, N., Zarco-Tejada, P. J., and Dextraze, L. (2002). Integrated narrow-band vegetation indices for prediction of crop chlorophyll content for application to precision agriculture. *Remote Sensing of Environment* 81, 416–426. doi: 10.1016/S0034-4257(02)00018-4.

Hassan, M. A., Yang, M., Rasheed, A., Jin, X., Xia, X., Xiao, Y., et al. (2018). Time-Series Multispectral Indices from Unmanned Aerial Vehicle Imagery Reveal Senescence Rate in Bread Wheat. *Remote Sensing* 10, 809. doi: 10.3390/rs10060809.

Herr, A. W., Adak, A., Carroll, M. E., Elango, D., Kar, S., Li, C., et al. (2023). Unoccupied aerial systems imagery for phenotyping in cotton, maize, soybean, and wheat breeding. *Crop Science.*

Iqbal, F., Lucieer, A., and Barry, K. (2018). Simplified radiometric calibration for UAS-mounted multispectral sensor. *European Journal of Remote Sensing* 51, 301–313. doi: 10.1080/22797254.2018.1432293.

Jang, G., Kim, J., Yu, J.-K., Kim, H.-J., Kim, Y., Kim, D.-W., et al. (2020). Review: Cost-Effective Unmanned Aerial Vehicle (UAV) Platform for Field Plant Breeding Application. *Remote Sensing* 12, 998. doi: 10.3390/rs12060998.

Lozada, D. N., Godoy, J. V., Ward, B. P., and Carter, A. H. (2020). Genomic Prediction and Indirect Selection for Grain Yield in US Pacific Northwest Winter Wheat Using Spectral Reflectance Indices from High-Throughput Phenotyping. *International Journal of Molecular Sciences* 21, 165. doi: 10.3390/ijms21010165.

Mir, R. R., Reynolds, M., Pinto, F., Khan, M. A., and Bhat, M. A. (2019). High-throughput phenotyping for crop improvement in the genomics era. *Plant Science* 282, 60–72. doi: 10.1016/j.plantsci.2019.01.007.

Montesinos López, O. A., Montesinos López, A., and Crossa, J. (2022). *Multivariate Statistical Machine Learning Methods for Genomic Prediction*. Cham: Springer International Publishing doi: 10.1007/978-3-030-89010-0.

Myneni, R. B., Hall, F. G., Sellers, P. J., and Marshak, A. L. (1995). The interpretation of spectral vegetation indexes. *IEEE Transactions on Geoscience and Remote Sensing* 33, 481–486. doi: 10.1109/TGRS.1995.8746029.

Ortiz, M. V., Sangjan, W., Selvaraj, M. G., McGee, R. J., and Sankaran, S. (2021). Effect of the Solar Zenith Angles at Different Latitudes on Estimated Crop Vegetation Indices. *Drones* 5, 80.

Pauli, D., Chapman, S. C., Bart, R., Topp, C. N., Lawrence-Dill, C. J., Poland, J., et al. (2016). The Quest for Understanding Phenotypic Variation via Integrated Approaches in the Field Environment. *Plant Physiology* 172, 622–634. doi: 10.1104/pp.16.00592.

Prasad, B., Carver, B. F., Stone, M. L., Babar, M. A., Raun, W. R., and Klatt, A. R. (2007). Potential Use of Spectral Reflectance Indices as a Selection Tool for Grain Yield in Winter Wheat under Great Plains Conditions. *Crop Science* 47, 1426–1440. doi: https://doi.org/10.2135/cropsci2006.07.0492.

Ray, D. K., Mueller, N. D., West, P. C., and Foley, J. A. (2013). Yield Trends Are Insufficient to Double Global Crop Production by 2050. *PLoS ONE* 8, e66428. doi: 10.1371/journal.pone.0066428.

Reynolds, M., Chapman, S., Crespo-Herrera, L., Molero, G., Mondal, S., Pequeno, D. N. L., et al. (2020). Breeder friendly phenotyping. *Plant Science* 295, 110396. doi: 10.1016/j.plantsci.2019.110396.

Reynolds, M., Foulkes, J., Furbank, R., Griffiths, S., King, J., Murchie, E., et al. (2012). Achieving yield gains in wheat. *Plant, cell & environment* 35, 1799–1823.

Rouse Jr, J. (1974). Monitoring the vernal advancement and retrogradation (green wave effect) of natural vegetation.

Sankaran, S., Khot, L. R., and Carter, A. H. (2015a). Field-based crop phenotyping: Multispectral aerial imaging for evaluation of winter wheat emergence and spring stand. *Computers and Electronics in Agriculture* 118, 372–379. doi: 10.1016/j.compag.2015.09.001.

Sankaran, S., Khot, L. R., Espinoza, C. Z., Jarolmasjed, S., Sathuvalli, V. R., Vandemark, G. J., et al. (2015b). Low-altitude, high-resolution aerial imaging systems for row and field crop phenotyping: A review. *European Journal of Agronomy* 70, 112–123. doi: 10.1016/j.eja.2015.07.004.

Sapkota, B. R., Adams, C. B., Kelly, B., Rajan, N., and Ale, S. (2023). Plant population density in cotton: Addressing knowledge gaps in stand uniformity and lint quality under dryland and irrigated conditions. *Field Crops Research* 290, 108762.

Sarkar, S., Oakes, J., Cazenave, A.-B., Burow, M. D., Bennett, R. S., Chamberlin, K. D., et al. (2022). Evaluation of the US peanut germplasm mini-core collection in the Virginia-Carolina region using traditional and new high-throughput methods. *Agronomy* 12, 1945.

Song, P., Wang, J., Guo, X., Yang, W., and Zhao, C. (2021). High-throughput phenotyping: Breaking through the bottleneck in future crop breeding. *The Crop Journal* 9, 633–645.

Taiz, L., Zeiger, E., Møller, I. M., and Murphy, A. (2015). *Plant physiology and development*. Sinauer Associates.

Tattaris, M., Reynolds, M. P., and Chapman, S. C. (2016). A Direct Comparison of Remote Sensing Approaches for High-Throughput Phenotyping in Plant Breeding. *Frontiers in Plant Science* 7, 1131. doi: 10.3389/fpls.2016.01131.

Visitacion, G. J., Saludes, R. B., Luyun Jr, R. A., Pinca, Y. M. M., and Eusebio, M. F. V. (2022). Statistical Analysis of Crop Water Stress in Rainfed Rice (Oryza sativa L.) Using Spectral and Non-spectral Indices. *Philippine Journal of Science* 15.

Wang, C., and Myint, S. W. (2015). A simplified empirical line method of radiometric calibration for small unmanned aircraft systems-based remote sensing. *IEEE Journal of selected topics in applied earth observations and remote sensing* 8, 1876–1885.

Wientjes, E., Philippi, J., Borst, J. W., and van Amerongen, H. (2017). Imaging the Photosystem I/Photosystem II chlorophyll ratio inside the leaf. *Biochimica et Biophysica Acta (BBA) - Bioenergetics* 1858, 259–265. doi: 10.1016/j.bbabio.2017.01.008.

Xie, C., and Yang, C. (2020). A review on plant high-throughput phenotyping traits using UAV-based sensors. *Computers and Electronics in Agriculture* 178, 105731.

Xiong, W., Reynolds, M., and Xu, Y. (2022). Climate change challenges plant breeding. *Current Opinion in Plant Biology* 70, 102308.

Xue, J., and Su, B. (2017). Significant remote sensing vegetation indices: A review of developments and applications. *Journal of sensors* 2017.

Yin, C., Lv, X., Zhang, L., Ma, L., Wang, H., Zhang, L., et al. (2022). Hyperspectral UAV Images at Different Altitudes for Monitoring the Leaf Nitrogen Content in Cotton Crops. *Remote Sensing* 14, 2576.

CHAPTER THREE: LARGE-SCALE BREEDING APPLICATIONS OF UAS ENABLED GENOMIC PREDICTION

Andrew W. Herr[1] Peter Schmuker[1], and Arron H. Carter [1]

[1]Department of Crop and Soil Sciences, Washington State University, Pullman, Washington, USA

(Accepted in The Plant Phenome Journal)

Citation

Herr, A.W.; Schmuker, P; & Carter, A.H. (2023). Large-scale breeding applications of UAS enabled genomic prediction. The Plant Phenome Journal

Attributions

The author contributions for CHAPTER THREE: LARGE-SCALE BREEDING APPLICATIONS OF UAS ENABLED GENOMIC PREDICTION for the first author Andrew W. Herr include the conceptualization, data collection, analysis, original draft preparation, review, and editing. The contributions of second author Peter Schmuker include conceptualization, review, and editing. The contributions of co-author Arron H. Carter include conceptualization, review, editing, and funding acquisition. All authors contributed to the article and approved the published version.

Abstract

Breeding for improved, reliable cultivars despite growing environment irregularity can be challenging. Unoccupied aircraft systems (UAS) are a popular high-throughput phenotyping technology that has been shown to help interpret the mechanisms associated with crop productivity and environmental response, creating potential for improved breeding strategies. Spectral reflectance indices (SRI), encompassing both vegetation and water indices like Normalized Difference Vegetation Index (NDVI), Normalized Difference Red-Edge Index (NDRE), and Normalized Water Index (NWI), were employed to assess 4,094 winter wheat genotypes across 11,593 breeding plots at Washington State University from 2019 through 2022. SRIs were then used with genomic data in univariate models as covariates and multivariate models as secondary response variables for predictions of grain yield. The prediction accuracy of models was evaluated on a leave-one-year-out validation strategy against a base genomic prediction method. Including SRI data as fixed effects in univariate genomic prediction models can improve prediction accuracy over the control but is unreliable across years. When used in multivariate models, SRIs improve prediction performance across years but requires high-performance computational resources that could limit feasibility. In univariate models, when test year NDVI data was available and used to calculate breeding values, prediction performance was at least 16% better than the control, ranging in prediction accuracy from 0.54 in 2019 to 0.93 in 2020. This study highlights the limited reliability of SRI use in genomic prediction of untested environments and locations. However, a significant application for the technology can be found in early season UAS data collection to aid accurate predictions in late season, a helpful tool in tight turnaround times commonly experienced in winter crop breeding programs.

Introduction

In an age of growing demand, unreliable growing conditions, and scarce resources, it is important for plant breeders, through the cultivar development process, to increase and maintain genetic gain to release high-quality, efficient, and reliable crops that can meet market demands. Plant breeders select for and improve upon many traits throughout the cultivar development process, improving the genetics available to producers and directly impacting the overall quality and quantity of the final product. Of the traits of interest, the most challenging and resource-intensive are highly quantitative, like grain yield. These traits' moderate to low heritability introduce the need for replicated phenotypic observations across many growing environments to capture reliable rates of increases in genetic gain over time (Bernardo, 2002). Dealing with environmental variability is a significant factor in a breeder successfully selecting for and improving quantitative traits. Extreme environmental variability introduced by severe weather and climate change can impact global food production and limit a breeder's ability to increase genetic gain (Brown et al., 2015; Xiong et al., 2022). It is relevant to look at new strategies that can increase decrease cycle time and improve grain yield despite growing challenges resulting from climate change and extreme environmental variability (Xiong et al., 2022).

Genomic technologies have provided breeders with large amounts of data to utilize genomic and marker-assisted selections in breeding strategy. Genomic selection (GS) has been shown to increase the genetic gain in traits of interest and enhance overall selection efficiency (Rutkoski et al., 2015; Michel et al., 2017). However, genomic data in and of itself has limited utility in robust prediction without the backing of phenotypic observation, creating a constraint in selection efficiency and restricting overall cultivar development (Mir et al., 2019). Additionally, when working with quantitative traits like grain yield, utilization of GS is limited due to unreliable prediction accuracy when predicting untested environments and genotypes (Crossa et al., 2017). Traditionally, when present in training populations, significant environmental variability reduces the ability of a model to predict for target environments (Hu et al., 2019).

A likely path for improving GS strategies, especially in historically challenging untested environments and years, is complementing genomic with high throughput phenotyping (HTP) data in GS (Rutkoski et al., 2016; Crain et al., 2018; Sun et al., 2019; Lozada et al., 2020; Montesinos-López et al., 2023). Rutkoski et al. (2016) highlight this potential well by using SRI-enabled multivariate genomic prediction to increase prediction performance across a diversity of environments. Sun et al. (2019) and Crain et al. (2018) reiterates the finding of Rutkoski et al. (2016), highlighting the stable prediction performance of SRI enabled GS within the same environment and cycle, but both studies also make a note of the struggle and inconsistency of prediction in untested environments and cycle. An unanswered question in the above studies that limits the ability to assess real world application is the lack of prediction for untested environments, breeding cycles, and genotypes. Lozada et al. (2020) utilized a breeding diversity panel in SRI aided GS to successfully predict untested early generation breeding lines in known environments. Montesinos-López et al. (2023) expanded upon this work by evaluating model prediction performance for partially untested genotypes and untested environments within a single breeding cycle, finding success and showing SRIs ability to aid in prediction performance when both genotype and environment are untested. Despite these findings, validation is needed to identify the reliability of SRI enabled GS to work well on a larger population predicting for partially untested genotypes and across diverse, untested years and environments.

While using a large hyperspectral range has shown promise for the prediction of grain yield (Montesinos-López et al., 2017), this strategy can require extensive data management and expensive sensors for capture. Luckly, plant canopy architecture produces most of its variation of reflectance in a few wavelengths associated with key physiological components (Xue and Su, 2017). UAS mounted multispectral sensors that target and collect these key wavelengths can be combined to calculate spectral reflectance indices (SRI), creating valuable traits that can aid in the selection of grain yield while minimizing sensor expense and reducing computational requirements. SRIs provide a standardized trait value that targets critical physiological characteristics in the plant canopy (Myneni et al., 1995; Xue and Su, 2017).

This study will use two types of SRIs: vegetation and water indices. Vegetation indices are developed by evaluating the reflectance value of the plant canopy at specific light bands associated with photosynthetic capacity. Of these, Normalized Difference Vegetation Index (NDVI) is a popular index in staple crops due to its strong relationship with grain yield performance and evaluation of overall plant stress (Babar et al., 2007; Lozada et al., 2020; Herr et al., 2023). NDVI evaluates the contrast in the maximum absorption of red relative to the maximum reflectance of near-infrared (NIR; Rouse et al., 1974). Another popular vegetation index used in wheat research is Normalized Difference Red-Edge Index (NDRE). The NDRE formula is similar to NDVI, but instead of focusing on red absorption, it evaluates red-edge absorption relative to NIR (Gitelson and Merzlyak, 1996). Unlike vegetation indices, water indices like Normalized Water Index (NWI) consider the contrast of reflectance within the NIR range (800 – 2500nm; Babar et al., 2006). SRIs vary in their ability to capture new information relative to the target trait of interest; crop, maturity, and target trait play a role in index success (Wientjes et al., 2017; Lozada et al., 2020; Herr et al., 2023). While limited in direct trait capture, SRIs are well established at estimating routine traits of interest like plot quality as well as both biotic and abiotic stresses (Sankaran et al., 2015; Guo et al., 2021; Sarkar et al., 2022; Sapkota et al., 2023). Additionally, SRIs are effective in their ability to quantify previously infeasible traits like chlorophyll content, nitrogen content, relative water content, leaf osmotic potential, stomatal conductance, and canopy temperature (Babar et al., 2006; Gutierrez et al., 2010; Xie and Yang, 2020; Bal et al., 2021; Visitacion et al., 2022; Yin et al., 2022). SRIs are an intriguing option when looking to improve GS. The relative ease of data collection and ability to capture previously infeasible aspects of genetic variability and photosynthetic performance across growing environments creates the potential for added value in prediction ability (Crain et al., 2018; Montesinos-López et al., 2023).

For most commodity crops like wheat, grain yield is the primary trait of interest for producers and, consequently, for breeders. The highly quantitative nature of wheat grain yield makes selection efficiency for the trait difficult (Reynolds et al., 2012). It has been established that UAS-derived SRIs correlate well with grain yield (Geipel et al., 2014; Gracia-Romero et al., 2017; Lozada et al., 2020; Herr and Carter, 2023). This makes grain yield an appealing trait for a breeder to focus on when implementing HTP into their breeding strategy (Reynolds et al., 2020; Montesinos López et al., 2022; Herr et al., 2023).

As mentioned above, genomic and SRI data have shown a lot of promise for improving GS strategies; however, how these two distinct data types are combined has been split between a few methods. For example, Montesinos-López et al. (2023) showed that when predicting within year with a seven-fold cross-validation strategy, UAS data, when used in multivariate and multi-kernel gBLUP models, improved prediction performance across test locations. Additionally, Sun et al. (2019) has shown that incorporating UAS data in a multivariate strategy can improve GS performance for grain yield across various growing conditions and breeding cycles. HTP traits have also been shown to benefit GS through use as fixed effects. Crain et al. (2018) and Sandhu et al. (2021) highlight the potential utility of HTP traits as fixed effects. These studies indicate that how a trait is utilized in a model plays a factor in how the data is interpreted and impacts prediction performance. In Crain et al. (2018), while SRIs aid in prediction as both covariates and secondary response variables, the environments in which each of these GS models preform best differs. Unlike genomic data which is consistent, SRIs are dynamic and vary among genotype and across environments.

This study aims to identify the ability of different UAS-derived SRIs to improve GS performance as covariates in a univariate model or secondary response variables in a multivariate model across years and locations with a large-scale breeding program. We believe this will provide insight into the general utility of combining genomic and UAS data as an applied breeding strategy and highlight potential methods for implementation, especially when dealing with extreme environmental variability.

Material and Methods

Study Population

This study uses the Washington State University soft white winter wheat (Triticum aestivum L.) breeding trials from 2019 to 2022. The population has a unique combination of within-year and across-year environmental variability. Data was collected on 11,593 plots of 4,094 genotypes across 60 individual trial experiments (trial/location/year). **Supplementary Table 1** details the study population characteristics, including location, year, trial design, total number of unique entries, and number of total plot observations. Across four years, varieties were evaluated across nine locations, ranging in average annual precipitation from 257 mm (Lind, WA) to 518 mm (Pullman, WA). Within this dataset, we see extreme variability across years. In Pullman, for example, there is a range in annual precipitation during the critical growing season (May-July) from 20 mm in 2021 to 155 mm in 2022.

Trial locations are divided into two general agronomic production regions for winter wheat in Washington State, a low rainfall deep furrow region (average annual precipitation of 125-400 mm) consisting of trials in the towns of Davenport, Lind, Ritzville, Harrington, and Kahlotus as well as a higher rainfall region (average annual precipitation of 400-660 mm) consisting of trials in the towns of Pullman, Walla Walla, Farmington, and Prescott. Plot trials from every phase of the breeding process were observed and utilized in this study. Single plot trials were unreplicated augmented trials of first plot observations of F5 and double haploid lines, typically one or two trials in each production region per year. Preliminary trials were alpha lattice trials of lines advanced from single plot trials and planted at one to two locations per production region per year. The Advance Soft White Yield 1 (AWY1) trial is an alpha lattice trial for the advanced testing of varieties in the lower rainfall region, whereas AWY2 is an advanced soft white yield trial targeted for the higher rainfall region. Advanced trials were observed from two to six locations for their respective product regions. Plots in the lower rainfall region were planted using a 4-row deep furrow planter at a seed density of 190 seeds per square meter, whereas the higher rainfall locations were planted using a double-disc 8-row small plot planter at a seed density of 220 seeds per square meter. The total plot size for all locations was 1.5 meters wide by 3.5 meters long.

Phenotypic Data Collection

All UAS phenotypic data was collected using a modified Sentera Quad Multispectral Sensor (Sentera, St Paul, MN) consisting of four sensors covering eight target bands (450nm – 970nm) used to calculate SRIs outlined in **Table 1**. UAS data was collected at anthesis, an established stage of maturity critical in the relationship between reflectance and grain yield (Duan et al., 2017; Lozada et al., 2020). Additionally, to minimize noise and maintain high data quality, UAS data was collected within a five-hour window of solar noon and only on days with clear skies, limiting solar radiation variability. During flights, the UAS flew a programmed route at an average altitude of 45 m, with an 85% bidirectional overlap of georeferenced images. Grain yield data were collected at all locations with a Zurn 150 harvester (Zurn Harvesting GmbH & Co. KG, Waldenburg, Germany).

Phenotypic Data Processing and Analysis

Collected UAS images from each flight were stitched and prepped for data extraction in Pix4Dmapper (Pix4D Inc., Denver, CO), creating a single orthomosaic reflectance image for each sensor per location/flight. Geographic Information System (QGIS) was then used to identify individual plots, georeference, and crop orthomosaic images for each trial. R Code utilizing 'FIELDimageR' (Matias et al., 2020) and 'raster' (Hijmans et al., 2015) was then used for calibration, index calculation, and single plot mean data extraction. In 2019, a single reflectance target (85% reflectance) was used for radiometric calibration on RBG and red edge bands. Quantum efficiency coefficients were used to calculate NIR using:

$$800nm = (2.921 \times 450nm) - (0.754 \times 680nm). \tag{1}$$

A coefficient of 3.07 was used in the normalization of NIR during the calculation of SRIs (Ortiz et al., 2021). For 2020 through 2022, a set of target panels was used (five panels ranging from 2%–85% reflectance, MosaicMill Oy, Vantaa, Finland) to standardize all flights and collected images. Using these panels, all eight raw band layers were adjusted based on the relationship:

$$SR = CRx \pm b \tag{2}$$

where the slope (*x*) and intercept (*b*) are based on the regression of the observed reflectance in target panels, collected reflectance (*CR*) is the raw observed pixel values, and surface reflectance (*SR*) is the true reflectance value (Iqbal et al., 2018). All datasets used adjusted multispectral band values to calculate indices. **Table 1** outlines the SRIs used in this study, including their abbreviation, equation, and reference. These indices were chosen based on past research that utilized similar genetic material and growing conditions as this study (Gizaw et al., 2016a; b; Lozada et al., 2020).

Table 1: Spectral Reflectance Index Equations

Spectral Reflectance Index	**Abbr.**	**Equation**	**Reference**
Normalized Difference Vegetation Index	NDVI	$\frac{800nm - 680nm}{800nm + 680nm}$	(Rouse et al., 1974)
Normalized Difference Red Edge 1	NDRE1	$\frac{800nm - 710nm}{800nm + 710nm}$	(Gitelson and Merzlyak, 1996)
Normalized Difference Red Edge 2	NDRE2	$\frac{800nm - 745nm}{800nm + 745nm}$	(Gitelson and Merzlyak, 1996)
Normalized Water Index 1	NWI1	$\frac{970nm - 800nm}{970nm + 800nm}$	(Gao, 1996)
Normalized Water Index 2	NWI2	$\frac{970nm - 900nm}{970nm + 900nm}$	(Gao, 1996)
Modified Triangular Vegetation Index	MTVI	$\frac{1.8(800nm - 550nm) - 3.75(680nm - 550nm)}{\sqrt{(2 * 800nm + 1)^2 - (6 * 800nm - 5\sqrt{680nm} - 0.5}}$	(Haboudane et al., 2004)

Heritability of grain yield and SRIs were calculated across years using the mixed linear model:

$$Y_{ijkl} = \mu + Block_i + Check_j + Gen_{k(j)} + Env_l + Block_i \times Env_l + Check_j \times Env_l + Gen_{k(j)} \times Env_l + \varepsilon_{ijkl} \quad (3)$$

that Y_{ijkl} are the designated traits of interest (i.e SRIs or grain yield) of the *i*th block and *j*th check of genotype *k* in environment *l*; μ is the mean effect; $Block_i$ is the random effect of the *i*th

block; $Check_j$ is the fixed effect of the *j*th replicated cultivar check; $Gen_{k(j)}$ is the random effect of genotype *k* in the *j*th check; Env_l is the random effect of the *l*th environment; × indicates random effect from interactions of variables, and ε_{ijk} are the residual errors. Variance components generated across years from model (3) were then used to calculate broad-sense heritability on a genotype-difference basis using the method:

$$H^2_{Cullis} = 1 - \frac{\bar{v}^{BLUP}_{\Delta}}{2\sigma^2_g} \tag{4}$$

where $2\sigma^2_g$ is the genotype variance and $\bar{v}^{BLUP}_{\Delta}$ is the mean-variance of the best linear unbiased predictors (BLUP; Cullis et al., 2006). In addition to broad sense heritability, Pearson correlations across the population were generated among grain yield and SRIs, using unadjusted plot values.

In comparing SRIs, a random forest model was used to evaluate SRI relative importance to grain yield. A random forest model was chosen because of its popularity as a machine learning algorithm that is both flexible in the datasets it can handle and ease of use in dealing with classification problems (Touw et al., 2013). The random forest model treated all unadjusted SRIs as predictors for unadjusted grain yield observations. From the original data, 1,000 bootstrap samples were drawn. An unpruned classification tree was generated from each of these bootstrap samples. However, instead of choosing the best split from all predictors, the best split is chosen by bagging a random subset of four of six predictors. A majority vote of the 1,000 trees based on the predictor performance in splits determines predictions and predictor variable importance to the trait of interest, in this case, grain yield. A random forest classification model produces two measures of variable merit for the primary trait of interest, node purity and mean square error (MSE). Node purity is a measure of the Gini Index and indicates the likelihood of a node split of the variable leading to misclassification averaged over all model trees (Witten and James, 2013). The percent decrease in MSE is based on the mean decrease in prediction accuracy when the given variable is excluded on out-of-bag samples. The R package 'randomForest' (Liaw and Wiener, 2002) was used in the analysis.

Genotypic Data

All 4,094 lines used in this study were genotyped through the North Carolina State Genomics Sciences laboratory in Raleigh, NC, using genotyping-by-sequencing (Elshire et al., 2011) and the restriction enzymes MspI and PstI (Poland et al., 2012). Sequences were aligned to the Chinese Spring International Wheat Genome Sequencing Consortium RefSeq v1.0 (Appels et al., 2018) using the Burrows-Wheeler Aligner 0.7.17 (Li and Durbin, 2010). Genetic markers with more than 20% missing data, minor allele frequency of less than 5%, and monomorphic ones were removed. Markers were then imputed using Beagle version 5.0 (Browning et al., 2018). After imputation and filtering, 46,681 single-nucleotide polymorphism (SNP) markers remained.

Genomic Prediction and Analysis

All models evaluated in this study utilize a two-step method for prediction. Adjusted means for grain yield and SRI data were calculated for each field experiment in both augmented and Alpha-lattice individual trials using two-dimensional penalized splines through the R package 'SpATS' (Rodríguez-Álvarez et al., 2018) written out as:

$$Y_{ijk} = f(u_i, v_i) + Block_j + Gen_{k(i)} + \varepsilon_{ijk} \tag{5}$$

where Y_{ijk} is the adjusted mean phenotypic value of the trait of interest, u_i *and* v_i denote trial position (column and row), $Block_j$ is the fixed effect of the jth block, $Gen_{k(i)}$ is a fixed effect of genotype *k* in position *i*, and ε_{ijk} are the residual errors. The smooth bivariate function $f(u_i, v_i)$ is modeled by the tensor product of B-spline bases (Dierckx, 1995). For both augmented and alpha lattice trials, row and column were treated as random effects, while block was treated as a fixed effect. In the second step, a mixed linear model employing adjusted means, generated from equation 5, was used to calculate genomic estimated breeding values (GEBVs; Ward et al., 2019; Merrick and Carter, 2021). A kinship matrix was generated utilizing the VanRaden Method (VanRaden, 2008).

Two basic statistical model structures were used to compare genomic prediction performance with incorporated SRIs. A univariate gBLUP model with grain yield as a response (Control) was used as a baseline for model performance.

$$Y = \mu + Zu + \varepsilon \tag{6}$$

where Y is a vector of BLUPs of the target response variable, in this case, grain yield, from equation 5, μ is the overall mean, Z is the marker-based relationship matrix (n×n), u is an array (1×n) of random genetic effect, and ε is the residual error. Univariate gBLUP models were also developed that utilized grain yield as a response variable and combinations of SRIs as covariates. This can be written as a modified version of equation 6:

$$Y = \mu + X\beta + Zu + \varepsilon \tag{7}$$

where X is the design matrix of SRIs as fixed effects, and β is a vector of fixed effect coefficients with all other equation variables remaining the same as equation 6. Finally, multivariate gBLUP models incorporating grain yield and SRIs response variables are represented as:

$$\begin{bmatrix} Y_1 \\ \vdots \\ Y_n \end{bmatrix} = \begin{bmatrix} X_1 & 0 \\ \vdots & \vdots \\ 0 & X_n \end{bmatrix} \begin{bmatrix} \mu_1 \\ \vdots \\ \mu_n \end{bmatrix} + \begin{bmatrix} Z_1 & 0 \\ \vdots & \vdots \\ 0 & Z_n \end{bmatrix} \begin{bmatrix} \mu_1 \\ \vdots \\ \mu_n \end{bmatrix} + \begin{bmatrix} \varepsilon_1 \\ \vdots \\ \varepsilon_n \end{bmatrix} \tag{8}$$

where n is the number of response variables (grain yield and a combination of SRIs), Y_1 is the vector of BLUPs from equation 5, X is a design matrix of fixed effects simplified to a vector of 1 for each trait representing the mean because only the markers were used in this model. Z is the design matrix for random effects with $\mu_{1\ldots n}$ indicating the marker random effects and the standard error being designated as $\varepsilon_{1\ldots n}$. Multivariate models incorporated SRI variables in the same combinations as the univariate models. SRI combinations were selected based on the potential value in selection and computational resource efficiency. Both univariate and multivariate gBLUP models were done using the ‘sommer’ package in R (Covarrubias-Pazaran, 2016).

Multivariate analysis based on equation (8), univariate analysis based on equation (7), and a univariate analysis (equation 7) utilizing test year SRI data were evaluated for prediction accuracy based on the correlations of predicted GEBVs and their respective adjusted means from equation (5). The GEBVs generated from the multivariate and univariate approaches were based on the kinship matrix. While for the univariate method utilizing test year SRIs, GEBVs were based on the genetic kinship prediction and SRI covariate effect.

This study aims to evaluate a model’s utility in breeding programs. A major use case for GS in breeding is predicting the next generation’s performance in an untested year/environment. To evaluate model performance and overall prediction accuracy and more closely simulate a real-world breeding scenario, models were evaluated on a leave-one-year-out (LOYO) scenario. The dataset used in this study consists of data collected across four years. Models were trained on three years and then used to predict the fourth year, meaning that each year was used as a testing set only once and used in the prediction set three times. Then the average prediction accuracy and standard error were calculated for the global average model performance across years to highlight model stability across years.

Results

SRI Correlation, Heritability, and Importance

Across all years, the correlation of SRIs and grain yield were calculated, from unadjusted plot observations, to identify SRIs that have a strong relationship with grain yield and identify what SRIs are strongly related to each other, potentially minimizing the trait redundancy in models. The best SRI correlations with grain yield were NDVI (0.79) and NDRE1 (0.66), as shown in **Figure 1**.

NWI1 and NWI2 show a negative correlation with vegetation indices and grain yield. This is expected as NWI indices estimate canopy water stress, with higher values indicating less canopy water content. Additionally, indices with multiple variations, in this case, NDRE and NWI, were found to have strong correlations of 0.79 and 1, respectively, between index variations. NWI and NDVI show a strong negative relationship with a correlation of -0.75; this is most likely due to water stress playing a significant role in the overall plant health of this study population. Interestingly, MTVI shows strong relationships with other SRIs. However, this relationship is positive with NDVI yet negative for both variations of NDRE and NWI.

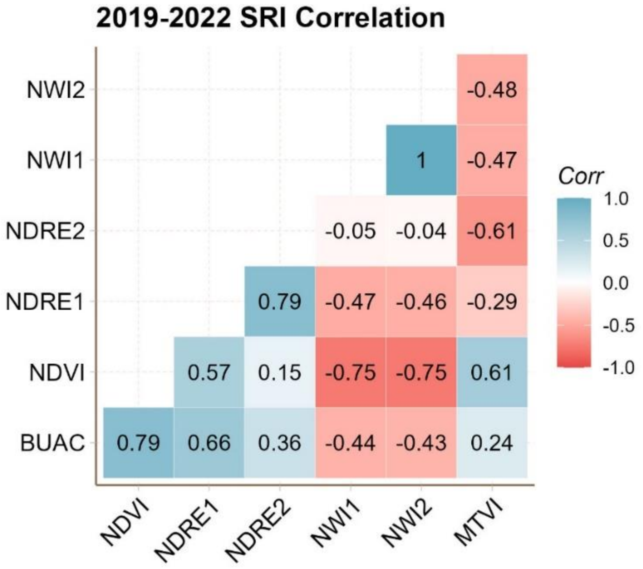

Figure 1. Pearson correlations of spectral reflectance indices (SRI) and grain yield from 2019 to 2022. Indices in the table are those outlined in Table 1. BUAC – Grain Yield.

For SRIs to have value in the prediction and selection of grain yield, it is crucial to consider the heritability of SRIs relative to the target trait of interest. If a HTP generated trait is less heritable than the primary trait of interest, it is unlikely that the HTP generated trait will add value to model predictions. Fortunately, in this study, with this population from 2019 to 2022, all SRIs evaluated have an average higher heritability (0.622-0.84) than grain yield (0.587). **Table 2** outlines the heritability of SRIs relative to our trait of interest across all years, making them viable candidates for use in GS as a means to account for previously uncaptured genetic variability, potentially improving overall prediction performance. As seen with correlation results, heritability shows a strong, potentially indifferent relationship between variations of the same index with close, if not identical, heritabilities.

Table 2: Trait Broad Sense Heritability 2019-2022

Year	Grain Yield	MTVI	NDRE1	NDRE2	NDVI	NWI1	NWI2
2019-2022	0.587	0.735	0.84	0.836	0.622	0.768	0.768
2019	0.608	0.835	0.877	0.839	0.665	0.842	0.842
2020	0.596	0.682	0.730	0.638	0.638	0.752	0.760
2021	0.658	0.741	0.648	0.650	0.690	0.736	0.736
2022	0.562	0.670	0.624	0.610	0.637	0.500	0.500

To further classify SRIs potential value for use in GS, a random forest classification model approach was evaluated for its ability to identify SRIs of importance that should be focused on in GS model development. NDRE2 and NDVI performed well across both metrics associated with a random forest analysis with high node purity and low MSE. Interestingly, **Figure 2** highlights the increased node purity of NDRE2 over NDRE1 in grain yield despite correlations indicating the reverse relationship, as seen in Figure 1. It is worth noting that while NDRE1 is not as valuable in node purity, it still has a higher value in model accuracy, indicating a potential to classify grain yield performance. Unsurprisingly, both NWI indices and MTVI did not perform well in either metric of the random forest. These results align with the indices' correlation to grain yield, indicating a moderate to insignificant relationship of the SRIs to grain yield for this population.

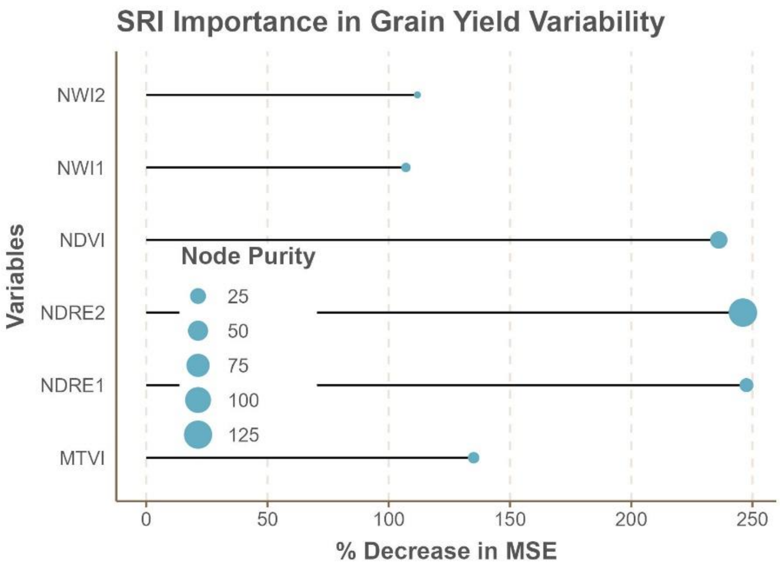

Figure 2. Results of a random forest identifying SRI importance in accounting for grain yield variability by node purity, a measure of the likelihood of a node split of an SRI and leading to misclassification, and MSE, the mean decrease in prediction accuracy when the given SRI is omitted on out-of-bag samples.

Genomic Prediction Accuracy

Genomic prediction accuracy was evaluated across four years of breeding trial data using a LOYO approach to closely simulate a real-world breeding scenario of predicting the next breeding cycle. Using this validation scheme, three different model strategies were evaluated across the inclusion of 13 different combinations of SRI data. Due to computational limitations, SRI combinations were limited to those that showed potential from high correlation to grain yield, low correlation to other SRI, high heritability, and high performance in the random forest analysis.

The control gBLUP univariate models performed well across years, especially considering the level of environmental variability in the population, with an accuracy range from 0.31 in 2019 to 0.64 in 2020 and an average across years of 0.47. When SRIs were included in the univariate gBLUP model, few SRIs or combinations of SRI fixed effects were able to improve upon the control model.

NDRE1 was the only index in a univariate model that raised average prediction accuracy above the control at 0.49. As shown in **Supplementary Figure 1,** the improvement of univariate models with SRIs as fixed effects ranged from a 41% increase over the control in 2022 with NDRE1 with an accuracy of 0.53 to a 67% decrease over the control, also in 2022, with NDVI and NDRE2 and an accuracy of 0.12.

In multivariate gBLUP models, SRIs did not improve prediction accuracy with any significance over the control. A few SRI models produced a higher average prediction accuracy, the best being 0.48 with NDVI, NWI2, and NDRE2. In 2019, models that included NDRE2 performed 6% better than the control, while in 2022, models that included MTVI were 11-16% worse than the control. While multivariate models that utilize SRIs seem more stable across years, they also provide less potential gains over the control when compared to univariate models with SRI fixed effects.

True improvement in prediction accuracy over the control can be seen in **Figure 3** when SRI data from the predicted year are included in calculating GEBVs from a univariate model with SRI fixed effects. Models that utilized NDVI consistently achieved average accuracies of 0.63, with the best being NDVI alone, having a prediction accuracy of 0.70. NDRE1 produced the best and worst performance across years with this model strategy. In 2019, NDRE1 had a prediction accuracy of -0.25. In 2022, however, NDRE1 did 102% better than the control with an accuracy of 0.76. While NDRE1 performed well, **Supplementary Figure 1** highlights NDVI's ability to perform reliably well with a minimum performance of 16% better than the control and ranging in prediction accuracy from 0.54 in 2019 to 0.93 in 2020. SRIs, when combined with NDVI into either model structure, rarely outperformed models using NDVI alone.

Additionally, **Supplementary Figure 2** highlights model predictions when looking at a subset of the testing datasets. When prediction accuracy is averaged over the four years evaluated, there are clear distinctions in how well each trial stage can be predicted. Prediction accuracy across model types and SRIs were higher in early generation trials (Single Plot and Preliminary trials). Alternatively, in the later generation advanced yield trials (AWY1 and AWY2), prediction accuracy was close to zero for all models that did not utilize test year SRI data.

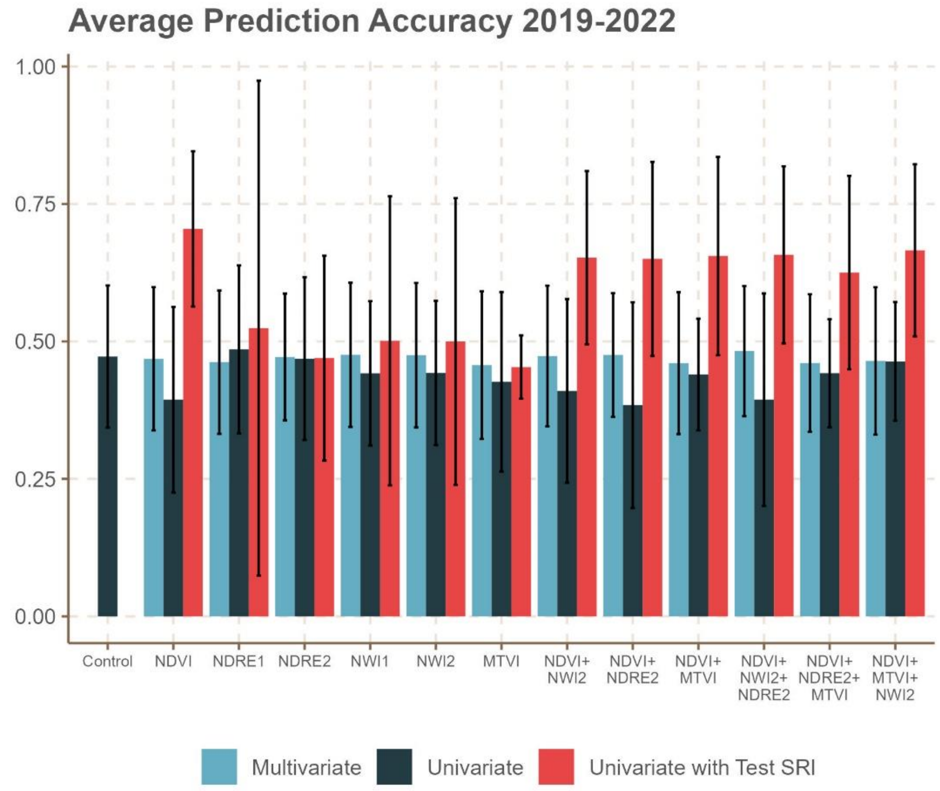

Figure 3. Average prediction accuracy of genomic selection models from 2019 to 2022 in a leave-one-year-out training scenario. Univariate and multivariate models were evaluated for success when incorporating SRIs as fixed effects and response variables, respectively. Additionally, SRIs were assessed for their ability to improve univariate models when test year data is available.

Discussion

SRI Correlation, Heritability, and Importance

From the inception of remote sensing technology, it has been essential to identify the potential for the collected traits to improve genetic gain. When working with SRIs, many options are available, all of which can inform upon and enhance the selection of a primary trait of interest (Jones and Vaughan, 2010; Guo et al., 2021). However, with limited resources and time, it is essential to narrow down the number of SRIs to a critical set that has a strong relationship to the traits of interest.

Calculating correlation allowed for the comparison of SRIs to each other and against grain yield. If the index does not correlate to grain yield, it will most likely not provide any valuable information in selecting that trait. Additionally, to maximize computational efficacy in later analysis, it is beneficial to identify what indices correlate highly with one another. Utilizing two highly correlated SRIs may provide redundant information unnecessary for improved understanding in selection. In this study, we see a vast correlation range between SRIs and grain yield, as shown in **Figure 1**. As expected, water indices (NWI) do not correlate well with the remaining vegetation indices, indicating the index's unique data capture. However, we do see a correlation of one between the two NWI indices, highlighting redundancy. In addition to identifying SRI redundancy and its relationship to grain yield, HTP generated traits provide little value if they are not more selectable than the trait of interest (Fukai and Fischer, 2012). Luckily, all SRIs evaluated in this study had an average heritability higher than grain yield. While correlation and heritability are essential for increasing selection efficiency relative to grain yield, we wanted to evaluate underutilized methods for winnowing down what SRIs to target for use in GS.

A random forest model provided an underutilized opportunity to analyze SRI variables with their direct ability to account for grain yield variability (Genuer et al., 2010). Random forest models are well established for use in prediction modeling, even when incorporating SRI data in genomic selection (Smith et al., 2013; Sandhu et al., 2021b). Data mining is an alternative use for a random forest model (Genuer et al., 2010). The quantity of data provided in UAS-HTP creates new challenges in efficiently subsetting the dataset into usable portions significant to the goal. This methodology has shown great potential in other research areas (Rossel and Behrens, 2010; Naidoo et al., 2012), but little has been done in plant breeding applications. In this study, this model strategy was able to distinguish significant differences between SRI with NDVI and NDRE variants performing the best relative to grain yield. This is most likely due to the large environmental variability across the dataset impacting grain yield. The capture of relative plant health, impacted by environmental effects, is a critical component of NDVI and NDRE.

These methods do not in and of themselves indicate how helpful SRIs will be in GS. They provide a basis on which to focus resources. With many SRIs available from a given sensor and many possibilities of crop and environment, it is valuable to have tools that can help identify the indices with the most potential in a given application.

From a breeding perspective it is important also to keep in mind what is being selected for when utilizing SRIs. Because of the inherent nature of SRIs having both a genetic and environmental element, there is potential for the introduction of unwanted bias introduced from SRIs and impacting breeder selections. Rutkoski et al. (2016) explores this idea with heading date. The study was set up very similarly to this one where UAS spectral data was tested for its ability to improve genomic prediction methods. They found that prediction performance was reduced when heading was corrected; however, this did not deter them from suggesting the uses of SRI in GS without correction, especially across untested environments where heading corrections were least effective. The potential of bias introduced from SRIs is possible, yet this should not deter from the potential for SRIs to provide value in selection, but create awareness for the breeder utilizing SRIs for potential unwanted indirect selection. Bias in selections is not a new issue. Maturity, for example, can impact SRI values but also impacts yield, so utilizing SRIs to make selections for grain yield could impact maturity, but solely selecting based on grain yield could have the same potential impact (Johnson et al., 1983; Fehr, 1991; Rutkoski et al., 2016). Further research needs to be done to evaluate the use of SRIs for selection and the bias that might be introduced from them, allowing breeders to mitigate unwanted indirect selection.

Genomic Prediction Accuracy

The potential for UAS-collected data to benefit GS has been well established. Crain et al. (2018) showed the potential for UAS data to improve GS across model strategies and irrigation regiments. Similarly, Sandhu et al. (2021a) used a spring wheat nested association mapping population to evaluate univariate and multivariate approaches to including SRI data in GS. Their results showed value in including SRI for predictions in and across cycles. Work by Montesinos-López et al. (2023), using the same dataset as this study, showed the potential of SRIs to improve GS performance within cycles and across environments. Across the literature, it has been well established that SRIs for use in GS of wheat show great promise. However, with many of the studies testing this methodology, the population sizes used and environmental factors are limited.

The hope for this study was to truly test the viability of the SRIs in GS in a challenging real-world scenario. Washington State University winter wheat breeding provided an ideal test of UAS-HTP when dealing with extreme environmental conditions, diverse growing locations and agronomic regions as well as considerable variation in trial design and replications. These factors generally increase GS models' difficulty in predicting untested years and environments (Cuevas et al., 2017; Crossa et al., 2017).

While potential has been shown for SRIs alone and as covariates to improve prediction performance (Crain et al., 2018; Sandhu et al., 2021a), in this study, when used as fixed effects in a univariate gBLUP model, improvement over the control was inconsistent, with some years having significantly worse prediction performance over the control, as highlighted in **Supplementary Figure 1**. Additionally, when used in multivariate models, SRIs were able to make slight improvements in prediction accuracy over the control while maintaining model stability across years and environments. Because of the genetic effect associated with both HTP traits and grain yield, it could be argued that HTP traits used as covariates introduces confounding factors that could impact model reliability across diverse genotypes and environments, as demonstrated in this study. It is potentially more appropriate to use a modeling strategy that deals with the relationship HTP traits have with grain yield, genotype, and environment through the use of multivariate analysis (Rutkoski et al., 2016; Sun et al., 2019) or multi-kernel analysis (Montesinos-López et al., 2023). However, it could also be argued that with the size of the dataset used in this study and the computational requirements of a multivariate model, the gain in prediction the model provided over the control was not enough to justify the additional time and computational resources necessary in a multivariate analysis.

In addition to evaluating univariate and multivariate models with untested environments, we also wanted to determine how models could be improved when early season test year SRI data was available. Incorporating test set SRI data in GS is not a new idea. Work by both Rutkoski et al. (2016) and Crain et al. (2018) utilized spectral data from test observations in the training dataset. However, in these studies, this strategy is limited to multivariate models.

Because of SRIs ability to expose environmental variability and the variety's genetic response, treating the trait like an environmental (Crossa et al., 2017; Tolhurst et al., 2022) or known genome-wide association signals (Rice and Lipka, 2019; Sehgal et al., 2020) allowed for GS models to better account for environmental variability in the test year and increase overall prediction accuracy. In its extreme case, this was shown in **Supplementary Figure 2,** where trials with considerable environmental variation (AWY1 and AWY2) produced deficient prediction performance across all model variations except those that incorporated test year SRI data. Interestingly, the models that performed well in predicting advanced yield trial data did only slightly better than model alternatives in early generation trials, most likely due to a strong environmental effect and lower yield variability in the advanced trials compared to a high genetic, lower environmental variance found in the earlier generation trials. Another reason the models might be performing this way is due to the population structure with distinct high and low rainfall regions in the advanced trials but combined in the early generation trials.

While utilizing test year SRI data in GS is less applicable to many breeding needs, i.e prediction for untested environments, years, and genotypes, it could provide valuable insight when trials have been planted and selections must be made quickly for either fall planting of winter crops or winter nurseries. For example, in the Washington State winter wheat breeding program, due to water limitations in 2021, many of the 2022 lower rainfall trials were planted in the higher rainfall region. Because 2022 was a cold, wet year, harvest was delayed, leading to an 11-day turnaround time for the 2023 planting of the low rainfall region trials. In this scenario, utilizing 2022 NDVI data as a fixed effect in a gBLUP model before harvest would have provided valuable insight into variety advancements, saving valuable time for the breeder.

Conclusion

This study evaluated the potential of utilizing UAS-collected SRI data in univariate and multivariate GS models to predict grain yield in a large-scale multi-year wheat breeding population of extreme environmental variability. Random forest was found to be a powerful data mining tool that can help deal with large amounts of generated SRI data and identify UAS traits that are most likely valuable in the primary trait of interest. In a leave-one-year-out validation scenario, SRI incorporated as fixed effects in univariate models and in multivariate models showed the potential to improve performance over the base gBLUP model. In dealing with environmental factors, utilizing test year SRI fixed effects, especially NDVI, in calculating GEBVs dramatically increased univariate models' prediction performance. UAS-collected reflectance data can account for variability in grain yield previously missed by genomic data alone, creating more robust and reliable prediction modeling. However, despite these facts, when no SRI data is available in the predicted environment, it is worth asking if the computational and time allocation necessary is worth the limited increase in prediction performance.

Supplementary Tables and Figures

Supplementary Table 1: Study Population

Location	Year	Trial	Design	Replication	Total Observations	Number of Entries
Davenport	2019	AWY1	Alpha-Lattice	3	144	49
Davenport	2019	AWY2	Alpha-Lattice	3	144	48
Davenport	2019	Preliminary	Alpha-Lattice	3	144	48
Lind	2019	Single Plot	Augmented Design with repeating checks	1	252	234
Pullman	2019	AWY1	Alpha-Lattice	3	144	48
Pullman	2019	AWY2	Alpha-Lattice	3	144	48
Pullman	2019	Preliminary	Alpha-Lattice	3	270	90
Pullman	2019	Single Plot	Augmented Design with repeating checks	1	232	215
Pullman	2019	Single Plot	Augmented Design with repeating checks	1	272	253
Pullman	2019	Single Plot	Augmented Design with repeating checks	1	629	603
Ritzville	2019	AWY1	Alpha-Lattice	3	144	48
Walla Walla	2019	AWY2	Alpha-Lattice	3	144	48
Walla Walla	2019	Preliminary	Alpha-Lattice	3	270	90
Farmington	2020	AWY2	Alpha-Lattice	3	144	48
Harrington	2020	AWY1	Alpha-Lattice	3	144	48
Lind	2020	AWY1	Alpha-Lattice	3	144	48
Lind	2020	Preliminary	Alpha-Lattice	3	198	66
Lind	2020	Single Plot	Augmented Design with repeating checks	1	304	281
Lind	2020	Single Plot	Augmented Design with repeating checks	1	406	375
Pullman	2020	AWY1	Alpha-Lattice	3	144	48
Pullman	2020	AWY2	Alpha-Lattice	3	144	48
Pullman	2020	Preliminary	Alpha-Lattice	3	216	72
Pullman	2020	Preliminary	Alpha-Lattice	3	216	72
Pullman	2020	Single Plot	Augmented Design with repeating checks	1	134	121
Pullman	2020	Single Plot	Augmented Design with repeating checks	1	223	208
Ritzville	2020	AWY1	Alpha-Lattice	3	144	48
Walla Walla	2020	AWY2	Alpha-Lattice	3	144	48
Walla Walla	2020	Preliminary	Alpha-Lattice	3	216	72

Davenport	2021	AWY1	Alpha-Lattice	3	144	48
Davenport	2021	AWY2	Alpha-Lattice	3	144	48
Davenport	2021	Preliminary	Alpha-Lattice	3	216	72
Harrington	2021	AWY1	Alpha-Lattice	3	144	48
Kahlotus	2021	AWY1	Alpha-Lattice	3	144	48
Lind	2021	AWY1	Alpha-Lattice	3	144	48
Lind	2021	Preliminary	Alpha-Lattice	3	216	72
Lind	2021	Single Plot	Augmented Design with repeating checks	1	99	93
Lind	2021	Single Plot	Augmented Design with repeating checks	1	129	113
Lind	2021	Single Plot	Augmented Design with repeating checks	1	414	382
Pullman	2021	AWY1	Alpha-Lattice	3	144	48
Pullman	2021	AWY2	Alpha-Lattice	3	144	48
Pullman	2021	Preliminary	Alpha-Lattice	3	216	72
Pullman	2021	Single Plot	Augmented Design with repeating checks	1	227	212
Pullman	2021	Single Plot	Augmented Design with repeating checks	1	468	433
Ritzville	2021	AWY1	Alpha-Lattice	3	144	48
Ritzville	2021	Single Plot	Augmented Design with repeating checks	1	414	382
Walla Walla	2021	AWY2	Alpha-Lattice	3	144	48
Walla Walla	2021	Preliminary	Alpha-Lattice	3	216	72
Davenport	2022	AWY1	Alpha-Lattice	3	126	42
Davenport	2022	AWY2	Alpha-Lattice	3	108	36
Davenport	2022	Preliminary	Alpha-Lattice	3	162	54
Farmington	2022	AWY2	Alpha-Lattice	3	108	36
Harrington	2022	AWY1	Alpha-Lattice	3	126	42
Prescott	2022	AWY1	Alpha-Lattice	3	126	42
Pullman	2022	AWY1	Alpha-Lattice	3	126	42
Pullman	2022	AWY2	Alpha-Lattice	3	108	36
Pullman	2022	Preliminary	Alpha-Lattice	3	180	60
Pullman	2022	Single Plot	Augmented Design with repeating checks	1	176	168
Pullman	2022	Single Plot	Augmented Design with repeating checks	1	194	183
Ritzville	2022	AWY1	Alpha-Lattice	3	126	42

Ritzville	2022	Preliminary	Alpha-Lattice	3	162	54

All locations were in Washington State. AWYI – advanced white yield trial for low rainfall region; AWY2 - advanced white yield trial for high rainfall region

Prediction Accuracy of Models for Grain Yield in Each Year

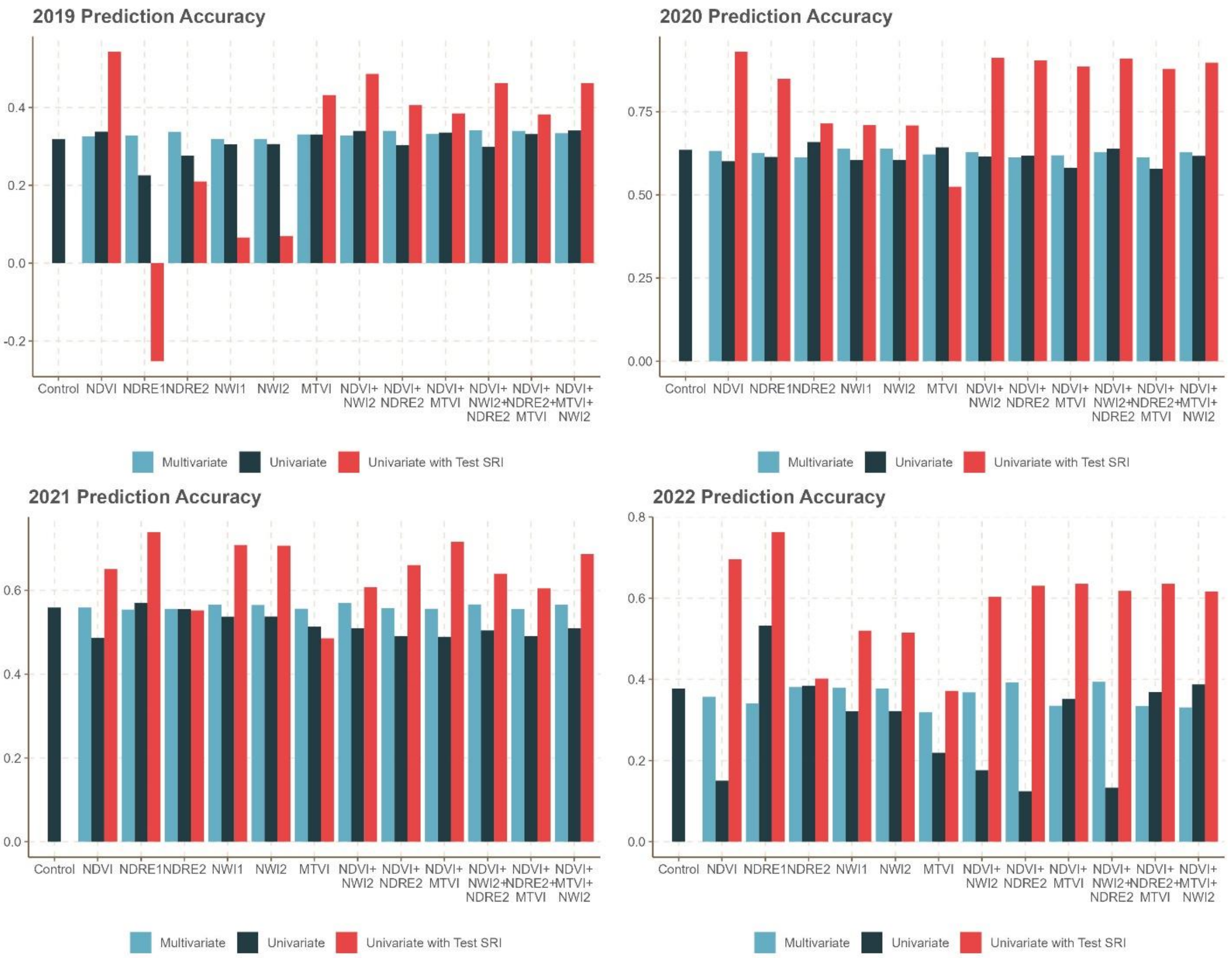

Supplementary Figure 1. Prediction accuracy of genomic selection models from 2019 to 2022. Univariate and multivariate models were evaluated for success when incorporating SRIs as fixed effects and response variables, respectively. Additionally, SRIs were assessed for their ability to improve univariate models when test year data is available.

Prediction Accuracy of Models for Grain Yield in Each Trial Type

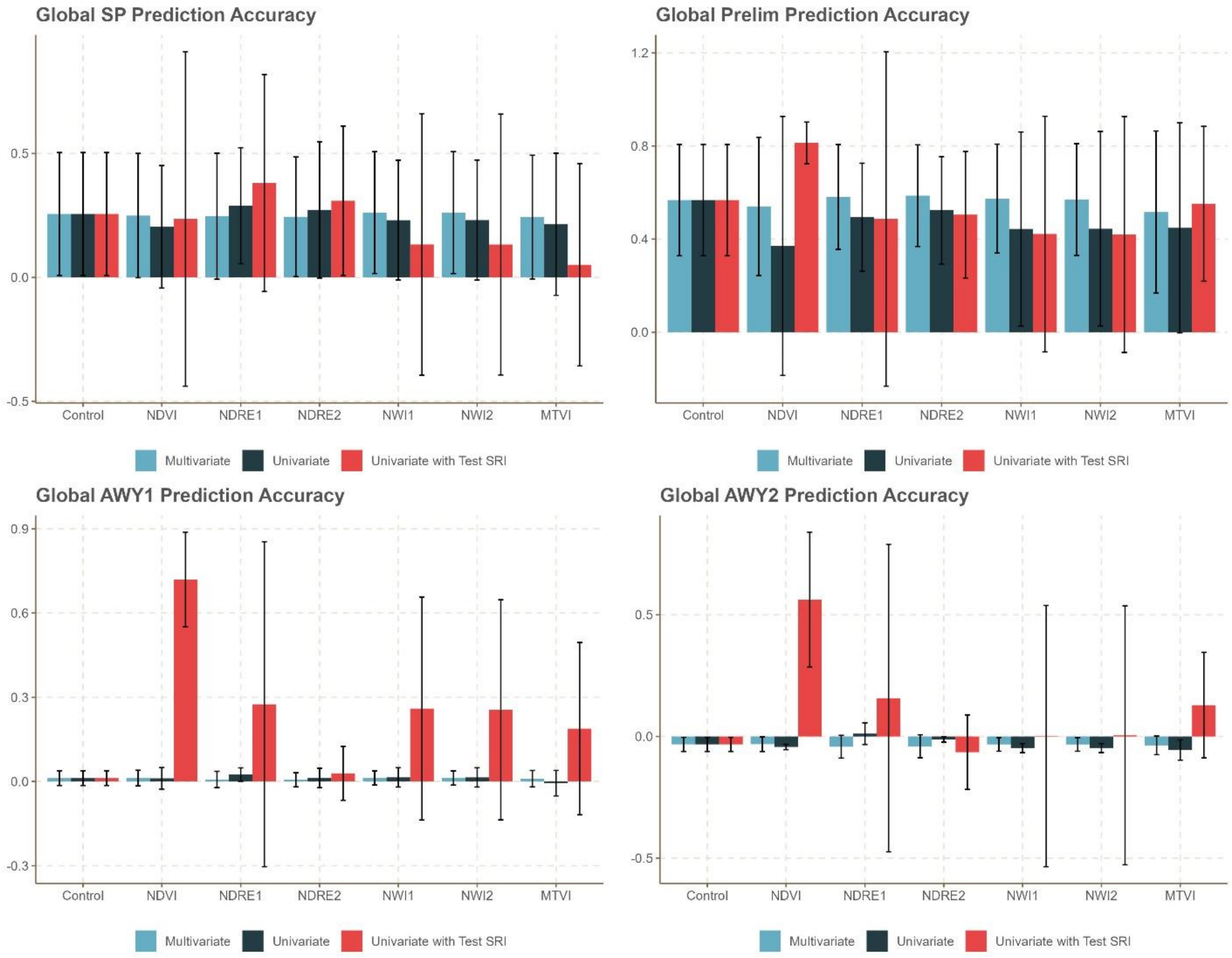

Supplementary Figure 2. Prediction accuracy of genomic selection models from 2019 to 2022. Univariate and multivariate models were evaluated for success when incorporating SRIs as fixed effects and response variables, respectively. Additionally, SRIs were assessed for their ability to improve univariate models when test year data is available. AWYI – advanced white yield trial for low rainfall region; AWY2 - advanced white yield trial for high rainfall region; Prelim – Preliminary yield trials; SP – Single Plot Yield trials

Acknowledgments

Research was partially supported by the Agriculture and Food Research Initiative Competitive Grant awards 2022-67013-36426 and 2022-68013-36439 (WheatCAP) from the National Institute of Food and Agriculture, Hatch project 1014919, and the O.A. Vogel Research Endowment at Washington State University.

Conflict of Interest

The authors declare no conflicts of interest.

Data Availability

All code and data used in the study can be found at (https://github.com/AW-Herr/Large-scale-breeding-applications-of-UAS-enabled-genomic-prediction).

References

Appels, R., K. Eversole, N. Stein, C. Feuillet, B. Keller, et al. 2018. Shifting the limits in wheat research and breeding using a fully annotated reference genome. Science 361(6403): eaar7191. doi: 10.1126/science.aar7191.

Babar, M.A., M. van Ginkel, M.P. Reynolds, B. Prasad, and A.R. Klatt. 2007. Heritability, correlated response, and indirect selection involving spectral reflectance indices and grain yield in wheat. Aust. J. Agric. Res. 58(5): 432–442. doi: 10.1071/AR06270.

Babar, M., M. Reynolds, M. Van Ginkel, A. Klatt, W. Raun, et al. 2006. Spectral reflectance to estimate genetic variation for in-season biomass, leaf chlorophyll, and canopy temperature in wheat. Crop science 46(3): 1046–1057.

Bal, S.K., G. Wakchaure, S. Potekar, B.U. Choudhury, R.L. Choudhary, et al. 2021. Spectral signature-based water stress characterization and prediction of wheat yield under varied irrigation and plant bio-regulator management practices. Journal of the Indian Society of Remote Sensing 49: 1427–1438.

Bernardo, R. 2002. Breeding for quantitative traits in plants. Stemma press Woodbury, MN.

Brown, M., J. Antle, P. Backlund, E. Carr, B. Easterling, et al. 2015. Climate change, global food security and the US food system. Washington DC: USDA Technical Document. doi: 10.7930/J0862DC7.

Browning, B.L., Y. Zhou, and S.R. Browning. 2018. A one-penny imputed genome from next-generation reference panels. The American Journal of Human Genetics 103(3): 338–348.

Covarrubias-Pazaran, G. 2016. Genome-assisted prediction of quantitative traits using the R package sommer. PloS one 11(6): e0156744.

Crain, J., S. Mondal, J. Rutkoski, R.P. Singh, and J. Poland. 2018. Combining high-throughput phenotyping and genomic information to increase prediction and selection accuracy in wheat breeding. The plant genome 11(1): 170043.

Crossa, J., P. Pérez-Rodríguez, J. Cuevas, O. Montesinos-López, D. Jarquín, et al. 2017. Genomic Selection in Plant Breeding: Methods, Models, and Perspectives. Trends in Plant Science 22(11): 961–975. doi: 10.1016/j.tplants.2017.08.011.

Cuevas, J., J. Crossa, O.A. Montesinos-López, J. Burgueño, P. Pérez-Rodríguez, et al. 2017. Bayesian Genomic Prediction with Genotype × Environment Interaction Kernel Models. G3 Genes|Genomes|Genetics 7(1): 41–53. doi: 10.1534/g3.116.035584.

Cullis, B.R., A.B. Smith, and N.E. Coombes. 2006. On the design of early generation variety trials with correlated data. Journal of Agricultural, Biological, and Environmental Statistics 11(4): 381–393. doi: 10.1198/108571106X154443.

Dierckx, P. 1995. Curve and surface fitting with splines. Oxford University Press.

Duan, T., S.C. Chapman, Y. Guo, and B. Zheng. 2017. Dynamic monitoring of NDVI in wheat agronomy and breeding trials using an unmanned aerial vehicle. Field Crops Research 210: 71–80. doi: 10.1016/j.fcr.2017.05.025.

Elshire, R.J., J.C. Glaubitz, Q. Sun, J.A. Poland, K. Kawamoto, et al. 2011. A Robust, Simple Genotyping-by-Sequencing (GBS) Approach for High Diversity Species. PLOS ONE 6(5): e19379. doi: 10.1371/journal.pone.0019379.

Fehr, W. 1991. Principles of cultivar development: Theory and technique.

Fukai, S., and K. Fischer. 2012. Field Phenotyping Strategies and Breeding for Adaptation of Rice to Drought†. Frontiers in Physiology 3. https://www.frontiersin.org/articles/10.3389/fphys.2012.00282.

Gao, B.-C. 1996. NDWI—A normalized difference water index for remote sensing of vegetation liquid water from space. Remote sensing of environment 58(3): 257–266.

Geipel, J., J. Link, and W. Claupein. 2014. Combined Spectral and Spatial Modeling of Corn Yield Based on Aerial Images and Crop Surface Models Acquired with an Unmanned Aircraft System. Remote Sensing 6(11): 10335–10355. doi: 10.3390/rs61110335.

Genuer, R., J.-M. Poggi, and C. Tuleau-Malot. 2010. Variable selection using random forests. Pattern Recognition Letters 31(14): 2225–2236. doi: 10.1016/j.patrec.2010.03.014.

Gitelson, A.A., and M.N. Merzlyak. 1996. Signature Analysis of Leaf Reflectance Spectra: Algorithm Development for Remote Sensing of Chlorophyll. Journal of Plant Physiology 148(3): 494–500. doi: 10.1016/S0176-1617(96)80284-7.

Gizaw, S.A., K. Garland-Campbell, and A.H. Carter. 2016a. Evaluation of agronomic traits and spectral reflectance in Pacific Northwest winter wheat under rain-fed and irrigated conditions. Field Crops Research 196: 168–179. doi: 10.1016/j.fcr.2016.06.018.

Gizaw, S.A., K. Garland-Campbell, and A.H. Carter. 2016b. Use of spectral reflectance for indirect selection of yield potential and stability in Pacific Northwest winter wheat. Field Crops Research 196: 199–206. doi: 10.1016/j.fcr.2016.06.022.

Gracia-Romero, A., S.C. Kefauver, O. Vergara-Díaz, M.A. Zaman-Allah, B.M. Prasanna, et al. 2017. Comparative Performance of Ground vs. Aerially Assessed RGB and Multispectral Indices for Early-Growth Evaluation of Maize Performance under Phosphorus Fertilization. Front. Plant Sci. 8. doi: 10.3389/fpls.2017.02004.

Guo, W., M.E. Carroll, A. Singh, T.L. Swetnam, N. Merchant, et al. 2021. UAS-Based Plant Phenotyping for Research and Breeding Applications. Plant Phenomics 2021: 1–21. doi: 10.34133/2021/9840192.

Gutierrez, M., M.P. Reynolds, and A.R. Klatt. 2010. Association of water spectral indices with plant and soil water relations in contrasting wheat genotypes. J Exp Bot 61(12): 3291–3303. doi: 10.1093/jxb/erq156.

Haboudane, D., J.R. Miller, E. Pattey, P.J. Zarco-Tejada, and I.B. Strachan. 2004. Hyperspectral vegetation indices and novel algorithms for predicting green LAI of crop canopies: Modeling and validation in the context of precision agriculture. Remote Sensing of Environment 90(3): 337–352. doi: 10.1016/j.rse.2003.12.013.

Herr, A.W., A. Adak, M.E. Carroll, D. Elango, S. Kar, et al. 2023. Unoccupied aerial systems imagery for phenotyping in cotton, maize, soybean, and wheat breeding. Crop Science 63: 1722–1749. doi: 10.1002/csc2.21028.

Herr, A.W., and A.H. Carter. 2023. Remote sensing continuity: a comparison of HTP platforms and potential challenges with field applications. Frontiers in Plant Science 14. https://www.frontiersin.org/articles/10.3389/fpls.2023.1233892.

Hijmans, R.J., J. Van Etten, J. Cheng, M. Mattiuzzi, M. Sumner, et al. 2015. Package 'raster.' R package 734: 473.

Hu, X., B.F. Carver, C. Powers, L. Yan, L. Zhu, et al. 2019. Effectiveness of Genomic Selection by Response to Selection for Winter Wheat Variety Improvement. The Plant Genome 12(3): 180090. doi: 10.3835/plantgenome2018.11.0090.

Iqbal, F., A. Lucieer, and K. Barry. 2018. Simplified radiometric calibration for UAS-mounted multispectral sensor. European Journal of Remote Sensing 51(1): 301–313. doi: 10.1080/22797254.2018.1432293.

Johnson, S.K., D.B. Helsel, and K.J. Frey. 1983. Direct and indirect selection for grain yield in oats (avena sativa L.). Euphytica 32(2): 407–413. doi: 10.1007/BF00021449.

Jones, H.G., and R.A. Vaughan. 2010. Remote sensing of vegetation: principles, techniques, and applications. Oxford University Press, USA.

Li, H., and R. Durbin. 2010. Fast and accurate long-read alignment with Burrows–Wheeler transform. Bioinformatics 26(5): 589–595.

Liaw, A., and M. Wiener. 2002. Classification and regression by randomForest. R news 2(3): 18–22.

Lozada, D.N., J.V. Godoy, B.P. Ward, and A.H. Carter. 2020. Genomic Prediction and Indirect Selection for Grain Yield in US Pacific Northwest Winter Wheat Using Spectral Reflectance Indices from High-Throughput Phenotyping. International Journal of Molecular Sciences 21(1): 165. doi: 10.3390/ijms21010165.

Matias, F.I., M.V. Caraza-Harter, and J.B. Endelman. 2020. FIELDimageR: An R package to analyze orthomosaic images from agricultural field trials. The Plant Phenome Journal 3(1): e20005.

Merrick, L.F., and A.H. Carter. 2021. Comparison of genomic selection models for exploring predictive ability of complex traits in breeding programs. The Plant Genome 14(3): e20158. doi: 10.1002/tpg2.20158.

Michel, S., C. Ametz, H. Gungor, B. Akgöl, D. Epure, et al. 2017. Genomic assisted selection for enhancing line breeding: merging genomic and phenotypic selection in winter wheat breeding programs with preliminary yield trials. Theoretical and Applied Genetics 130: 363–376.

Mir, R.R., M. Reynolds, F. Pinto, M.A. Khan, and M.A. Bhat. 2019. High-throughput phenotyping for crop improvement in the genomics era. Plant Science 282: 60–72. doi: 10.1016/j.plantsci.2019.01.007.

Montesinos-López, O.A., A.W. Herr, J. Crossa, and A.H. Carter. 2023. Genomics combined with UAS data enhances prediction of grain yield in winter wheat. Frontiers in Genetics 14. https://www.frontiersin.org/articles/10.3389/fgene.2023.1124218.

Montesinos-López, O.A., A. Montesinos-López, J. Crossa, G. de los Campos, G. Alvarado, et al. 2017. Predicting grain yield using canopy hyperspectral reflectance in wheat breeding data. Plant Methods 13(1): 4. doi: 10.1186/s13007-016-0154-2.

Myneni, R.B., F.G. Hall, P.J. Sellers, and A.L. Marshak. 1995. The interpretation of spectral vegetation indexes. IEEE Transactions on Geoscience and Remote Sensing 33(2): 481–486. doi: 10.1109/TGRS.1995.8746029.

Naidoo, L., M.A. Cho, R. Mathieu, and G. Asner. 2012. Classification of savanna tree species, in the Greater Kruger National Park region, by integrating hyperspectral and LiDAR data in a Random Forest data mining environment. ISPRS Journal of Photogrammetry and Remote Sensing 69: 167–179. doi: 10.1016/j.isprsjprs.2012.03.005.

Ortiz, M.V., W. Sangjan, M.G. Selvaraj, R.J. McGee, and S. Sankaran. 2021. Effect of the Solar Zenith Angles at Different Latitudes on Estimated Crop Vegetation Indices. Drones 5(3): 80. doi: 10.3390/drones5030080.

Poland, J., J. Endelman, J. Dawson, J. Rutkoski, S. Wu, et al. 2012. Genomic Selection in Wheat Breeding using Genotyping-by-Sequencing. The Plant Genome 5(3). doi: 10.3835/plantgenome2012.06.0006.

Reynolds, M., J. Foulkes, R. Furbank, S. Griffiths, J. King, et al. 2012. Achieving yield gains in wheat. Plant, cell & environment 35(10): 1799–1823.

Rice, B., and A.E. Lipka. 2019. Evaluation of RR-BLUP Genomic Selection Models that Incorporate Peak Genome-Wide Association Study Signals in Maize and Sorghum. The Plant Genome 12(1): 180052. doi: 10.3835/plantgenome2018.07.0052.

Rodríguez-Álvarez, M.X., M.P. Boer, F.A. van Eeuwijk, and P.H.C. Eilers. 2018. Correcting for spatial heterogeneity in plant breeding experiments with P-splines. Spatial Statistics 23: 52–71. doi: 10.1016/j.spasta.2017.10.003.

Rossel, R.A.V., and T. Behrens. 2010. Using data mining to model and interpret soil diffuse reflectance spectra. Geoderma 158(1): 46–54. doi: 10.1016/j.geoderma.2009.12.025.

Rouse, J.W., R.H. Hass, J.A. Schell, D.W. Deering, and J.C. Harlan. 1974. Monitoring the vernal advancement and retrogradation (green wave effect) of natural vegetation. NASA, Greenbelt, MD, USA.

Rutkoski, J., J. Poland, S. Mondal, E. Autrique, L.G. Pérez, et al. 2016. Canopy Temperature and Vegetation Indices from High-Throughput Phenotyping Improve Accuracy of Pedigree and Genomic Selection for Grain Yield in Wheat. G3: Genes, Genomes, Genetics 6(9): 2799–2808. doi: 10.1534/g3.116.032888.

Rutkoski, J., R.P. Singh, J. Huerta-Espino, S. Bhavani, J. Poland, et al. 2015. Genetic Gain from Phenotypic and Genomic Selection for Quantitative Resistance to Stem Rust of Wheat. The Plant Genome 8(2): plantgenome2014.10.0074. doi: 10.3835/plantgenome2014.10.0074.

Sandhu, K.S., P.D. Mihalyov, M.J. Lewien, M.O. Pumphrey, and A.H. Carter. 2021a. Combining Genomic and Phenomic Information for Predicting Grain Protein Content and Grain Yield in Spring Wheat. Front. Plant Sci. 12. doi: 10.3389/fpls.2021.613300.

Sandhu, K., S.S. Patil, M. Pumphrey, and A. Carter. 2021b. Multitrait machine- and deep-learning models for genomic selection using spectral information in a wheat breeding program. The Plant Genome 14(3): e20119. doi: 10.1002/tpg2.20119.

Sehgal, D., U. Rosyara, S. Mondal, R. Singh, J. Poland, et al. 2020. Incorporating Genome-Wide Association Mapping Results Into Genomic Prediction Models for Grain Yield and Yield Stability in CIMMYT Spring Bread Wheat. Frontiers in Plant Science 11. https://www.frontiersin.org/articles/10.3389/fpls.2020.00197.

Smith, P.F., S. Ganesh, and P. Liu. 2013. A comparison of random forest regression and multiple linear regression for prediction in neuroscience. Journal of Neuroscience Methods 220(1): 85–91. doi: 10.1016/j.jneumeth.2013.08.024.

Sun, J., J.A. Poland, S. Mondal, J. Crossa, P. Juliana, et al. 2019. High-throughput phenotyping platforms enhance genomic selection for wheat grain yield across populations and cycles in early stage. Theor Appl Genet 132(6): 1705–1720. doi: 10.1007/s00122-019-03309-0.

Tolhurst, D.J., R.C. Gaynor, B. Gardunia, J.M. Hickey, and G. Gorjanc. 2022. Genomic selection using random regressions on known and latent environmental covariates. Theoretical and Applied Genetics 135(10): 3393–3415. doi: 10.1007/s00122-022-04186-w.

Touw, W.G., J.R. Bayjanov, L. Overmars, L. Backus, J. Boekhorst, et al. 2013. Data mining in the Life Sciences with Random Forest: a walk in the park or lost in the jungle? Briefings in Bioinformatics 14(3): 315–326. doi: 10.1093/bib/bbs034.

VanRaden, P.M. 2008. Efficient Methods to Compute Genomic Predictions. Journal of Dairy Science 91(11): 4414–4423. doi: 10.3168/jds.2007-0980.

Visitacion, G.J., R.B. Saludes, R.A. Luyun Jr, Y.M.M. Pinca, and M.F.V. Eusebio. 2022. Statistical Analysis of Crop Water Stress in Rainfed Rice (Oryza sativa L.) Using Spectral and Non-spectral Indices. Philippine Journal of Science 15(2): 587–603.

Ward, B.P., G. Brown-Guedira, P. Tyagi, F.L. Kolb, D.A. Van Sanford, et al. 2019. Multienvironment and Multitrait Genomic Selection Models in Unbalanced Early-Generation Wheat Yield Trials. Crop Science 59(2): 491–507. doi: 10.2135/cropsci2018.03.0189.

Wientjes, E., J. Philippi, J.W. Borst, and H. van Amerongen. 2017. Imaging the Photosystem I/Photosystem II chlorophyll ratio inside the leaf. Biochimica et Biophysica Acta (BBA) - Bioenergetics 1858(3): 259–265. doi: 10.1016/j.bbabio.2017.01.008.

Witten, D., and G. James. 2013. An introduction to statistical learning with applications in R. springer publication.

Xie, C., and C. Yang. 2020. A review on plant high-throughput phenotyping traits using UAV-based sensors. Computers and Electronics in Agriculture 178: 105731. doi: 10.1016/j.compag.2020.105731.

Xiong, W., M. Reynolds, and Y. Xu. 2022. Climate change challenges plant breeding. Current Opinion in Plant Biology 70: 102308.

Xue, J., and B. Su. 2017. Significant remote sensing vegetation indices: A review of developments and applications. Journal of sensors 2017(Article ID 1353691): 17 pages. doi: 10.1155/2017/1353691.

Yin, C., X. Lv, L. Zhang, L. Ma, H. Wang, et al. 2022. Hyperspectral UAV Images at Different Altitudes for Monitoring the Leaf Nitrogen Content in Cotton Crops. Remote Sensing 14(11): 2576.

CHAPTER FOUR: SPATIAL ANALYSIS WITH UAS DATA IN WHEAT BREEDING YIELD TRIALS

Andrew W. Herr[1], Kimberly Garland Campbell[2], Xianran Li[2], and Arron H. Carter[1]

[1]Department of Crop and Soil Sciences, Washington State University, Pullman, WA 99164-6420

[2]USDA–ARS, Wheat Health, Genetics, and Quality Research Unit, Pullman, WA 99164-6420

(Submitted in The Plant Phenome Journal)

Citation

Herr, A.W.; Campbell, K. G.; Li, X.; & Carter, A.H. (2023). Spatial analysis with UAS data in wheat breeding yield trials. The Plant Phenome Journal

Attributions

The author contributions for CHAPTER FOUR: SPATIAL ANALYSIS WITH UAS DATA IN WHEAT BREEDING YIELD TRIALS for the first author Andrew W. Herr include the conceptualization, data collection, analysis, original draft preparation, review, and editing. The contributions of author Kimberly G. Campbell and Xianran Li include conceptualization, review, and editing. The contributions of co-author Arron H. Carter include conceptualization, review, editing, and funding acquisition. All authors contributed to the article and approved the published version.

Abstract

An important aspect of reliable cultivar development is good field trial evaluations. In more extensive field experiments, trial design and modeling of spatial variability are critical to control field variability and minimize error in genotype evaluations. Unoccupied aircraft systems (UAS) are a popular high-throughput phenotyping tool that has been used to successfully evaluate plant stress and other canopy characteristics. In precision agriculture applications, UAS imagery has been used to identify spatial variability in field settings. Here we use UAS spectral imagery to improve field trial spatial analysis, better control spatial variability and reduce error for more reliable selections. UAS imagery data was collected across 47 breeding trials planted in augmented complete block design (ACBD) or alpha-lattice replicated designs from 2020 through 2023. Trials were evaluated using three spatial analysis strategies: linear models incorporating block effect, row-column effect, or 2D splines. UAS-derived spectral reflectance indices (SRI) were combined with each model as covariates. Modeling strategies were used across all trials and evaluated for autocorrelation, model fitness, and coefficient of variation (CV). Akaike information criterion (AIC) was used to assess model fitness. For spatial analysis trials, SRIs improved model AIC by an average of 38.4 for alpha-lattice trials and 69.1 for ACBD trials. CV scores were also improved when SRIs were utilized, with average CV values being 2.6 lower for alpha-lattice and 2.1 for ACBD trials. This study highlights the potential for SRIs to improve the analyses of field breeding trials, despite extreme environmental variables and climate conditions.

Introduction

Plant breeding is an essential aspect of reliable agricultural production and improvement. Plant breeders work to maintain and increase the genetic output of cultivars, meeting market needs by developing and providing reliable trait characteristics. Regardless of the crop of interest, breeding goals will focus on several target traits generally defined by grower and consumer needs. Many of these traits are polygenic, making selection more complex and resource intensive. One of the most critical traits in this category is crop yield. The quantitative nature and moderate heritability of crop yield requires extensive replicated multi-year field trials across target environments (Bernardo, 2002). Environmental variability is a significant factor that must be addressed when working with agricultural field experiments like those utilized by breeders in crop yield evaluation (Smith et al., 2005). Spatial variability introduced by soil heterogeneity, slope, elevation, and management practices will reduce a breeder's ability to distinguish genetic effects from local environmental effects, limiting selection efficiency and overall genetic gain (van Es and van Es, 1993; Morales et al., 2022). It is imperative to establish strategies to minimize the bias of treatment estimates and maximize the reliability and efficiency of field-based breeding yield trial experiments (Stringer et al., 2012).

Local spatial variability in yield trial experiments is most often addressed through the experimental design which corrects for variability using randomization and replication of experimental units. In plant breeding field trials, the plot is the experimental unit which is part of a larger block. The randomized complete block design (RCBD), a popular design strategy, utilizes blocking and full replication of experimental units across blocks to minimize spatial variability within a block and maximize it across blocks (Stringer et al., 2012; Piepho et al., 2015). However, homogeneity within blocks is challenging to maintain when the number of genotypes evaluated increases (Brownie et al., 1993; Yang et al., 2004). Alpha-lattice designs are able to handle a large number of genotypes by utilizing unreplicated incomplete subblocks of a larger complete replication to minimize experimental error (Patterson and Thompson, 1971; Yang et al., 2004). In early-stages of a breeding cycle, resources are generally limited, so replicated multi-location trials can be impractical. Unreplicated augmented complete block designs (ACBD) are commonly used when many genotypes need to be evaluated, and resources limit the replication of observations (Federer and Raghavarao, 1975). In an ACBD design, replicated check plots are utilized systematically throughout the trial in a block pattern and then augmented with unreplicated test plots.

The trial design is only part of the process of accounting for spatial variability in yield trial experiments. Corrections through spatial statistical analysis can further increase data reliability (Borges et al., 2019). Without spatial analysis, reaching the desired level of precision in the dataset may be challenging due to irregular heterogeneity and autocorrelation present in the experiment (Piepho et al., 2008; Piepho and Williams, 2010).

In plant breeding, field trial design and spatial analysis strategies are well-established and reliable methods for dealing with field trial spatial heterogeneity (Hinkelmann, 2012; Borges et al., 2019). Many statistical methods for spatial modeling have been developed to account for and minimize within-trial effects through rows and columns, blocks, or nearest-neighbor correlations (Gilmour et al., 1997; Piepho et al., 2008, 2015; Piepho and Williams, 2010; Boer et al., 2020). Additionally, advanced spatial models, such as splines, can be utilized to model several covariates concurrently (Piepho et al., 2022). One such model focuses on P-Splines, a class of splines developed by Eilers and Marx (1996). Recently Rodríguez-Álvarez et al. (2018) highlighted the utility of using two-dimensional P-Splines for spatial analysis of field trials by modeling covariance as a smooth spatial trend.

New technologies, such as high throughput phenotyping (HTP), can also be used to improve spatial analysis in breeding trials but have not been thoroughly explored. In the field of precision agriculture, however, HTP strategies for remote sensing have become promising and valuable in identifying spatial trends (Zhang and Kovacs, 2012; Cohen et al., 2013; Geipel et al., 2014).

. For breeding applications, HTP can be incorporating using unoccupied aircraft systems (UAS), an ideal combination of scalability while maintaining data resolution (Reynolds et al., 2020;

Guo et al., 2021; Herr and Carter, 2023). Breeders use UAS spectral data among to provide trait information to aid in the selection of critical traits through the capture of spectral reflectance indices (SRI) to estimate routine traits of interest like plot quality, biotic, and abiotic stresses (Sankaran et al., 2015; Guo et al., 2021; Sarkar et al., 2022; Sapkota et al., 2023). SRIs collected with UAS provide standardized data focused on essential plant physiological characteristics by targeting critical wavelengths of light associated with critical components of the plant canopy (Myneni et al., 1995; Xue and Su, 2017). One of the early and most popular SRIs is Normalized Difference Vegetation Index (NDVI) which has been shown to accurately measure photosynthetic capacity and overall plant stress in crops and especially in wheat (Lozada et al., 2020; Herr et al., 2023). Another popular vegetation index used in wheat research is Normalized Difference Red-edge Index (NDRE). NDRE is similar to NDVI in its ability to identify plant stress, but instead of focusing on red absorption, it evaluates red-edge absorption relative to NIR (Gitelson and Merzlyak, 1996).

Spectral data collected from UAS have been utilized in many different ways to improve the breeding strategy by improving the collection of commonly utilized traits (Tirado et al., 2020; Lozada et al., 2020), allowing for the collection of previously infeasible traits (Adak et al., 2021; Yin et al., 2022), fueling machine learning modeling (Ferreira et al., 2019; Etienne et al., 2021), and aiding in genomic selection (Crain et al., 2018; Jarquin et al., 2018; Sun et al., 2019). Morales et al. (2022) provide promising results where the use of NDVI enhanced the detection of spatial heterogeneity and genomic selection among inbred and hybrid maize field evaluations over traditional methods. Here we further explore the potential of UAS-derived SRI data for use in the improvement of modeling for spatial heterogeneity in a wheat breeding application.

Material and Methods

Study Population

UAS spectral data and yield were collected from Washington State University soft white winter wheat (*Triticum aestivum* L.) breeding trials from 2020 through 2022 . Data were collected across 47 individual trial experiments (trial/location/year) encompassing 8,660 plots. **Supplementary Table 1** outlines the study population attributes, including location, year, trial design, number of unique entries, and number of plot observations. Experimental breeding trials were evaluated across nine locations ranging in average annual precipitation from 257 mm (Lind, WA) to 518 mm (Pullman, WA). Across years, the trials examined experienced extreme environmental variability. In Pullman, WA, for example, total precipitation during the key growing season (May-July) ranged from 20 mm in 2021 to 155 mm in 2022.

In Washington State, winter wheat production is generally divided into two agronomic production regions. The first is a low rainfall wheat fallow region (average annual precipitation of 125-400 mm) consisting of trials in the towns of Davenport, Lind, Ritzville, Harrington, and Kahlotus, WA. In this region, the wheat crop is planted every other year into stored soil moisture retained from the fallow year. The second target production region has a higher annual rainfall (average annual precipitation of 400-660 mm), consisting of trials in Pullman, Walla Walla, Farmington, and Prescott, WA. In this region, winter wheat is rotated annually with spring crops. This study utilized field trials from three of the main phases of large plot observation in the breeding program, Early generation, Preliminary, and Advanced yield trials.. The Early-generation trials of genotypes in a large plot setting were evaluated in ACBD trials derived from either F_5 (F_5 Single Plots) or double haploid (DH Single Plots) lines. These trials utilized a set of checks replicated throughout the trial, while test genotypes are a single observation. Due to seed limitations, one or two of these trials were evaluated annually in each production region. Genotypes selected from the

ACBD single-plot trials were advanced to a three block, three replication alpha-lattice trial denoted as a Preliminary trial. Each year, Preliminary yield trials were evaluated at one to two locations per production region. The final phase for breeder evaluation occurred in Advanced yield (AY) trials. Like Preliminary trials, AY trials were designed in a three block, three replication alpha-lattice. Trials denoted as AY1 were targeted for testing varieties in the lower rainfall region, whereas AY2 is an advanced trial targeted for the higher rainfall region. Depending on the year, each AY trial was evaluated in three to five locations in the targeted production region. Plots in the lower rainfall region were planted using a 4-row deep furrow planter at a seed density of 190 seeds per square meter. The higher rainfall locations were planted using a double-disc, 8-row small plot planter at a seed density of 220 seeds per square meter. The total plot size for all locations was 1.5 meters wide by 3.5 meters long.

Phenotypic Data Collection

Grain yield data for all trials was collected with a Zurn 150 harvester (Zurn Harvesting GmbH & Co. KG, Waldenburg, Germany) equipped with the Harvest Master Grain Gauge. UAS spectral data was collected with a modified Sentera Quad Multispectral Sensor (Sentera, St. Paul, MN) consisting of four sensors covering eight target bands (450 – 970nm). These spectral bands were then used to calculate the SRIs outlined in **Table 1**. For data collection, the UAS was flown at an approximate altitude of 45 m with an 85% bidirectional overlap of georeferenced images. Flights were conducted at anthesis due to the established relationship between reflectance data collected at that maturity and grain yield (Duan et al., 2017; Lozada et al., 2020). UAS flights were only conducted within a five-hour window of solar noon and on days with clear skies.

Table 1: Spectral Reflectance Index Equations

Spectral Reflectance Index	Abbreviation	Equation	Reference

Normalized Difference Vegetation Index	NDVI	$\frac{800nm - 680nm}{800nm + 680nm}$	(Rouse et al., 1974)
Normalized Difference Red Edge	NDRE	$\frac{800nm - 710nm}{800nm + 710nm}$	(Gitelson and Merzlyak, 1996)
Green Normalized Difference Vegetation Index	GNDVI	$\frac{800nm - 560nm}{800nm + 560nm}$	(Bushmann and Nagel, 1993)
Percent Canopy Cover	%CC	$\frac{1}{N}\sum_{i=1}^{N} GNDVI_i$	(Sankaran et al., 2015)

Phenotypic Data Processing and Analysis

Orthomosaic reflectance images were created from each sensor per location and flight using Pix4Dmapper (Pix4D Inc., Denver, CO). After stitching, images were georeferenced, and individual plots were identified using Geographic Information System (QGIS). Image standardization, index calculation, and mean plot data extraction of all spectral data were performed utilizing the R packages 'FIELDimageR' (Matias et al., 2020) and 'raster' (Hijmans et al., 2015). Image standardization across flights was done using a set of target panels (five panels ranging from 2%–85% reflectance, MosaicMill Oy, Vantaa, Finland). Using these panels, all eight raw band layers collected were adjusted based on the relationship:

$$SR = a \times CR + b \tag{1}$$

where the slope (*a*) and intercept (*b*) are based on the regression of the observed reflectance in target panels, collected reflectance (*CR*) is the raw observed pixel values, and surface reflectance (*SR*) is the true reflectance value (Iqbal et al., 2018). **Table 1** outlines the SRIs produced from this methodology and utilized in this study, including their abbreviation, equation and reference. An example of how these phenotypic traits look when displayed in a trial layout can be seen in **Figure 1.**

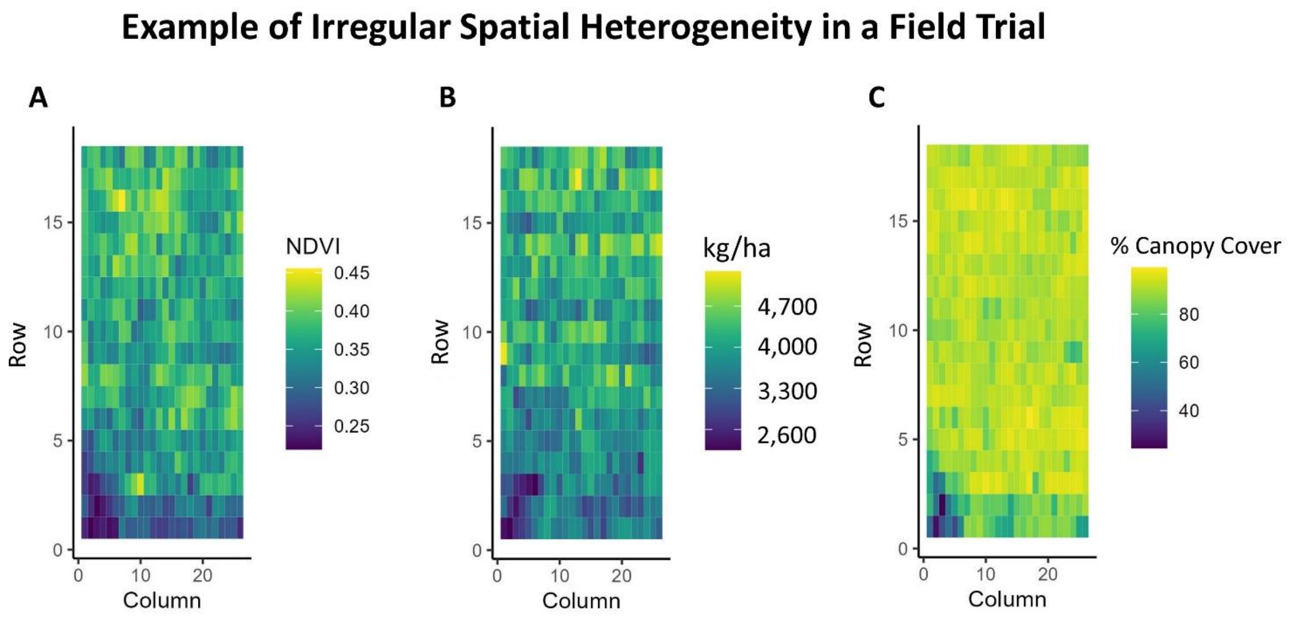

Figure 1. Heat map of average plot values for (A) NDVI, (B) grain yield in kilograms per hectare, and (C) percentage of plot canopy cover in the 2021 Pullman F5 Single plot trials. This figure highlights the severity of spatial heterogeneity in field experiments.

Spatial Modeling and Analysis

The study population consists of 47 field trials in which genotypes were evaluated in an experimental unit (plot) in one of two experimental designs: alpha-lattice or ACBD. These field trials were used to compare three spatial analysis strategies with and without SRI covariates.

The control method for this study was to utilize linear mixed models and the trial design alone to account for spatial variability. This will be referred to as the "Block Effect" method. For ACBD trials, the block effect was adjusted using the model:

$$Y_{ijk} = Gen_{i(j)} + Block_j + Check_k + \varepsilon_{ijk} \tag{2}$$

that Y_{ijk} is the phenotypic value for grain yield of the ith genotype in the jth block; $Gen_{i(j)}$ is the random effect of genotype i in the jth block; $Block_j$ is the random effect of the jth block; $Check_k$ is the fixed effect of the kth replicated cultivar check; and ε_{ijk} is the residual error. For alpha-lattice trials, the block effect was adjusted for with the model:

$$Y_{ijk} = Gen_i + Block_j + Sub_{k(j)} + \varepsilon_{ijk} \tag{3}$$

where Y_{ijk} is the phenotypic value for grain yield of the ith genotype and the jth block; Gen_i is the fixed effect of genotype i; $Block_j$ is the random effect of the jth block; $Sub_{k(j)}$ is the random effect of the sub-block k in the jth block; and ε_{ijk} is the residual error.

The second method for spatial adjustments used in this study is based on the block effect models shown in equations 2 and 3 but will incorporate row and column of plots as random effects in the model. These will be referred to as the "Row-Column Effect" method. For ACBD trials, this analysis is represented as:

$$Y_{ijklm} = Gen_{i(j)} + Block_j + Check_k + Row_l + Col_m + \varepsilon_{ijklm} \tag{4}$$

where Row_l is a random effect of the lth row and Col_m is the random effect of the mth column are added to equation 2. Similarly, in alpha-lattice trials, the row-column effect is incorporated as:

$$Y_{ijklm} = Gen_i + Block_j + Sub_{k(j)} + Row_l + Col_m + \varepsilon_{ijklm} \tag{5}$$

that Row_l is the random effect of the lth row and Col_m is the random effect of the mth column added to equation 3.

The final method utilized for spatial analysis are 2D Splines. Two-dimensional anisotropic tensor product P-splines can create a spatial field indicating spatial dependence (Rodríguez-Álvarez et al., 2018). This spatial trend can be used in conjunction with standard mixed model effects. For ACBD trials, the model is written as:

$$Y_{hijklm} = f(u_h, v_h) + Gen_{i(j)} + Block_j + Check_k + Row_l + Col_m + \varepsilon_{hijklm} \tag{6}$$

where Y_{hijklm} is the phenotypic value for grain yield; $f(u_h, v_h)$ is the P-spline framework denoted by row and column position u_h and v_h, respectively; $Block_j$ is the random effect of the jth block; $Check_k$ is the fixed effect of the kth replicated cultivar check; $Gen_{i(j)}$ is the random effect of genotype i in the ith check; Row_l is the random effect of the lth row; Col_m is the random effect of the mth column; and ε_{hijklm} is the residual error. More information on how the P-Spline framework is modeled can be found in Rodríguez-Álvarez et al. (2018). Alpha- Lattice trials are similarly modeled as:

$$Y_{hijklm} = f(u_h, v_h) + Gen_i + Block_j + Sub_{k(j)} + Row_l + Col_m + \varepsilon_{hijklm} \tag{7}$$

where Y_{hijklm} is the phenotypic value for grain yield; $f(u_h, v_h)$ is the P-spline framework denoted by row and column position u_h and v_h, respectively; Gen_i is the fixed effect of genotype i; $Block_j$ is the random effect of the jth block; $Sub_{k(j)}$ is the random effect of the sub-block k in the jth block; Row_l is the random effect of the lth row; Col_m is the random effect of the mth column; and ε_{hijklm} is the residual error.

Each of these models, denoted in equations 2-7, was evaluated alone and with the inclusion of an SRI as a fixed effect. Each model was evaluated with NDVI, NDRE, and percent canopy cover (%CC). All models were generated using R's “sommer” package (Covarrubias-Pazaran, 2016).

The first statistical method used to evaluate the validity of using SRIs in spatial analysis models was to conduct a Moran I test to identify the different spatial analyses that best reduced trial autocorrelation. The Moran I test utilizes model residuals and plot position to determine overall experiment spatial observation trends and distribution (clustered, random, or dispersed) (Arlinghaus, 2020). Models were compared for model fitness for the trial data they were generated from. Akaike information criterion (AIC) was calculated for each model as a function associated with the model output using the R package "sommer" (Covarrubias-Pazaran, 2016). AIC was chosen over other methods (BIC or Log Likelihood) because of its ability to deal with and compare models containing a different number of parameters while not biasing against model complexity, yet still avoiding overfitting (Chakrabarti and Ghosh, 2011). Another method used in the comparison of spatial model success was the calculation of the coefficient of variation (CV) based on the model-adjusted standard deviation of grain yield divided by the mean trial yield. CV is a popular method for determining the reliability and overall power of the data produced in a field experiment.

Results

A unique factor that plays a significant role in the results of this study is the years and growing conditions that are evaluated. In 2021, growing conditions were hot, with below-average precipitation. In 2020 and 2022, growing conditions led to less plant stress with cooler temperatures and above-average precipitation. For example, during the key growing season (May-July) in Pullman, WA, the average daily temperature was 14.6 C in 2020, 17.8 C in 2021, and 14.7 C in 2022. Similarly, total precipitation in this growing window was 113 mm in 2020, 20 mm in 2021, and 155 mm in 2022. As expected, this weather impacted crop performance across years dramatically. In the Pullman AY2 trial, the average grain yield was 11,184 kg/ha in 2020, 5,138 kg/ha in 2021, and 9,375 kg/ha in 2022. As will be discussed later, the environmental variation found in this study population across years significantly impacts how results should be interpreted. It highlights the inconsistency or stability of the methodologies tested across diverse experimental conditions.

Autocorrelation

After spatial analysis, trials were evaluated for a clustering effect of the adjusted yield. The distribution of the Moran I statistic across the study population highlights the minimal impact **of** spatial modeling (**Supplementary Figure 1).** However, evaluating autocorrelation does highlight the impact trial design and yearly environmental effects can have on the correlation of neighboring plot values within an experimental trial. The distribution of the Moran I statistic for all trials and model iterations, as shown in Figure 2, is centered around 0, indicating that spatial analysis maintained a complete random spatial distribution. Omitting some outliers, alpha-lattice produced autocorrelation values that point to no clustering within the trial datasets, with most having a value lower than 0. The alpha-lattice outliers produced were from the 2021 growing season, which saw unprecedented water stress in many locations. In general, 2021 saw a shift in trial values that indicated more clustering and spatial correlation of plots, which was unsurprising considering the year's growing conditions. Moran distributions centered around 0 for 2020 and 2022 growing seasons with few water stress events.

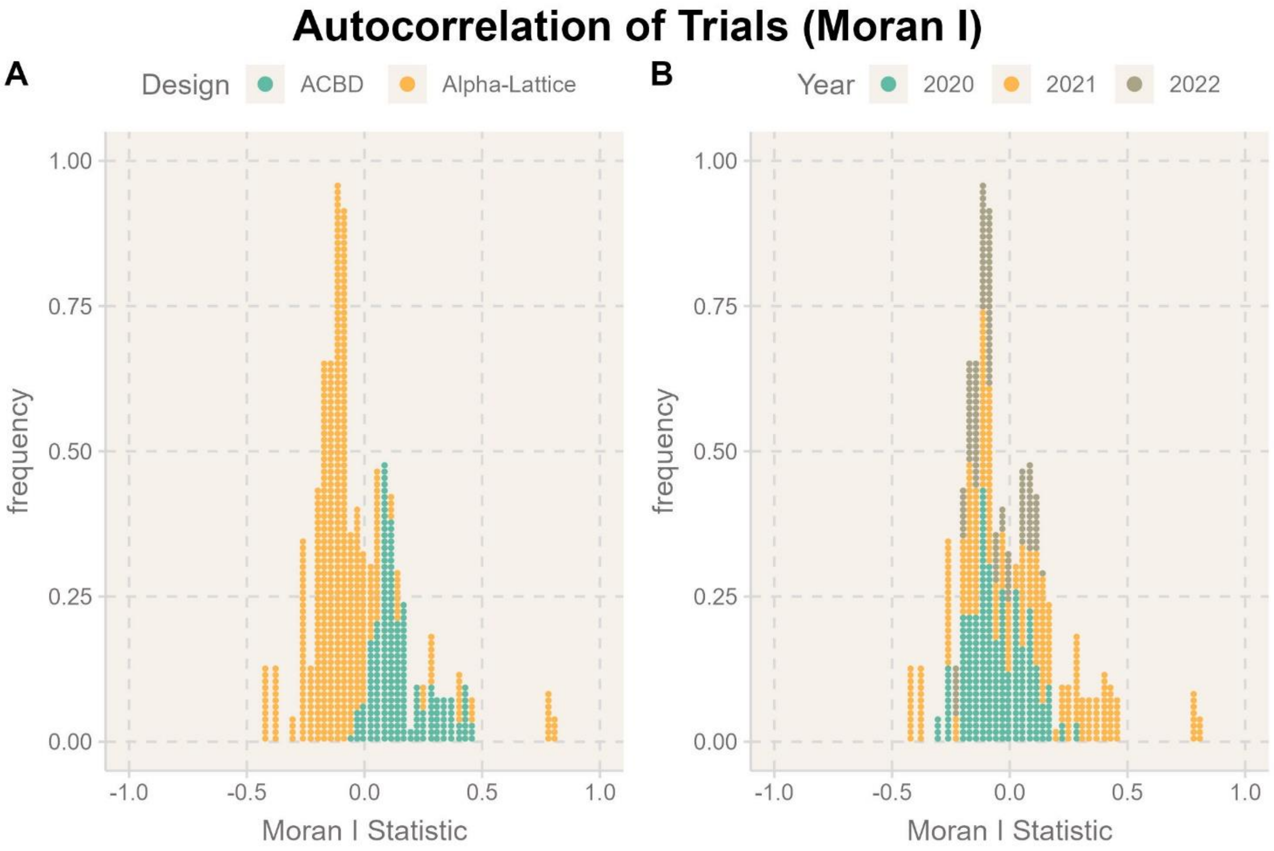

Figure 2. Distribution of trial autocorrelation by (A) trial design and (B) year. A Moran I value of 1 indicates plots are entirely clustered (high correlations present), 0 indicates a completely random distribution, and -1 indicates no correlations with a perfect distribution pattern. ACBD – Augmented Complete Block Design

Model Fit

Evaluation of model fit is the best way to identify the modeling strategy that works in a particular scenario and with a specific dataset (Chakrabarti and Ghosh, 2011). Spatial analysis was conducted on 47 trials using models outlined in equations 2-7, both with and without SRIs (NDVI, NDRE, and %CC) as covariates. These models were then evaluated for model fitness by calculating

AIC. The distribution of AIC of the models is found in **Figure 3,** where a lower AIC indicated a better model fit.

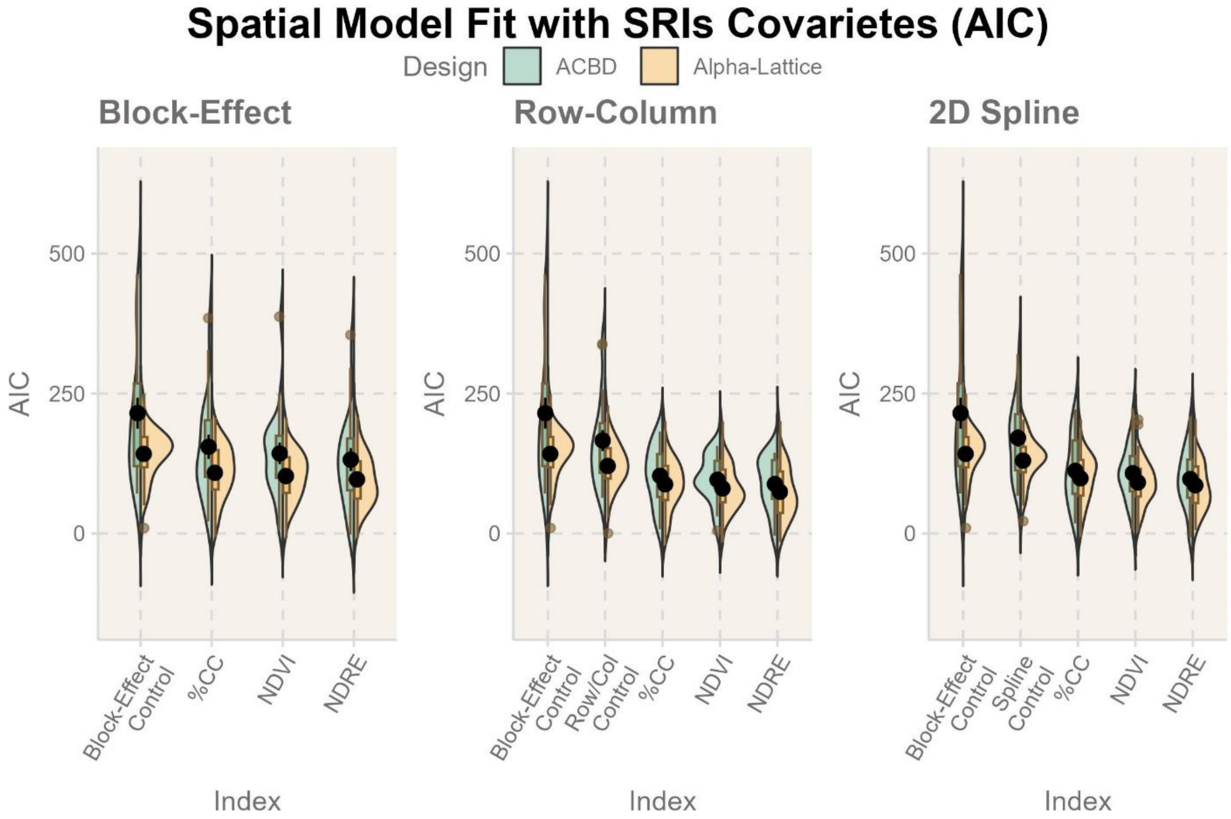

Figure 3. Comparison of the distribution of model fit across individual experiments for trial design and spatial model strategy. NDVI – Normalized Difference Vegetation Index; NDRE – Normalized Difference Red Edge; %CC – Percent Canopy Cover; AIC - Akaike Information Criterion; ACBD – Augmented Complete Block Design.

The alpha-lattice performed better than the comparable ACBD trials with an overall average AIC of 100.93 and 132.14, respectively. across modeling strategies, both with and without SRI variables, This trend was expected due to the replication of genotypes in the more robust alpha-lattice design. The robustness of the alpha-lattice is also shown in the limited ability of SRIs to improve model fitness for trials over the control models. SRIs, however, have a significant effect on model fit when used for ACBD trials. This is most apparent in ability of SRI's to minimize poor outlier AIC scores in augmented trials regardless of the base model used ,an indication of improved model reliability and overall robustness. Identification and decreasing the influence of outliers is critical when trait data are used in selection indices, especially genomic selection indices. Among SRIs, there is little difference in model fitness. Each index evaluated improved overall model fitness similarly regardless of base model or trial design. As shown in **Supplementary Table 2**, the best spatial modeling strategy across this study population was the Row-Column Effect model with NDRE as a covariate with an AIC average of 73.74 and 88.27 for alpha-lattice and ACBD, respectively. The poorest fitting models were the Block-Effect control models, where alpha-lattice had an average AIC of 141.07 and ACBD with 214.92.

Coefficient of Variation

CV follows a similar trend to that found with model fitness, where alpha-lattice trials produce a lower, better average CV value across all models (10.38) than the comparable models for ACBD trials (14.02), again highlighting the ability of alpha-lattice design to deal with and minimize irregular trial heterogeneity very well. As seen in **Figure 4,** the difference in CV performance did not change between alpha-lattice and ACBD in the same model strategy, even when utilizing SRIs. However, SRIs lowered CV scores by an average of 2.55 for alpha-lattice and 2.1 for ACBD trials. As was expected, the poorest average CV was produced by the Block Effect control model, with a CV of 12.69 for alpha-lattice and 15.77 for ACBD. Dissimilar to AIC, the best improvement in average CV for alpha-lattice (8.84) was using the 2D Spline with NDVI as a covariate, while for ACBD (12.73), the 2D Spline with NDRE had the lowest CV.

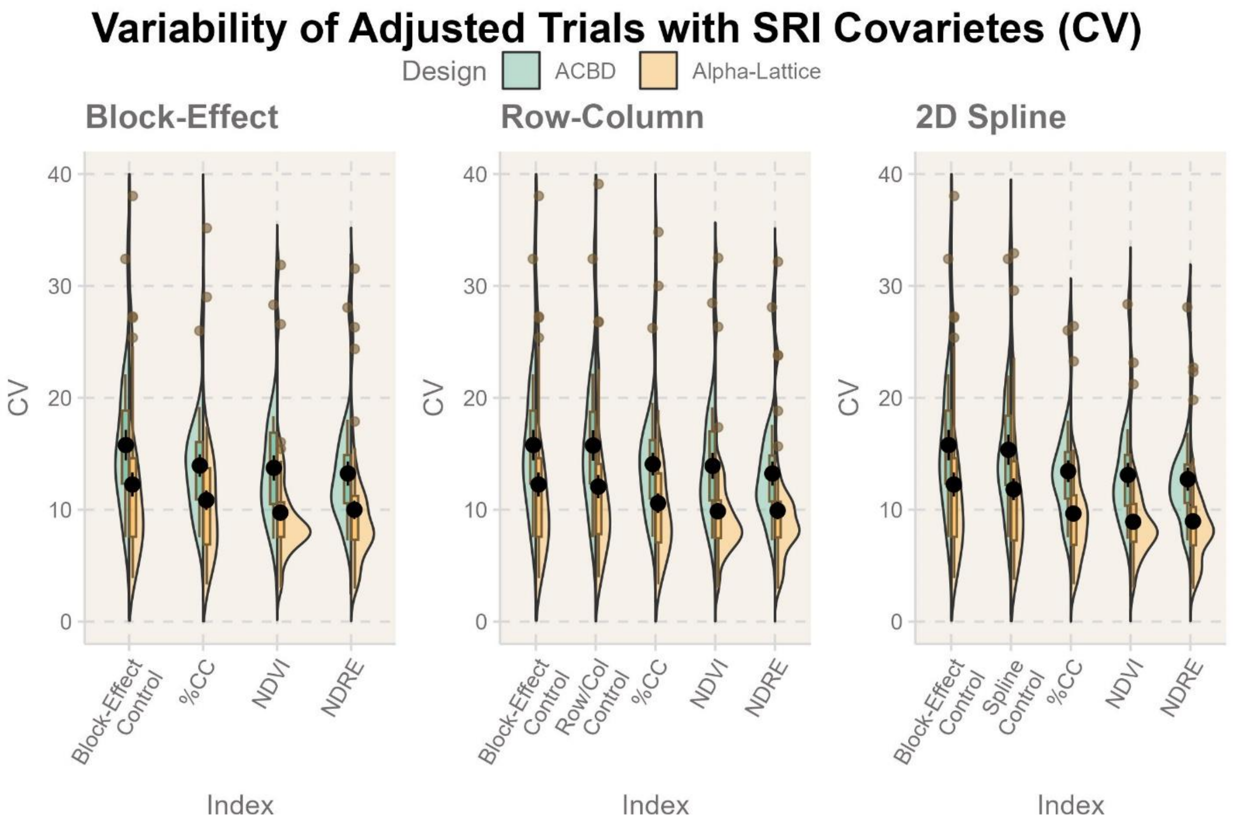

Figure 4. Comparison of the coefficient of variation (CV) distribution across individual experiments for trial design and spatial model strategy. NDVI – Normalized Difference Vegetation Index; NDRE – Normalized Difference Red Edge; %CC – Percent Canopy Cover; AIC - Akaike Information Criterion; ACBD – Augmented Complete Block Design.

Discussion

This research evaluated the validity of utilizing UAS-derived SRI data to improve spatial models for the evaluation of grain yield in individual field experiments. All SRIs evaluated, NDVI, NDRE, and %CC, were found to enhance model fitness for trial design (Block-Effect), row-column effect, and 2D Spline model trends. These results were found amidst trials that were evaluated in a diversity of environments and growing conditions. SRIs improved model fitness and account for more significant amounts of spatial variability in both alpha-lattice and ACBD trials. ACBD trials saw much more significant gains in model performance from SRIs.

The study population evaluated was made up of trials utilizing one of two trial designs: alpha-lattice or ACBD. These trials were observed over three extreme environmental years, testing both water stress tolerance and limits of yield potential under ideal growing conditions. Because of this, the trials evaluated have distinct characteristics and challenges that must be dealt with in spatial analysis.. In 2021, a severe drought year, the trials exhibited increased autocorrelation and clustering, indicating irregular spatial heterogeneity. Less spatial clustering was observed in the more ideal growing seasons of 2020 and 2022,

The design of a field trial and how it is analyzed play a significant role in the quality and reliability of the data it produces. The reality of field experimentation is that irregular spatial heterogeneity will be present and introduce errors and outliers into the trial trait data. Trial design and, secondarily, spatial analysis work to mitigate this error (Gilmour et al., 1997; Stringer et al., 2012; Borges et al., 2019). Breeders can have increased confidence that trait data represents genetic potential. UAS-collected SRIs have a unique ability to capture plant stress and other trial characteristics like canopy cover.

While UAS-collected spectral data has become a popular tool for breeders, it is still expensive and requires specialized labor and equipment. To maximize the value of the UAS, it is important to find as many uses for the data it produces as possible, maximizing overall utility. Extensive research has been done in popular areas of plant breeding where there is clear potential for UAS data to provide valuable insight into trait selection (Sankaran et al., 2015; Xue and Su, 2017; Herr et al., 2023). It is well established that UAS data can improve tools for trait selection that a breeder already uses, such as genomic selection (Crain et al., 2018; Sun et al., 2019; Lozada et al., 2020). This study aims to expand the work of Morales et al (2022) to determine if UAS data can benefit field trial design and analysis for minimizing spatial variability across a diversity of trial types, locations, and environmental conditions.

CV is a popular tool to identify how much variability has been introduced into a field experiment, indicating the overall reliability of the collected data. It works well to highlight the improvement SRI-enabled spatial modeling can have on the data collected. The trends found in the distribution of model CV match those found with AIC. SRIs improve a trial's uniformity and reduce deviation around the trial mean.

While the results of this study are promising, it is worth further exploring how indices utilized in spatial modeling impact phenotypic values and genotype rank. It is feasible that the improved models, while reducing spatial variation, could introduce unwanted bias into the data utilized in breeder selections. The next steps for this research will focus on what impact SRIs have on genotype trial rank, if any.

Conclusion

This study highlights the powerful potential of SRI to improve the overall efficiency of field trial design and analysis in a breeding program, providing decision-makers with more reliable field trial datasets. The results presented have generated many more questions that need attention, including how these models differ in producing ranks of evaluated genotypes and how that impacts breeder selection. The next steps will include assessing how these spatial models impact selection results and the introduction of potential bias created by using a specific SRI.

Supplementary Tables and Figures

Supplementary Table 1

Location	Year	Trial	Design	Observations	Genotypes
Farmington, WA	2020	AY2	Alpha-Lattice	144	48
Harrington, WA	2020	AY1	Alpha-Lattice	144	48
Lind, WA	2020	AY1	Alpha-Lattice	144	48
Lind, WA	2020	DH Single Plots	Augmented	406	375
Lind, WA	2020	F5 Single Plots	Augmented	304	281
Lind, WA	2020	Preliminary	Alpha-Lattice	198	66
Pullman, WA	2020	AY1	Alpha-Lattice	144	48
Pullman, WA	2020	AY2	Alpha-Lattice	144	48
Pullman, WA	2020	DH Single Plots	Augmented	134	121
Pullman, WA	2020	F5 Single Plots	Augmented	223	208
Pullman, WA	2020	Preliminary	Alpha-Lattice	216	72
Pullman, WA	2020	Preliminary	Alpha-Lattice	216	72
Ritzville, WA	2020	AY1	Alpha-Lattice	144	48
Walla Walla, WA	2020	AY2	Alpha-Lattice	144	48
Walla Walla, WA	2020	Preliminary	Alpha-Lattice	216	72
Davenport, WA	2021	AY1	Alpha-Lattice	144	48
Davenport, WA	2021	AY2	Alpha-Lattice	144	48
Davenport, WA	2021	Preliminary	Alpha-Lattice	216	72
Harrington, WA	2021	AY1	Alpha-Lattice	144	48
Kahlotus, WA	2021	AY1	Alpha-Lattice	144	48
Lind, WA	2021	AY1	Alpha-Lattice	144	48
Lind, WA	2021	DH Single Plots	Augmented	129	113
Lind, WA	2021	DH Single Plots	Augmented	99	93
Lind, WA	2021	F5 Single Plots	Augmented	414	382
Lind, WA	2021	Preliminary	Alpha-Lattice	216	72
Pullman, WA	2021	AY1	Alpha-Lattice	144	48
Pullman, WA	2021	AY2	Alpha-Lattice	144	48
Pullman, WA	2021	DH Single Plots	Augmented	227	212
Pullman, WA	2021	F5 Single Plots	Augmented	468	433
Pullman, WA	2021	Preliminary	Alpha-Lattice	216	72
Ritzville, WA	2021	AY1	Alpha-Lattice	144	48
Ritzville, WA	2021	F5 Single Plots	Augmented	414	382
Walla Walla, WA	2021	AY2	Alpha-Lattice	144	48
Walla Walla, WA	2021	Preliminary	Alpha-Lattice	216	72
Davenport, WA	2022	AY1	Alpha-Lattice	126	42

Davenport, WA	2022	AY2	Alpha-Lattice	108	36
Davenport, WA	2022	Preliminary	Alpha-Lattice	162	54
Farmington, WA	2022	AY2	Alpha-Lattice	108	36
Harrington, WA	2022	AY1	Alpha-Lattice	126	42
Prescott, WA	2022	AY1	Alpha-Lattice	126	42
Pullman, WA	2022	AY1	Alpha-Lattice	126	42
Pullman, WA	2022	AY2	Alpha-Lattice	108	36
Pullman, WA	2022	F5 Single Plots	Augmented	194	183
Pullman, WA	2022	F5 Single Plots	Augmented	176	168
Pullman, WA	2022	Preliminary	Alpha-Lattice	180	60
Ritzville, WA	2022	AY1	Alpha-Lattice	126	42
Ritzville, WA	2022	Preliminary	Alpha-Lattice	162	54

DH – Double Haploid; AY – Advanced Yield Trial

Supplementary Table 2

	AIC		CV	
Model	Alpha- Lattice	Augmented	Alpha- Lattice	Augmented
Global Average	100.93	132.14	10.38	14.02
Block Effect - Control	141.07	214.92	12.69	15.77
Block Effect - %CC	108.05	154.83	10.74	13.94
Block Effect - NDVI	102.34	142.97	9.64	13.74
Block Effect - NDRE	96.45	131.9	9.88	13.24
Block Effect - Index AVG	102.28	143.23	10.09	13.64
2D Spline - Control	129.03	170.8	11.68	15.35
2D Spline - %CC	97.93	111.85	9.57	13.44
2D Spline - NDVI	90.8	107.65	8.84	13.11
2D Spline - NDRE	85.74	97.28	8.88	12.73
2D Spline - Index AVG	91.49	105.59	9.09	13.09
Row-Column - Control	119.1	166.14	12.55	15.74
Row-Column - %CC	87.01	103.11	10.48	14.07
Row-Column - NDVI	79.85	95.95	9.78	13.91
Row-Column - NDRE	73.74	88.27	9.83	13.23
Row-Column - Index AVG	80.2	95.77	10.03	13.74

AIC - Akaike information criterion; CV - coefficient of variation; NDVI - normalized difference vegetation index; NDRE - normalized difference red-edge index; %CC - percentage canopy cover

Acknowledgments

Research was partially supported by the Agriculture and Food Research Initiative Competitive Grant awards 2022-67013-36426 and 2022-68013-36439 (WheatCAP) from the National Institute of Food and Agriculture, Hatch project 1014919, and the O.A. Vogel Research Endowment at Washington State University. Thank you to Dr. Julia Piaskowski, who ran the workshop "Incorporating Spatial Analysis into Agricultural Field Experiments" (https://idahoagstats.github.io/guide-to-field-trial-spatial-analysis/), demonstrating many of the statistical methods utilized in this study.

Conflict of Interest

The authors declare no conflicts of interest.

Data Availability

All code and data used in the study can be found at (https://github.com/AW-Herr/Spatial_analysis_with_UAS_data_in_wheat_breeding_yield_trials).

References

Adak, A., S.C. Murray, S.L. Anderson, S.C. Popescu, L. Malambo, et al. 2021. Unoccupied aerial systems discovered overlooked loci capturing the variation of entire growing period in maize. The Plant Genome 14(2): e20102.

Arlinghaus, S., editor. 2020. Practical Handbook of Spatial Statistics. CRC Press, Boca Raton.

Bernardo, R. 2002. Breeding for quantitative traits in plants. Stemma press Woodbury, MN.

Boer, M.P., H.-P. Piepho, and E.R. Williams. 2020. Linear Variance, P-splines and Neighbour Differences for Spatial Adjustment in Field Trials: How are they Related? Journal of Agricultural, Biological and Environmental Statistics 25(4): 676–698. doi: 10.1007/s13253-020-00412-4.

Borges, A., A. González-Reymundez, O. Ernst, M. Cadenazzi, J. Terra, et al. 2019. Can Spatial Modeling Substitute for Experimental Design in Agricultural Experiments? Crop Science 59(1): 44–53. doi: 10.2135/cropsci2018.03.0177.

Brownie, C., D.T. Bowman, and J.W. Burton. 1993. Estimating Spatial Variation in Analysis of Data from Yield Trials: A Comparison of Methods. Agronomy Journal 85(6): 1244–1253. doi: 10.2134/agronj1993.00021962008500060028x.

Bushmann, C., and E. Nagel. 1993. In vivo spectroscopy and internal optics of leaves as basis for remote sensing of vegetation. International Journal of Remote Sensing 14(4): 711–722. doi: 10.1080/01431169308904370.

Chakrabarti, A., and J.K. Ghosh. 2011. AIC, BIC and Recent Advances in Model Selection. In: Bandyopadhyay, P.S. and Forster, M.R., editors, Philosophy of Statistics. North-Holland, Amsterdam. p. 583–605

Cohen, S., Y. Cohen, V. Alchanatis, and O. Levi. 2013. Combining spectral and spatial information from aerial hyperspectral images for delineating homogenous management zones. Biosystems Engineering 114(4): 435–443. doi: 10.1016/j.biosystemseng.2012.09.003.

Covarrubias-Pazaran, G. 2016. Genome-assisted prediction of quantitative traits using the R package sommer. PloS one 11(6): e0156744.

Crain, J., S. Mondal, J. Rutkoski, R.P. Singh, and J. Poland. 2018. Combining high-throughput phenotyping and genomic information to increase prediction and selection accuracy in wheat breeding. The plant genome 11(1): 170043.

Duan, T., S.C. Chapman, Y. Guo, and B. Zheng. 2017. Dynamic monitoring of NDVI in wheat agronomy and breeding trials using an unmanned aerial vehicle. Field Crops Research 210: 71–80. doi: 10.1016/j.fcr.2017.05.025.

Eilers, P.H.C., and B.D. Marx. 1996. Flexible smoothing with B-splines and penalties. Statistical Science 11(2): 89–121. doi: 10.1214/ss/1038425655.

van Es, H.M., and C.L. van Es. 1993. Spatial Nature of Randomization and Its Effect on the Outcome of Field Experiments. Agronomy Journal 85(2): 420–428. doi: 10.2134/agronj1993.00021962008500020046x.

Etienne, A., A. Ahmad, V. Aggarwal, and D. Saraswat. 2021. Deep Learning-Based Object Detection System for Identifying Weeds Using UAS Imagery. Remote Sensing 13(24): 5182.

Federer, W.T., and D. Raghavarao. 1975. On Augmented Designs. Biometrics 31(1): 29–35. doi: 10.2307/2529707.

Ferreira, A. dos S., D.M. Freitas, G.G. da Silva, H. Pistori, and M.T. Folhes. 2019. Unsupervised deep learning and semi-automatic data labeling in weed discrimination. Computers and Electronics in Agriculture 165: 104963. doi: 10.1016/j.compag.2019.104963.

Geipel, J., J. Link, and W. Claupein. 2014. Combined Spectral and Spatial Modeling of Corn Yield Based on Aerial Images and Crop Surface Models Acquired with an Unmanned Aircraft System. Remote Sensing 6(11): 10335–10355. doi: 10.3390/rs61110335.

Gilmour, A.R., B.R. Cullis, and A.P. Verbyla. 1997. Accounting for Natural and Extraneous Variation in the Analysis of Field Experiments. Journal of Agricultural, Biological, and Environmental Statistics 2(3): 269–293. doi: 10.2307/1400446.

Gitelson, A.A., and M.N. Merzlyak. 1996. Signature Analysis of Leaf Reflectance Spectra: Algorithm Development for Remote Sensing of Chlorophyll. Journal of Plant Physiology 148(3): 494–500. doi: 10.1016/S0176-1617(96)80284-7.

Guo, W., M.E. Carroll, A. Singh, T.L. Swetnam, N. Merchant, et al. 2021. UAS-Based Plant Phenotyping for Research and Breeding Applications. Plant Phenomics 2021: 1–21. doi: 10.34133/2021/9840192.

Herr, A.W., A. Adak, M.E. Carroll, D. Elango, S. Kar, et al. 2023. Unoccupied aerial systems imagery for phenotyping in cotton, maize, soybean, and wheat breeding. Crop Science 63: 1722–1749. doi: 10.1002/csc2.21028.

Herr, A.W., and A.H. Carter. 2023. Remote sensing continuity: a comparison of HTP platforms and potential challenges with field applications. Frontiers in Plant Science 14. https://www.frontiersin.org/articles/10.3389/fpls.2023.1233892.

Hinkelmann, K. 2012. Design and analysis of experiments. Volume 3, Special designs and applications. Wiley-Interscience, Hoboken, NJ.

Iqbal, F., A. Lucieer, and K. Barry. 2018. Simplified radiometric calibration for UAS-mounted multispectral sensor. European Journal of Remote Sensing 51(1): 301–313. doi: 10.1080/22797254.2018.1432293.

Jarquin, D., R. Howard, A. Xavier, and S. Das Choudhury. 2018. Increasing Predictive Ability by Modeling Interactions between Environments, Genotype and Canopy Coverage Image Data for Soybeans. Agronomy 8(4): 51. doi: 10.3390/agronomy8040051.

Lozada, D.N., J.V. Godoy, B.P. Ward, and A.H. Carter. 2020. Genomic Prediction and Indirect Selection for Grain Yield in US Pacific Northwest Winter Wheat Using Spectral Reflectance Indices from High-Throughput Phenotyping. International Journal of Molecular Sciences 21(1): 165. doi: 10.3390/ijms21010165.

Morales, N., M.A. Gore, L.A. Mueller, and K.R. Robbins. 2022. Spatio-temporal modeling of high-throughput multi-spectral images improves agronomic trait genomic prediction in hybrid maize. Authorea Preprints.

Myneni, R.B., F.G. Hall, P.J. Sellers, and A.L. Marshak. 1995. The interpretation of spectral vegetation indexes. IEEE Transactions on Geoscience and Remote Sensing 33(2): 481–486. doi: 10.1109/TGRS.1995.8746029.

Patterson, H.D., and R. Thompson. 1971. Recovery of inter-block information when block sizes are unequal. Biometrika 58(3): 545–554. doi: 10.1093/biomet/58.3.545.

Piepho, H.-P., M.P. Boer, and E.R. Williams. 2022. Two-dimensional P-spline smoothing for spatial analysis of plant breeding trials. Biometrical Journal 64(5): 835–857. doi: 10.1002/bimj.202100212.

Piepho, H.-P., C. Richter, and E. Williams. 2008. Nearest Neighbour Adjustment and Linear Variance Models in Plant Breeding Trials. Biometrical Journal 50(2): 164–189. doi: 10.1002/bimj.200710414.

Piepho, H.P., and E.R. Williams. 2010. Linear variance models for plant breeding trials. Plant Breeding 129(1): 1–8. doi: 10.1111/j.1439-0523.2009.01654.x.

Piepho, H.-P., E.R. Williams, and V. Michel. 2015. Beyond Latin Squares: A Brief Tour of Row-Column Designs. Agronomy Journal 107(6): 2263–2270. doi: 10.2134/agronj15.0144.

Reynolds, M., S. Chapman, L. Crespo-Herrera, G. Molero, S. Mondal, et al. 2020. Breeder friendly phenotyping. Plant Science 295: 110396. doi: 10.1016/j.plantsci.2019.110396.

Rodríguez-Álvarez, M.X., M.P. Boer, F.A. van Eeuwijk, and P.H.C. Eilers. 2018. Correcting for spatial heterogeneity in plant breeding experiments with P-splines. Spatial Statistics 23: 52–71. doi: 10.1016/j.spasta.2017.10.003.

Rouse, J.W., R.H. Hass, J.A. Schell, D.W. Deering, and J.C. Harlan. 1974. Monitoring the vernal advancement and retrogradation (green wave effect) of natural vegetation. NASA, Greenbelt, MD, USA.

Sankaran, S., L.R. Khot, and A.H. Carter. 2015. Field-based crop phenotyping: Multispectral aerial imaging for evaluation of winter wheat emergence and spring stand. Computers and Electronics in Agriculture 118: 372–379. doi: 10.1016/j.compag.2015.09.001.

Smith, A.B., B.R. Cullis, and R. Thompson. 2005. The analysis of crop cultivar breeding and evaluation trials: an overview of current mixed model approaches. The Journal of Agricultural Science 143(6): 449–462. doi: 10.1017/S0021859605005587.

Stringer, J.K., A.B. Smith, and B.R. Cullis. 2012. Spatial analysis of agricultural field experiments. Design and analysis of experiments: special designs and applications. Wiley-Interscience, Hoboken, NJ. p. 109–136

Sun, J., J.A. Poland, S. Mondal, J. Crossa, P. Juliana, et al. 2019. High-throughput phenotyping platforms enhance genomic selection for wheat grain yield across populations and cycles in early stage. Theor Appl Genet 132(6): 1705–1720. doi: 10.1007/s00122-019-03309-0.

Tirado, S.B., C.N. Hirsch, and N.M. Springer. 2020. UAV-based imaging platform for monitoring maize growth throughout development. Plant direct 4(6): e00230.

Xue, J., and B. Su. 2017. Significant remote sensing vegetation indices: A review of developments and applications. Journal of sensors 2017(Article ID 1353691): 17 pages. doi: 10.1155/2017/1353691.

Yang, R.-C., T.Z. Ye, S.F. Blade, and M. Bandara. 2004. Efficiency of Spatial Analyses of Field Pea Variety Trials. Crop Science 44(1): 49–55. doi: 10.2135/cropsci2004.4900.

Yin, C., X. Lv, L. Zhang, L. Ma, H. Wang, et al. 2022. Hyperspectral UAV Images at Different Altitudes for Monitoring the Leaf Nitrogen Content in Cotton Crops. Remote Sensing 14(11): 2576.

Zhang, C., and J.M. Kovacs. 2012. The application of small unmanned aerial systems for precision agriculture: a review. Precision Agriculture 13(6): 693–712. doi: 10.1007/s11119-012-9274-5.

CHAPTER FIVE: BANDWAGON EFFECT AND OTHER MUSINGS

Throughout my time in graduate school, working on the projects outlined here, in the back of my mind I was forced to remember a paper Dr. Rex Bernardo published (Bernardo, 2016). In this publication, he outlines the idea initially discussed by N. W. Simmonds (1991) that in plant breeding, we are subject to bandwagon ideas and technology that become increasingly fashionable and popular as more people buy into them. Between Simmonds and Bernardo, many topics are discussed, and examples are given of when bandwagons enter plant breeder research, grow in hype, true potential is realized, and finally, the reality of how these tools can be utilized is settled. Bernardo illustrates this trend well in **Figure 1** (Bernardo, 2016)

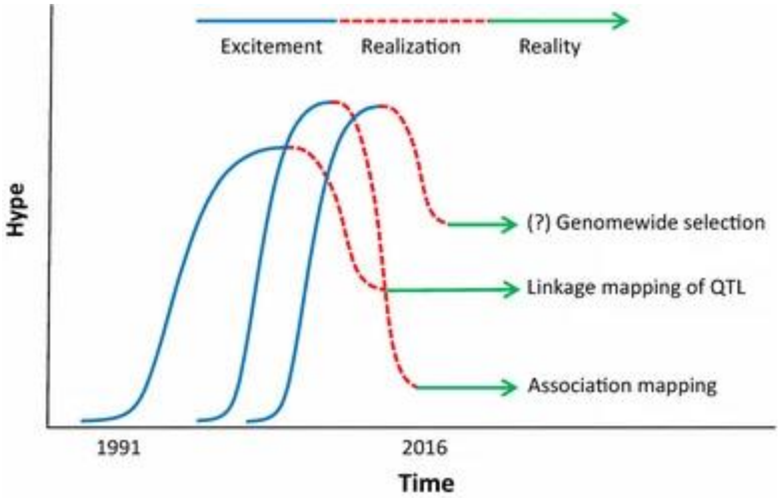

Figure 1. (Bernardo, 2016) Life cycle of a bandwagon, with QTL mapping, association mapping, and genomewide selection as examples. The reality level for association mapping is low, because the approach typically lacks power for detecting rare variants, which are what plant breeders most often seek. The (?) before genomewide selection indicates that the eventual level of usefulness of the procedure is still being discovered.

I wonder where high throughput phenotyping (HTP), especially with unoccupied aerial systems (UAS), will inevitably end up on that graph. Bernardo himself recognizes that HTP and

UAS imagery are on the rise of hype in breeding. This trend is also discussed in Chapter 1, where an evident surge in publications and citations can be seen (Herr et al., 2023).

The issues of a bandwagon can partly be blamed on human nature. We, in and of ourselves, are imperfect in conducting perfect research. The reality is that our passions, theories, and desires impact our research. Bandwagons exist because they allow us to be a part of an accepted community, where if we play our cards right, they will land us as a technology pioneer. Because of this, and mixed with an intense curiosity, I think scientists tend to hold onto ideas longer than they should, pushing concepts and strategies down rabbit holes with no applied or practical conclusion.

I struggle to decide if the hype for HTP and UAS for breeding applications should continue to rise or taper off. I feel that my research is conflicted in answering this question as well. Methods for data collection are still very labor intensive and require at least a part-time specialized technician. UAS data improves genomic selection, but is the increased prediction worth the resources necessary? At the same time, if you have early UAS data and disaster strikes your trials, model predictions can get very high prediction accuracy for how those genotypes would have performed. Finally, UAS have shown great promise in changing how we design and implement field experiments, reducing spatial error and improving field experiment reliability.

Another factor to consider in how UAS are used is that HTP traits are only slightly more heritable than the primary agronomic traits of interest. Genomic data, for example, is unchanging for genotypes across years and locations. In contrast, HTP data, because it is a phenotypic observation, indicates a response to both genotype and environment with no consistent relationship to either. This is also highlighted in prediction modeling strategies. When the genetic factor of HTP data is not taken into account, the reliability of predictions across environments and scenarios decreases (Crain et al., 2018; Rutkoski et al., 2016; Sun et al., 2019)

I believe we are most likely at the peak of the curve entering into the realization phase in Bernardo's illustration. When at conferences and meetings for breeding, HTP and UAS imagery are always some of the most talked about topics. The research outlined here, however, has highlighted some of the limitations in the technology and the reality of how it might practically be used in the industry. Additionally, where HTP ends up on Bernardo's figure depends in part on the cost of implementation on the breeder's part. Like with genomic selection, as the technology has gotten cheaper, the ease of use and tools available have increased. This has led to higher utilization across breeding programs, which was previously too resource-demanding. HTP will forever be part of the field of plant breeding. The ability to collect previously infeasible trait data and improve a breeder's understanding and selection ability is too valuable not to be utilized to some extent. The magnitude to which it is used depends on the ease of collection and utility in improving section efficiency and accuracy.

References

Bernardo, R. (2016). Bandwagons I, too, have known. *Theoretical and Applied Genetics*, *129*(12), 2323–2332. https://doi.org/10.1007/s00122-016-2772-5

Crain, J., Mondal, S., Rutkoski, J., Singh, R. P., & Poland, J. (2018). Combining high-throughput phenotyping and genomic information to increase prediction and selection accuracy in wheat breeding. *The Plant Genome*, *11*(1), 170043.

Herr, A. W., Adak, A., Carroll, M. E., Elango, D., Kar, S., Li, C., Jones, S. E., Carter, A. H., Murray, S. C., & Paterson, A. (2023). Unoccupied aerial systems imagery for phenotyping in cotton, maize, soybean, and wheat breeding. *Crop Science*, *63*, 1722–1749. https://doi.org/10.1002/csc2.21028

Rutkoski, J., Poland, J., Mondal, S., Autrique, E., Pérez, L. G., Crossa, J., Reynolds, M., & Singh, R. (2016). Canopy Temperature and Vegetation Indices from High-Throughput Phenotyping Improve Accuracy of Pedigree and Genomic Selection for Grain Yield in Wheat. *G3: Genes, Genomes, Genetics*, *6*(9), 2799–2808. https://doi.org/10.1534/g3.116.032888

Simmonds, N. (1991). *Bandwagons I have known.*

Sun, J., Poland, J. A., Mondal, S., Crossa, J., Juliana, P., Singh, R. P., Rutkoski, J. E., Jannink, J.-L., Crespo-Herrera, L., Velu, G., Huerta-Espino, J., & Sorrells, M. E. (2019). High-throughput phenotyping platforms enhance genomic selection for wheat grain yield across populations and cycles in early stage. *Theoretical and Applied Genetics*, *132*(6), 1705–1720. https://doi.org/10.1007/s00122-019-03309-0